AD NUMBER

AD904852

NEW LIMITATION CHANGE

TO

Approved for public release, distribution unlimited

FROM

Distribution authorized to U.S. Gov't. agencies only; Test and Evaluation; 11 Sep 1972. Other requests shall be referred to Commander, Naval Air Systems Command, Attn: AIR-50174, Washington, DC 20360.

AUTHORITY

USNASC ltr, 1 Nov 1973

KINEMATIC RANGING
in an
AIR-AIR MISSILE

by

R.J. LaSpisa and F.D. Powell

Report Number 9500-920254

October, 1972

Final Report on Naval Air Systems Command

Contract N00019-71-C-0259

Bell Aerospace Company DIVISION OF textron

POST OFFICE BOX ONE   •   BUFFALO, NEW YORK 14240

Bell Aerospace Company DIVISION OF textron

BUFFALO, NEW YORK 14240   716-297-1000

KINEMATIC RANGING IN AN AIR-AIR MISSILE

by

R. J. LaSpisa & F. D. Powell

Report Number 9500-920254

October, 1972

Final Report on Naval Air Systems Command

Contract N00019-71-C-0259

Bell Aerospace Company

ABSTRACT

Methods are explored for estimating Range and Range-Rate
from the geometry and kinematics of the air-air homing-missile
combat situation rather than from direct measurements. The
methods reported herein use the various signals available from
the missile autopilot, plus the inertial rotation-rate of the
Line of Sight provided by the seeker.

It is shown that acceleration of the target in the radial
direction, parallel to the Line of Sight, precludes successful
estimation by the classical techniques such as adaptive parame-
ter identification, Kalman filter estimation, or the various
minimum-variance estimation methods. A nonlinear estimator is
described which estimates the target acceleration and velocity
components and can yield accurate range and range-rate esti-
mates if correctly initialized at launch. This estimator is
able to take advantage of the many inequalities which constrain
the maneuvering of an air-air target. Errors and performance
of this estimator are demonstrated by computer simulations.

Bell Aerospace Company

TABLE OF CONTENTS

Bell Aerospace Company

TABLE OF CONTENTS

Page

LIST OF FIGURES

LIST OF FIGURES

LIST OF FIGURES

Bell Aerospace Company

LIST OF TABLES

Page

1. INTRODUCTION

Proper use of range and range-rate data, or the equivalent "time-to-go," can improve the performance of an air-air missile. At the same time, instruments which directly measure range and/or range-rate, such as radars, are expensive. The purpose of this study was to determine whether adaptive parameter identification techniques could enable estimation of range and range-rate from less expensive sensors which are used for example in infrared seekers.

1.1 Background

The trajectory of an air-air homing missile may be regarded as the response of a closed loop to an external command. In this case, the external command is the trajectory of the target, which must be assumed to be maneuvering either to conduct its attack or to attempt to evade the missile. The closed loop consists of the geometry which yields the inertial Line of Sight (LOS) rotation-rate, the navigation or guidance computer which forms commands to the missile as a function of the LOS rate, and the missile's dynamic response to that command, which closes the loop. The inertial LOS rate is, as viewed from the missile, a dynamic function of the target and missile accelerations perpendicular to the LOS, and the range and range-rate.

1

If signals of the LOS rate and the missile acceleration perpendicular to the LOS are available measurements, it might be possible to deduce the dynamics of the geometry, which may be regarded as a "plant" within the closed loop of the entire system.

As stated, the purpose of this research study was to explore means of estimating the missile-target range and range-rate by applying adaptive parameter identification techniques to this "plant" or geometry.

This approach to estimation of range and range-rate uses the missile dynamics as a probe with which to examine the geometry or kinematics of the system. It is therefore called "Dynamic Ranging," or "Kinematic Ranging."

Figure 1.1, right, shows the closed loop from target acceleration through the kinematics and dynamics to the missile response, in the upper portion. The lower part of the diagram shows, in a symbolic form, the parameter esti-mation computer whose ultimate outputs are the target range and range-rate. Consider the "box" containing the geometry and kinematics: its output, the LOS rate, is a measurable signal, while the two inputs are the target and the missile accelerations perpendicular to the LOS. But while the missile acceleration is an available signal, the target acceleration is not; estimation of range and range-rate

2

therefore must depend significantly on the characteris-
tics of the target acceleration perpendicular to the LOS.
It will be seen that the target acceleration parallel to
the LOS also has a strong effect on the estimation problem.
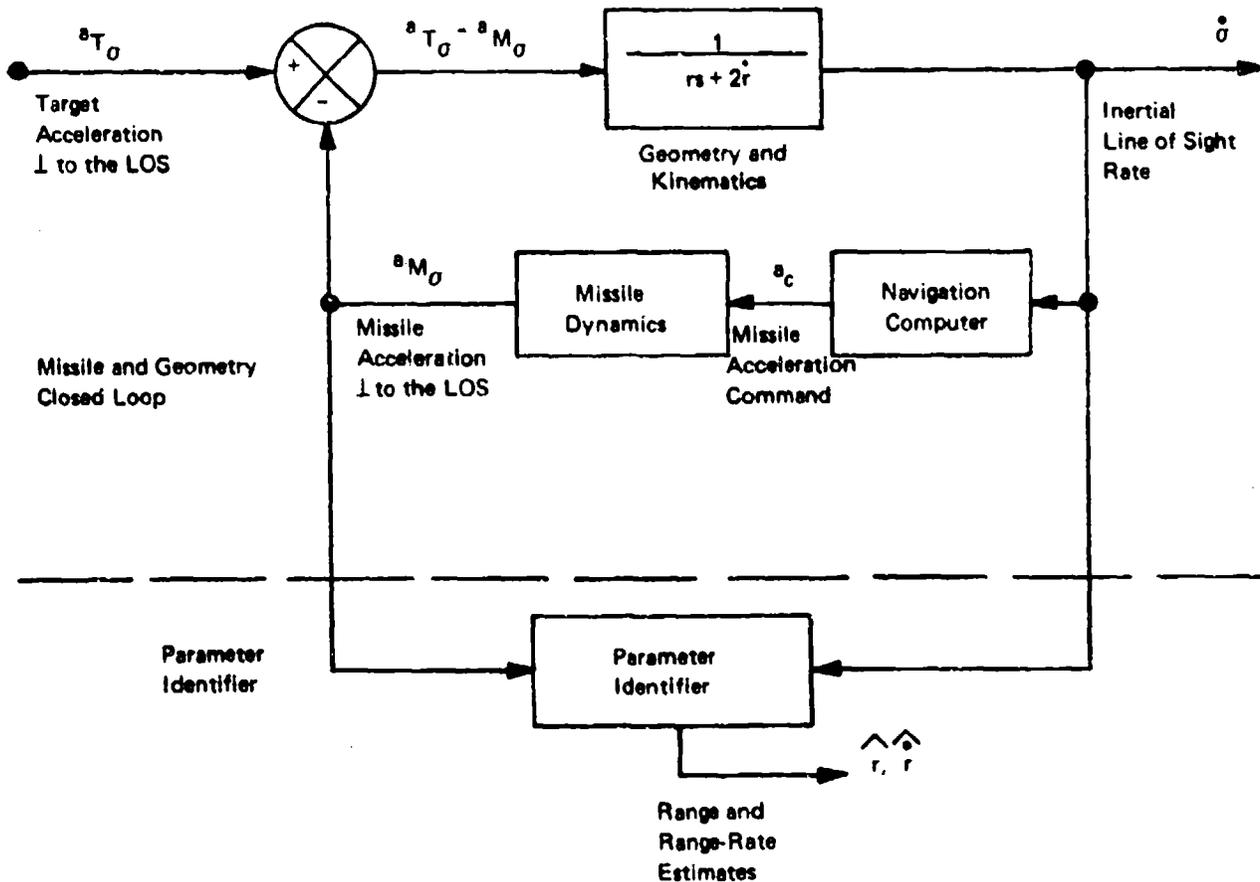
Fig. 1.1
System Configuration

1.2 Organization of the Report

The principal results of this study and the conclusions are gathered in Section 2. The problem is described and mathematically posed in Section 3. A nonlinear range and range-rate estimator is described in Section 4, together with an error and performance analysis. Several linear estimators are described in Section 5, together with comments on the conditions for which the problem is mathematically observable. A technological forecast is presented as Section 6. References are gathered in Section 7. Appendix A contains some details of the derivation of the nonlinear estimator, and Appendix B contains tabulations of the time-varying coefficients of its error propagation equation for a variety of typical trajectories.

2. SUMMARY AND CONCLUSIONS

A summary of the findings of this study is presented. The principal conclusions are stated and discussed.

2.1 Summary

Methods are explored for estimating Range and Range-Rate from the geometry and kinematics of the air-air homing-missile combat situation rather than from direct measurements. The methods reported herein use the various signals available from the missile autopilot, plus the inertial rotation rate of the Line of Sight provided by the seeker.

It is shown that acceleration of the target in the radial direction, parallel to the LOS, precludes successful estimation by the classical techniques such as adaptive parameter identification, Kalman filter estimation, or the various minimum-variance estimation methods, unless the sensor noise levels are very low and the geometry of the combat is favorable. A nonlinear estimator is described which estimates the target's aspect angle, its velocity and acceleration components plus turn-rate and roll-rate, and can yield accurate range and range-rate estimates if correctly initialized at launch. This estimator is able to take advantage of the many inequalities which constrain the maneuvering of an air-air target. Errors and performance of this estimator are demonstrated by computer simulations.

2.2 Conclusions

1. Target trajectories which have significant
acceleration parallel to the line of sight occur in most
combat geometries except head-on and tail-chase configu-
rations. If the target has significant acceleration
parallel to the line of sight, then range and range-rate
are mathematically unobservable from the kinematics by
linear methods.

In practice this means that range and range-rate
can be estimated only in favorable geometries and while
active maneuvering of the missile occurs and that the
sensor noise levels must be so low that very short aver-
aging times in the estimating filter will yield acceptable
accuracy. Filter averaging times of the order of one-
quarter second to one second yield range-rate errors as
large as 30 to 50% when the target has 3 to 6g acceleration
parallel to the LOS.

2. Two approaches are available to resolve these
difficulties. A method which uses linear principles
combines the kinematic techniques with stadimetric methods.
Stadimetric methods require that the seeker be able to
measure some function of the target's area or angular size
and rely on the assumption that the target is of constant
size. Using stadimetric data relieves but does not eliminate
the difficulties noted in conclusion (1), above. A second
method consists of a nonlinear estimator, discussed below.

3. A nonlinear estimator which estimates the target velocity vector components and acceleration components relative to the line of sight and also estimates the target turn-rate, and its rate of change, can be devised. As a stand-alone unit, this estimator requires initialization of range and range-rate. In combination with other equipment it can be used as a filter to exclude impossible target accelerations due to seeker noise or noise originating in some other method of ranging. Its principle of operation is based on the constraints on the target maneuverability dynamics, and, in particular, on the fact that the target airspeed cannot be significantly changed during an air-air missile engagement.

3. THE MATHEMATICAL MODEL OF KINEMATIC RANGING

The study is restricted to the Maneuver plane.

The key assumption guiding and restricting this study is that the seeker in the missile provides the line-of-sight (LOS) rate only; it does not yield any indication of target-size, or shape or changes thereof, as television or mosaic-type infrared seekers can, nor does it provide any range or range-rate information directly, as a radar does, nor even yield the variations of intensity of signal from the target. The simplest type of seeker, simply pointing at the target and carrying a rate gyro to sense the LOS rate, is assumed. On the other hand, the missile is assumed to have a pair of accelerometers in the maneuver plane, so that its accelerations may be resolved about the line of sight. Similarly, it is assumed that missile air-speed, or its estimate, can be provided if needed and that no data are transferred from the launch-airplane to the missile after the missile has been launched. The two areas which describe the problem are:

> (a) The geometry and the equations which define the kinematic relations from which we hope to estimate Range and Range-Rate, and
>
> (b) The constraints on the target.

These areas are discussed in detail below. The problem which we attack is estimation of Range and Range-Rate from the kinematics and dynamics of the combat.

3.1 Kinematics

Under these circumstances, a polar coordinate geometry with the moving origin located at the missile is the logical coordinate system. Figure 3.1 shows the geometry.
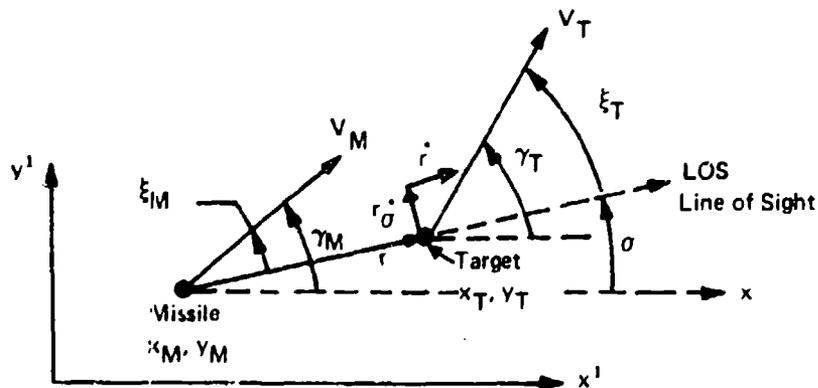
Figure 3.1 - Geometry

We first derive expressions for the velocity components parallel and perpendicular to the LOS. Similar expressions for the accelerations follow.

The instantaneous linear components of velocity parallel to the Line-of-Sight (LOS) yield the polar coordinate component,

$$\dot{r} = V_T \cos (\gamma_T - \sigma) - V_M \cos (\gamma_M - \sigma)$$

(3.1)

9

while the components perpendicular to the LOS are

$$r \dot{\sigma} = V_T \sin (\gamma_T - \sigma) - V_M \sin (\gamma_M - \sigma).$$

(3.2)

The angle ξ_T may be called "The Target Aspect Angle" as it represents the attitude of the target velocity vector relative to the LOS, and is closely related to the target body attitude with respect to the LOS.

As missile acceleration components are assumed to be measured, we differentiate (3.1) and (3.2) so that the acceleration terms will become explicitly evident, yielding

$$\ddot{r} = [\dot{V}_T \cos (\gamma_T - \sigma) - V_T \dot{\gamma}_T \sin (\gamma_T - \sigma)] - [\dot{V}_M \cos (\gamma_M - \sigma)$$
$$- V_M \dot{\gamma}_M \sin (\gamma_M - \sigma)] + \dot{\sigma} [V_T \sin (\gamma_T - \sigma) - V_M \sin (\gamma_M - \sigma)]$$

(3.3)

and

$$r\ddot{\sigma} + \dot{r}\dot{\sigma} = [\dot{V}_T \sin (\gamma_T - \sigma) + V_T \dot{\gamma}_T \cos (\gamma_T - \sigma)] -$$
$$[\dot{V}_M \sin (\gamma_M - \sigma) + V_M \dot{\gamma}_M \cos (\gamma_M - \sigma)] -$$
$$\dot{\sigma} [V_T \cos (\gamma_T - \sigma) - V_M \cos (\gamma_M - \sigma)].$$

(3.4)

The components of acceleration of target and missile parallel to the instantaneous line-of-sight are the first two terms of the right of (3.3), respectively.

Therefore define $a_{T_r} = \dot{V}_T \cos(\gamma_T - \sigma) - V_T \dot{\gamma}_T \sin(\gamma_T - \sigma)$

$$\tag{3.5}$$

$$a_{M_r} = \dot{V}_M \cos(\gamma_M - \sigma) - V_M \dot{\gamma}_M \sin(\gamma_M - \sigma).$$

$$\tag{3.6}$$

The third term on the right of (3.3) represents the apparent acceleration due to the LOS rotation-rate.

Now multiply (3.2) by $\dot{\sigma}$ and substitute $(r\dot{\sigma}^2)$ for the third term on the right of (3.3); with this substitution and the definitions (3.5) and (3.6), (3.3) yields

$$\ddot{r} - r\dot{\sigma}^2 - a_{T_r} + a_{M_r} = 0.$$

$$\tag{3.7}$$

Equation (3.4) is similarly simplified.

As before, define the components of target and missile accelerations across the instantaneous line-of-sight by

$$a_{T_\sigma} = \dot{V}_T \sin(\gamma_T - \sigma) + V_T \dot{\gamma}_T \cos(\gamma_T - \sigma)$$

$$\tag{3.8}$$

$$a_{M_\sigma} = \dot{V}_M \sin(\gamma_M - \sigma) + V_M \dot{\gamma}_M \cos(\gamma_M - \sigma)$$

$$\tag{3.9}$$

and substitute these for the first and second terms on the right of (3.4). Again, the third term on the right of (3.4) is the apparent acceleration due to the LOS rotation-rate. Now multiply (3.1) by $\dot{\sigma}$ and substitute

11

$(\dot{r}\,\dot{\sigma})$ for the third term on the right of (3.4), yielding the acceleration equation

$$r\,\ddot{\sigma} + 2\,\dot{r}\,\dot{\sigma} - a_{T_\sigma} + a_{M_\sigma} = 0.$$

(3.10)

If we use the notation

$$\xi_T = \gamma_T - \sigma$$

$$\xi_M = \gamma_M - \sigma$$

(3.11)

then the velocity equations (3.1) and (3.2) may be expressed as

$$\dot{r} - V_T \cos \xi_T + V_M \cos \xi_M = 0$$

(3.12)

$$r\,\dot{\sigma} - V_T \sin \xi_T + V_M \sin \xi_M = 0$$

(3.13)

and, with the more compact notation

$$V_{M_r} = V_M \cos \xi_M \,, \quad V_{T_r} = V_T \cos \xi_T \,,$$

$$V_{M_\sigma} = V_M \sin \xi_M \,, \quad V_{T_\sigma} = V_T \sin \xi_T \,,$$

(3.14)

for the components of target and missile velocity parallel and perpendicular to the LOS, we have the velocity equations in the form

$$\dot{r} - V_{T_r} + V_{M_r} = 0$$

(3.15)

$$r\,\dot{\sigma} - V_{T_\sigma} + V_{M_\sigma} = 0 \,.$$

(3.16)

Equations (3.1) and (3.2) or their equivalents (3.12) and
(3.13) or (3.15) and (3.16), together with (3.7) and (3.10)
form the key elements of the mathematical model of the
kinematics. The assumed noise levels, bias, initialization
errors, etc., which determine the errors of the proposed
solution, are gathered in Section 4.

The term $r\dot{\sigma}^2$ in (3.7) deserves a brief discussion.
This term, a component of the range-acceleration, is due
purely to the geometry. Its physical significance can
easily be perceived. Assume you, (M), are standing
motionless at the coordinates $X = 0$, $Y = Y_0$ where $|Y_0|$ is
small, so that $V_{M_r} = V_{M_\sigma} = a_{M_r} = a_{M_\sigma} = 0$. A vehicle,(T), is
approaching at constant velocity on the X-axis; $\dot{X}$ may be
positive or negative but $\dot{r}$ is negative as the vehicle is
approaching. The target is not accelerating,so that
$a_{T_r} = a_{T_\sigma} = 0$. At the start of the problem, $\dot{r} \simeq - |\dot{X}|$,
while at the end $\dot{r} \simeq + |\dot{X}|$; Range-Rate, $\dot{r}$, has changed
from $-|\dot{X}|$ to $+ |\dot{X}|$; the polar-coordinate acceleration signal
which expresses this change is $r\dot{\sigma}^2$. If the offset Y_0 is
very small, the change from $-|\dot{X}|$ to $+|\dot{X}|$ can occur very
suddenly, implying large values of $\ddot{r}$. In an air-air
combat situation, it is therefore possible for very large
range-accelerations to occur, due to the geometry alone,
even though neither missile nor target maneuvers.

3.2 Constraints on the Target

The constraints under which the target airplane operates form an essential part of the system. An airplane can increase or decrease its airspeed by changing its thrust or by use of the earth gravitation vector component; in either case or in combination the longitudinal acceleration increment is not more than 1g. An airplane can also change its airspeed by increasing its drag; this can be accomplished deliberately by use of speed brakes or involuntarily as a result of the induced drag due to the lift resulting from the airplane's evasive maneuvers. But the target of an air-air missile attack must try to maintain airspeed to conserve maneuverability. We therefore consider that

$$|\dot{V}_T| \leq 1 \text{ g}$$

is a plausible constraint for deliberate airspeed changes, and we neglect the involuntary changes in this study.

The target turn-rate, $\dot{\gamma}_T$, is governed by several inequality constraints. At high airspeed, $|V_T\dot{\gamma}_T|$ is limited by the ability of the pilot (or structure) to withstand g-loads, equal to $V_T\dot{\gamma}_T$, while at low airspeed the turn-rate is limited by aerodynamic stall related to bank angle ϕ_T. In addition, the target pilot and aircraft roll-dynamics establish a minimum time in which a maneuver can be performed or changed by the target so that $|\ddot{\gamma}_T|$, or $|\dot{\phi}_T|$, is limited.

The high-speed condition provides the acceleration constraint, due to pilot or structural strength limits,

14

$$V_T |\dot{\gamma}_T| \leq 6 \text{ g}.$$

Further, turning is achieved by bank-angle. Taking the pilot's characteristics into account, the bank angle, ϕ_T, cannot be changed from hard-turn in one direction to the other in less than 1 second. This yields the constraint

$$|\dot{\phi}_T| \leq 2 |\phi_T|_L.$$

Figure 3.2 shows acceleration limit, turn-rate limit, and the bank angle for a coordinated turn, as functions of V/V_S where V_S is the stall speed for a fighter in combat configuration and $V_S = 200$ ft/sec. is assumed as a nominal value. The relationships for a coordinated turn are

$$
\begin{aligned}
\text{Acceleration Limit} \quad N_L &= \begin{cases} (V_T/V_S)^2, & V_T \leq 2.45\, V_S \\ 6.0, & V_T > 2.45\, V_S \end{cases} \\[2mm]
\text{Bank Angle} \quad |\phi_T|_L &= \cos^{-1}(1/N_L). \\[2mm]
\text{Roll Rate} \quad |\dot{\phi}_T|_L &= 2\,\phi_{T_L} = 2\cos^{-1}(1/N_L) \\[2mm]
\text{Turn-Rate Limit} \quad |\dot{\gamma}_T|_L &= \frac{(g/V_S)}{(V/V_S)}\sqrt{N_L^2 - 1} = \frac{g/V_S}{V/V_S}\tan|\phi_T|_L. \\[2mm]
\text{Turn-Acceleration Limit} \quad |\ddot{\gamma}|_L &= 2|\dot{\gamma}_T|_L \\[2mm]
\text{Airspeed change;} \quad |\dot{V}_T|_L &\leq 1.0 \text{ g}.
\end{aligned}
\tag{3.17}
$$

15

Equations 3.17 and Figure 3.2 thus represent the statement of the constraints which form part of the mathematical model. In an air-air combat situation, it will usually be the case that the target will be flying at a relatively high speed, so that the left of Fig. 3.2, representing the condition $V_T \overset{\le}{=} 2.45 \ V_S$, may be disregarded, and only a relatively narrow range of V_T/V_S can be realistically expected.
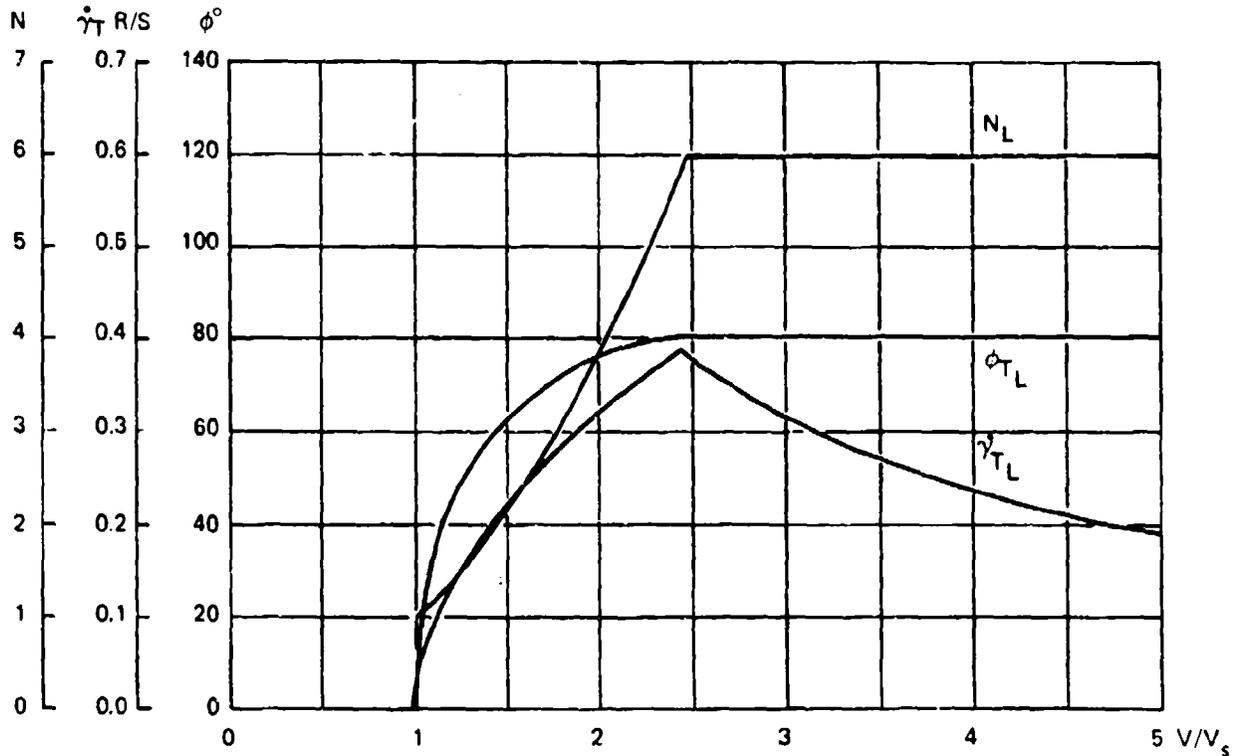
Figure 3.2. Bank-Angle and the Limits of Target Turn-Rate and Acceleration versus V/V_S ($V_S = V_{STALL} = 200$ '/S)

Bell Aerospace Company

4. A NONLINEAR ESTIMATOR

A derivation of a nonlinear range/range-rate estimation filter is presented below.

This filter has a format such that it is very easy to impose and take advantage of the physical constraints which limit the maneuverability of an airborne target. It therefore could be appropriately used alone if initialized or preset at launch with range and range-rate; thereafter it will correctly keep track of those variables. Alternately it may be used as a nonlinear filter in conjunction with other ranging methods, whether direct or indirect. The analysis below assumes that this estimator will be initialized or preset at launch. The error analysis and performance of Sections 4.2 and 4 3 show the effects of errors in initializing as well as the effects of various other error sources.

This nonlinear filter has as its physical origin, and therefore motivation, the hypotheses that (a) the target cannot easily change airspeed, and (b) range-acceleration is not trivial and must be estimated.

4.1 Theoretical Basis

The equations which present the components of velocity parallel and perpendicular to the LOS are, respectively, from (3.15) and (3.16),

$$\dot{r} = V_{T_r} - V_{M_r} \tag{4.1}$$

$$r\dot{\sigma} = V_{T_\sigma} - V_{M_\sigma} , \tag{4.2}$$

where the subscripts (T) and (M) refer to target and missile, respectively, while the subscripts (r) and (σ) refer to the components parallel to the LOS ⁀⁀pendicular thereto. Thus, for example, the targe̤ velocity component perpendicular to the LOS is V_{T_σ}.

Similarly, the equations which present the components of acceleration parallel and perpendicular to the LOS are, respectively, from (3.7) and (3.10),

$$\ddot{r} - r\dot{\sigma}^2 - a_{T_r} + a_{M_r} = 0 \tag{4.3}$$

$$r\ddot{\sigma} + 2\dot{r}\dot{\sigma} - a_{T_\sigma} + a_{M_\sigma} = 0, \tag{4.4}$$

wher̤ ᴛhe components use the same subscript code described above, so the target acceleration across the LOS is a_{T_σ}. Consider Eqn. (4.3); we can measure $\dot{\sigma}$ direct̤y from the seeker and can therefore compute $r\dot{\sigma}^2$, as initial values of r and $\dot{r}$ are assumed given. We can also directly sense the missile acceleration component a_{M_r}. If we could also estimate a_{T_r}, we could compute $\ddot{r}$ and then by integration continue to estimate $\dot{r}$ and r. This would enable us to close a computation loop and keep the estimation process going. It will be shown that we can estimate a_{T_r} by using the assumption that target airspeed is quasi-const̤nt during the brief interval of an air-air encounter. This is significant, as linear estimators uniformly fail to operate successfully whenever a_{T_r} is not negligible, as will be seen in Section ̤.

Let us solve Eqns. (4.1) and (4.2) for the target velocity components V_{T_r} and V_{T_σ}. We know that the total velocity, or airspeed, V_T, of the target can be determined from these components by the relationship

$$V_{T_r}^2 + V_{T_\sigma}^2 = V_T^2 \, , \tag{4.5}$$

due to the definitions $V_{T_r} = V_T \cos \xi_T$ and $V_{T_\sigma} = V_T \sin \xi_T$.

An air-air combat target cannot easily change its airspeed V_T. Since V_T is nearly constant, $\dot{V}_T$ is nearly zero, so that differentiation of (4.5) yields

$$V_{T_r} a_{T_r} + V_{T_\sigma} a_{T_\sigma} = V_T \dot{V}_T \approx 0 \tag{4.6}$$

where a_{T_r} and a_{T_σ} are the components of target acceleration parallel and perpendicular to the LOS. The considerable algebraic effort required to show that this differentiation is valid is presented in Appendix A.

We may solve (4.6) for a_{T_r}, so that we may estimate

$$\hat{a}_{T_r} = - \frac{V_{T_\sigma} a_{T_\sigma}}{V_{T_r}} \, . \tag{4.7}$$

We now substitute for a_{T_σ}, V_{T_σ}, and V_{T_r} from (4.1), (4.2) and (4.4) so that (4.7) becomes

$$\hat{a}_{T_r} = - \frac{\left(r\dot{\sigma} + V_{M_\sigma}\right)\left(r\ddot{\sigma} + 2\dot{r}\dot{\sigma} + a_{M_\sigma}\right)}{\left(\dot{r} + V_{M_r}\right)} \, . \tag{4.8}$$

All quantities on the right of (4.8) may be measured or estimated in the missile, so that we can compute $\hat{a}_{T_r}$. But we also have, from Section 3, Eqn. (3.8)

$$a_{T_\sigma} = \dot{V}_T \sin \xi_T + V_T \dot{\gamma}_T \cos \xi_T$$

and if $\dot{V}_T \approx 0$, then

(4.9)

$$a_{T_\sigma} \approx V_T \dot{\gamma}_T \cos \xi_T = V_{T_r} \dot{\gamma}_T .$$

We may therefore compute $\hat{a}_{T_r}$ in a different way, as

$$\hat{a}_{T_r} = -\ (r\dot{\sigma} + V_{M_\sigma})\ \frac{V_T \hat{\dot{\gamma}}_T \cos \xi_T}{V_T \cos \xi_T} = -(r\dot{\sigma} + V_{M_\sigma})\hat{\dot{\gamma}}_T = -\ V_{T_\sigma}\hat{\dot{\gamma}}_T$$

(4.10)

where $\hat{\dot{\gamma}}_T$ is the estimate of $\dot{\gamma}_T$, the target turn-rate.

Eqns. (4.8) and (4.10) present different forms of the same result; either may be used as appropriate to the available physical constraints. In particular, the relationship

$$\dot{\gamma}_T = \frac{a_{T_\sigma}}{V_{T_r}}$$

(4.11)

may be used to estimate $\hat{\dot{\gamma}}_T$.

If we substitute (4.11) into (4.7) we have

$$\hat{a}_{T_r} = -V_{T_\sigma} \dot{\gamma}_T .$$

(4.12)

This is an obvious result: V_{T_σ} is the target velocity across the LOS, and $\dot{\gamma}_T$ is its turn-rate, therefore the product is the acceleration of the target in the range

direction. Its magnitude is at a maximum when the target is flying perpendicular to the LOS and vanishes in a head-on or tail-chase combat configuration.

Equation (4.11) is a very convenient result, for it enables implementation of the constraints, described in Section 3, on the target maneuver capability:

(1) The estimates $\hat{a}_{T_r}$ and $\hat{a}_{T_\sigma}$ may be limited to 6g magnitude.

(2) Since $\dot{\gamma}_T$ may be estimated as $\hat{\dot{\gamma}}_T = \dfrac{\hat{a}_{T_\sigma}}{\hat{V}_{T_r}}$,

it is possible to limit the quotient to a realistic turn-rate which may be either a nominal constant or a function of the target's estimated airspeed $\hat{V}_T$.

(3) Further, if $\hat{\dot{\gamma}}_T$ is formed in a rate-limited net, it is possible to impose a physically motivated constraint on $\hat{\ddot{\gamma}}_T$, to represent the finite time required by the target to change its turn-rate, e.g., a right turn to a left turn. These limit-properties are of great value, for they make it possible to estimate $\hat{\dot{\gamma}}_T$. Without these limits, the division in (4.11) would fail due to a "division by zero" whenever the target velocity vector is nearly perpendicular to the

LOS. This condition can occur in a dogfight situation. Further, the limit on $\hat{\dot{\gamma}}_T$ noted above in (3) enables exclusion of noise which implies impossible roll-rates, just as the limits (1 & 2) preclude undue sensitivity to noise implying impossible turn-rates and accelerations.

The result of the analysis above is the estimator

$$\hat{\ddot{r}} = \hat{r} \; \dot{\sigma}^2 - a_{M_r} - \hat{V}_{T_\sigma} \; \overset{\text{c}}{\gamma}_T. \tag{4.13}$$

Fig. 4.1 shows an estimator configuration, which requires 6 multiplications for its instrumentation in the given format. The locations and character of the limits which impose the physical constraints are shown. The adaptive algorithm which determines $\hat{\overset{\text{c}}{\gamma}}_T$ is shown as part of the overall diagram. It is assumed that missile acceleration components are sensed with respect to the seeker centerline; it is also assumed that the missile velocity components with respect to the seeker centerline are available. This net can be formed in a variety of equivalent ways; the configuration shown in Fig. 4.1 is representative but not unique.

A brief discussion of Fig. 4.1 follows. The block
at the extreme upper left shows the process of inserting
the initial values of range and range-rate at launch.
The three blocks immediately below show the various
signals used in this estimator, gathered by their several
sources. Block A shows the two integrations relating
$\hat{\ddot{r}}$ to $\hat{\dot{r}}$ and $\hat{r}$. Block B shows the formation of $\hat{a}_{T_\sigma}$ from
the relationship

$$\hat{a}_{T_\sigma} = \hat{r}\ddot{\sigma} + 2\hat{\dot{r}}\dot{\sigma} + a_{M_\sigma} . \qquad (4.14)$$

Blocks C and D show the formation of $\hat{V}_{T_r}$ and $\hat{V}_{T_\sigma}$,
respectively, from the relationships

$$\hat{V}_{T_r} = \hat{\dot{r}} + V_{M_r} \qquad (4.15)$$

$$\hat{V}_{T_\sigma} = \hat{r}\dot{\sigma} + V_{M_\sigma} . \qquad (4.16)$$

Block E shows the formation of $\hat{\ddot{r}}$ as

$$\hat{\ddot{r}} = \hat{r}\dot{\sigma}^2 - a_{M_r} + \hat{a}_{T_r} . \qquad (4.17)$$

We have stated that the term $\hat{a}_{T_r}$ is estimated as

$$\hat{a}_{T_r} = -\hat{V}_{T_\sigma}\hat{\dot{\gamma}}_T \qquad (4.18$$

and that this may be limited to 6g, or some similar limit representative of the abilities of the target airplane and pilot. This limited product is contained within Block F.

We now consider estimation of $\hat{\dot{\gamma}}_T$, noting that if $\dot{V}_T \equiv 0$, then

$$\dot{\gamma}_T = a_{T_\sigma} \Big/ V_{T_r} \ .$$

We do not have the true values of a_{T_σ} and V_{T_r}, but only their estimates. The procedure for estimating $\hat{\dot{\gamma}}_T$ is to form an error

$$\epsilon = \hat{a}_{T_\sigma} - \hat{\dot{\gamma}}_T \hat{V}_{T_r} \tag{4.19}$$

as shown in Block G. A least mean magnitude algorithm is

$$\hat{\ddot{\gamma}}_T = k\hat{V}_{T_r} \ \text{sgn}(\epsilon) \tag{4.20}$$

where $\text{sgn}(\epsilon)$ is defined as

$$\text{sgn}(\epsilon) \equiv \begin{cases} + 1 \ , & \epsilon > 0 \\ - 1 & \epsilon < 0 \end{cases}$$

i.e., "the sign of ϵ". One simple way to limit $\hat{\ddot{\gamma}}_T$

to the values permitted by the constraint relationship is
to replace $\hat{V}_{T_r}$ by $\text{sgn}(\hat{V}_{T_r})$, and to choose k equal to
the constraint limit. It is essential that the algorithm
contain at least the sign of $\hat{V}_{T_i}$ and the sign of ϵ if it
is to be stable for $\hat{\dot{\gamma}}_T > 0$ and also for $\hat{\dot{\gamma}}_T < 0$. With these
comments, the $\hat{\dot{\gamma}}_T$ algorithm is now

$$\hat{\ddot{\gamma}}_T = k \ \text{sgn}(\hat{V}_{T_r}) \ \text{sgn}(\epsilon). \qquad (4.21)$$

The least mean magnitude algorithm is preferred to the
least mean square as it yields more rapid solution for
this class of problem, and is less complex to instrument.
In some extreme trajectories the target is flying nearly
perpendicular to the LOS and $\hat{V}_{T_r}$ may be quite small.
To preclude instability of the $\hat{\dot{\gamma}}_T$ algorithm it is useful
to disable integration of $\hat{\ddot{\gamma}}_T$ when $|\hat{V}_{T_r}|$ is less than some
minimum value, such as 60'/sec. Assume a target airspeed
of $V_T = 1000'$/sec. This limit is 6% of the airspeed,
implying that the angle ζ_T between the LOS and the target
velocity vector is in the range $86° < |\zeta_T| < 94°$.
With this restriction, algorithm (4.21) becomes

$$\hat{\ddot{\gamma}}_T = \begin{cases} k \ \text{sgn}(\hat{V}_{T_r}) \ \text{sgn}(\epsilon) \ , & |\hat{V}_{T_r}| \geq \hat{V}_{T_{r_{min}}} \\ 0 & , \text{ otherwise} \end{cases} \qquad (4.22)$$

An alternate form of (4.22) which contains the entire
algorithm in one expression is

$$\ddot{\hat{\gamma}}_T = k \; \text{sgn}(\hat{V}_{T_r}) \; \text{sgn}(\epsilon) \left[\frac{1 + \text{sgn}\left(|\hat{V}_{T_r}| - V_{T_{r_{min}}} \right)}{2} \right] .$$

(4.22a)

We found that $k = 0.4$ and $\hat{V}_{T_{r_{min}}} = 60$ ft/sec are satisfactory values for the missile and target which we assumed. Eqn. (4.22) is instrumented in Block H. The integration of $\ddot{\hat{\gamma}}_T$ to form $\dot{\hat{\gamma}}_T$ and the limitation of $\dot{\hat{\gamma}}_T$ to the constrained range appear in Block K. The expression in the square brackets [ ] in (4.22a) introduces the dead-space in the algorithm and is visible in Block H. The nonlinearity in the feedback path in Block K is an analog representation of a saturation limiter which imposes the constraint $\dot{\gamma}_{T_L}$ on turn-rate estimate $\dot{\hat{\gamma}}_T$. The net of Fig. 4.1 can be mechanized in analog or digital formats with equal ease. The choice of an analog format for this Figure is arbitrary.

26
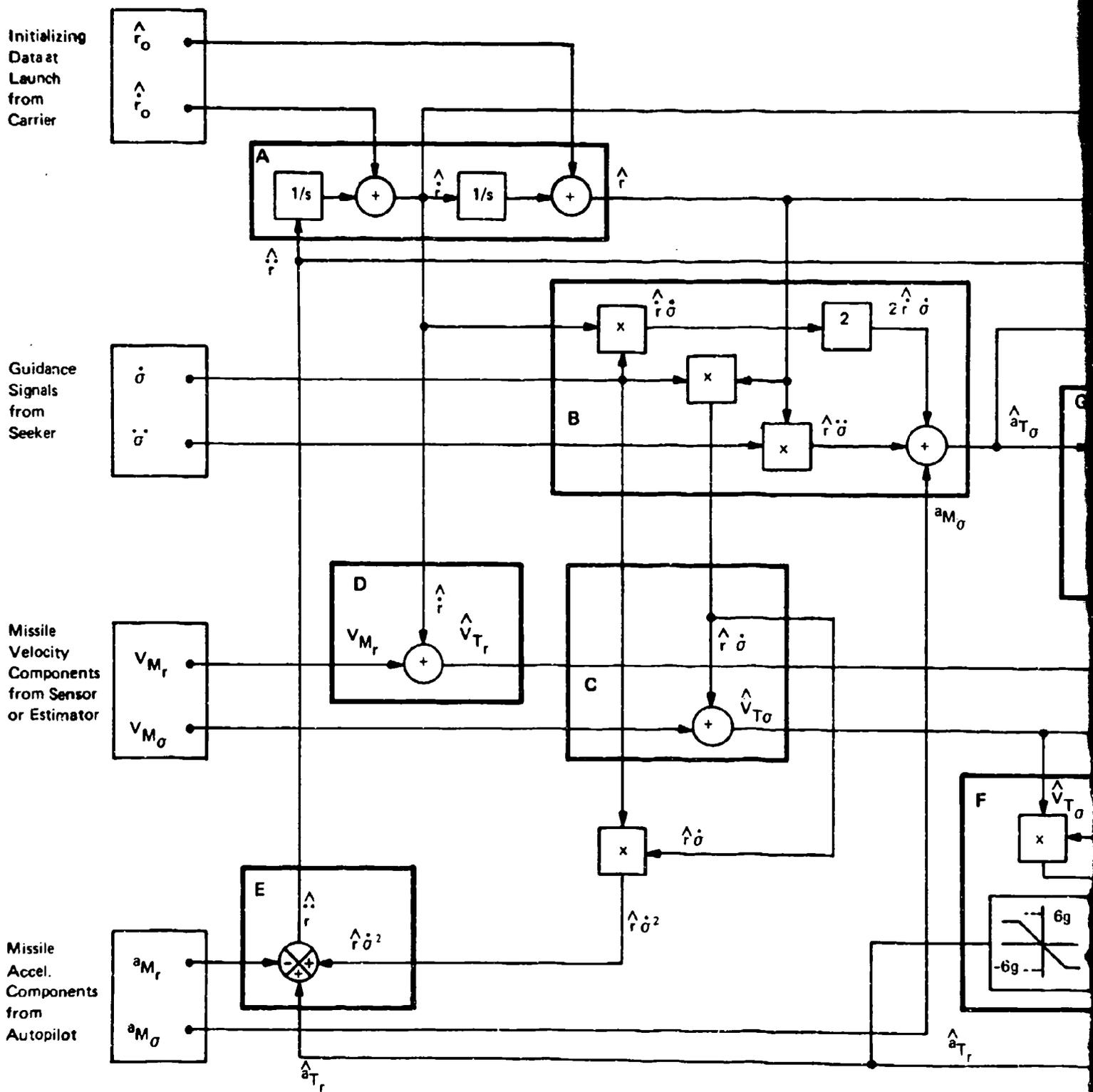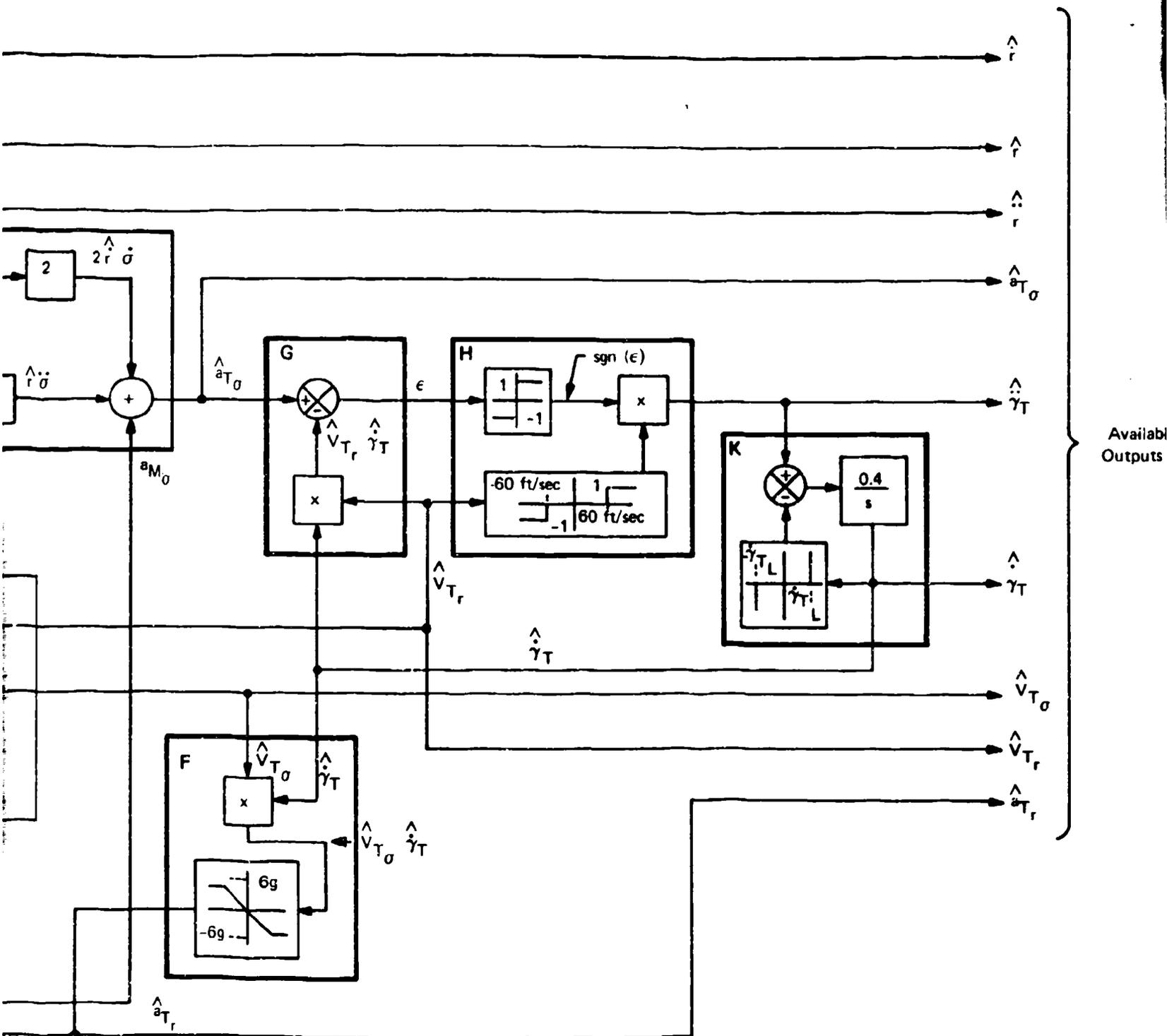
Figure 4.1. Range and Range-Rate Estimator Configuration

27

4.2 Error Analysis

The true value of the range acceleration is

$$\ddot{r} = r\dot{\sigma}^2 - a_{M_r} + a_{T_r} .$$

and we have shown that

$$a_{T_r} = \dot{V}_T \cos \xi_T - V_T \dot{\gamma}_T \sin \xi_T = (V_T \dot{V}_T - V_{T_\sigma} a_{T_\sigma})/V_{T_r}$$

where $V_{T_r} = V_T \cos \xi_T = \dot{r} + V_M \cos \xi_M$

$$V_{T_\sigma} = V_T \sin \xi_T = r\dot{\sigma} + V_M \sin \xi_M$$

and $a_{T_\sigma} = \dot{V}_T \sin \xi_T + V_T \dot{\gamma}_T \cos \xi_T = r\ddot{\sigma} + 2\dot{r}\dot{\sigma} + a_{M_\sigma} .$

Disregarding the effects of target velocity-change $\dot{V}_T$, the algorithm estimates a_{T_r} as

$$\hat{a}_{T_r} = - \frac{(\hat{r}\dot{\sigma} + \hat{V}_M \sin \hat{\xi}_M)}{(\hat{\dot{r}} + \hat{V}_M \cos \hat{\xi}_M)} (\hat{r}\ddot{\sigma} + 2 \hat{\dot{r}}\dot{\sigma} + a_{M_\sigma}), \tag{4.23}$$

imposing limits on $|\hat{a}_{T_r}|$, $|\hat{\dot{\gamma}}_T|$, and $|\hat{\ddot{\gamma}}_T|$ in the process.

We consider in this section the several sources of error and their significance. The principal sources of error are discussed below.

(1) $\dot{V}_T$. The target may change its airspeed, although relatively slowly.

(2) $\hat{r}_o$, $\hat{\dot{r}}_o$. Range and range-rate may be initialized with errors.

28

(3) $\hat{V}_M$. The missile airspeed is required. It may be sensed or may be provided adaptively, but with an error in either case.

(4) $\hat{\xi}_M$. The missile angle of attack must be estimated to form $\hat{\xi}_M = -\alpha - \lambda$ in order to resolve the missile velocity into the components $V_M \sin \xi_M$ and $V_M \cos \xi_M$. Errors enter as incorrect estimates of λ and α, as discussed in the simulation results. The angle λ is the angle from the missile centerline to the seeker centerline.

(5) $\dot{\sigma}$. The LOS rate may have random noise errors plus a bias.

(6) a_{M_r}, a_{M_σ}. The accelerometers sensing missile acceleration parallel and perpendicular, respectively, to the LOS may have bias errors and random noise.

We define $x = r - \hat{r}$, $\dot{x} = \dot{r} - \dot{\hat{r}}$, $\ddot{x} = \ddot{r} - \ddot{\hat{r}}$, so that x is the range error, and $V_i = \hat{V}_i + N_i$ where

$$V_1 = a_{M_r}$$

$$V_2 = 0; \quad N_2 = \dot{V}_T; \quad \text{shows } \dot{V}_T \neq 0$$

$$V_3 = V_M$$

$$V_4 = \dot{\sigma}$$

$$V_5 = \xi_M$$

$$V_6 = \ddot{\sigma}$$

$$V_7 = a_{M_\sigma}$$

Thus, N_i represents the deviation from the actual value of V_i, i.e., the additive noise. The error $x(t)$ is then governed by the equation

$$\ddot{x} + a_1(t)\dot{x} + a_2(t)x = \sum_{i=1}^{7} b_i(t)N_i \qquad (4.24)$$

where the coefficients a_i, b_i are defined as

$$a_1 = 2\dot{\sigma}\tan\xi_T - \dot{\gamma}_T\tan\xi_T$$

$$a_2 = -\dot{\sigma}^2 + \dot{\gamma}_T\dot{\sigma} + \ddot{\sigma}\tan\xi_T$$

$$b_1 = -1$$

$$b_2 = \sec\xi_T$$

$$b_3 = -\dot{\gamma}_T\sec\xi_T\sin(\gamma_M-\gamma_T)$$

$$b_4 = -r\dot{\gamma}_T - 2\dot{r}\tan\xi_T + 2r\dot{\sigma}$$

$$b_5 = -V_M\dot{\gamma}_T\sec\xi_T\cos(\gamma_M-\gamma_T)$$

$$b_6 = -r\tan\xi_T$$

$$b_7 = -\tan\xi_T .$$

The coefficients of x and $\dot{x}$ are functions of time. The trajectory of the errors of range estimate, x, and range-rate estimate, $\dot{x}$, may be found by solving this linear differential equation with time-varying coefficients, subject to the initial conditions x_o and $\dot{x}_o$, which are the assumed initialization errors of range and range rate. As (4.24) is linear, super-position is valid so that it may be solved for the individual terms. The coefficients a_i and b_i are tabulated in Appendix B for a number of typical trajectories.

4.3 Performance

The air-air missile homing situation was programmed on the digital computer. The simulation used parameters from a typical short-range highly maneuverable air-air missile. The guidance method used for the simulation was the conventional proportional guidance:

$$a_c = 5 \, V_M \, \dot\sigma,$$

where $\dot\sigma$ is the LOS angular inertial rate and a_c is the acceleration command across the LOS. The transfer function describing the missile characteristics was

$$\frac{a(s)}{a_c(s)} = \frac{-53s^2 + 106.6s + 27000}{s^3 + 72s^2 + 2160s + 27000}$$

where a is the cross-body acceleration. This corresponds to a simplified and linearized second order model for the missile airframe combined with a first order model for actuator lag. The estimates of range and range-rate were thus not used in the guidance loop as they might be in an actual missile system. The missile was started with a specified velocity with the airframe state variables at rest at the beginning of the trajectory. The geometry of the combat situation is shown in Fig. 4.2.

A discretization step size of .005 seconds was found to result in negligible error in the numerical output of the digital program as a substitute for the actual continuous model airframe being analyzed.

30
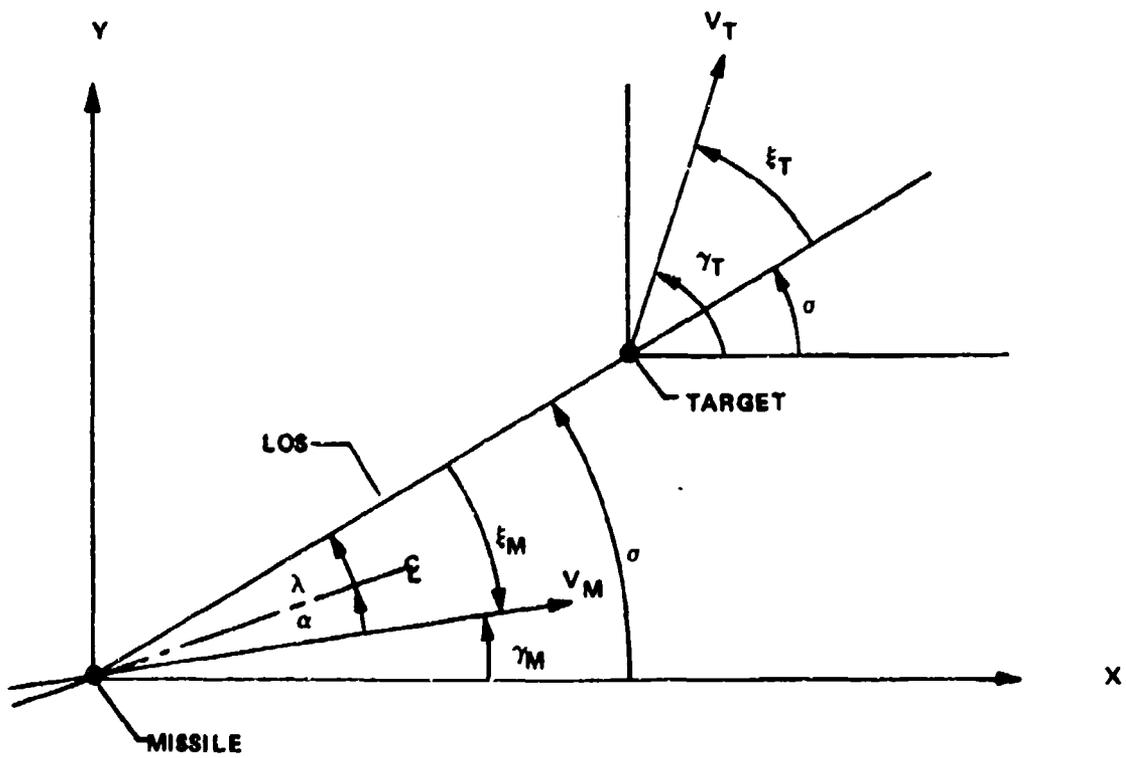
Figure 4-2. Definition of Positive Geometric Angles

Several different geometrical situations were simulated, corresponding to different angular orientations and bank angle of the target. Missile velocity was Mach 2.0 or 2144 ft/sec at 10,000 ft. altitude, and target velocity 1,000 ft/sec. The missile airspeed was assumed constant; this does not restrict the generality of the results.

The simulations which follow are arranged in ten groups, each corresponding to a different starting situation. The angle ϕ_T is defined as the bank angle of the target. For example, $80°$ represents a hard left turn of approximately 5.7 g's lateral acceleration. The angle Ψ_T represents the target's initial heading, measured positive counter-clockwise from a reference heading parallel to the attacking missile's initial centerline, which is the x-axis.

Most of the ten groupings of plots have six separate graphs, arranged in pairs on facing pages.

The first graph is a view looking down at the two dimensional chase. In each case the target is intercepted as a result of the homing navigation. This also shows initial physical orientation of the target. Connecting the missile and target at corresponding successive instants of time are dashed lines representing the position of the line-of-sight (LOS) as the chase evolves.

The second graph shows the actual values of range, range-rate, and range-acceleration as functions of time,

from t = 0 to t = time-of-intercept. These variables represent the true values of the parameters which are estimated.

Graphs 3 and 4 in the group plot the errors in the range estimate due to various error sources. The plot lettered (a) has no error sources and represents the good estimates of range and range-rate obtainable with this method. The reason (a) is not identically zero arises from the inaccuracies of the algorithm and computation; it is intended as a control in analyzing the other graphs. The other plots show the effects of various errors. For example, in plot (b) range is initialized incorrectly at 99% of its actual value. A listing of the sources of error is as follows:

(a) No errors, except those inherent to the algorithm itself.

(b) Range initialized with 1% error.

(c) Range-rate initialized with 1% error.

(d) The signal $\dot{\sigma}$ is erroneously biased by the amount 0.5 deg/sec.

(e) The signal G, the lateral accelerometer output, is biased by 3 ft/sec^2.

(f) The signal H, the longitudinal accelerometer output, is biased by 3 ft/sec^2.

(g) The seeker angle relative to the missile centerline, λ, is biased by 0.1 degrees.

(h) The error in measuring missile velocity V_M, is taken as 1% or 21.44 ft/sec.

33

(i) The error in estimating angle of attack, α, was taken to be a bias of 1 degree.

(j) In this case the target velocity is increased with an acceleration of 1g, thus illustrating the effect of violating the assumption $\dot{V}_T = 0$.

In all cases, only the particular source of error mentioned was included, i.e., the other error sources were removed.

Graphs 3 shows the errors from sources (a) through (e) above. Graph 4 shows error sources (f) through (j).

In the case of Figure 4.6, an additional source of error is analyzed. Figure 4.6.4 shows the effect of additive noise in the LOS rate as used by the kinematic ranging algorithm. The corrupted LOS rate was also fed to the guidance loop.

Graphs 5 and 6 of each group show the corresponding errors in range-rate instead of the error in range. Separation of cases (a) through (j) is the same as above in graphs 3 and 4.

Figure 4.12 is also an exception to the format specified. This figure displays the geometry when the target changes its maneuver during the flight of the missile. The target starts with a turn to the left, changing to a turn to the opposite direction of equal magnitude.

Figure 4.12.2 shows both the error in range and range-rate from the estimation algorithm. This error represents the numerical accuracy of the algorithm, and is not due to other sources.
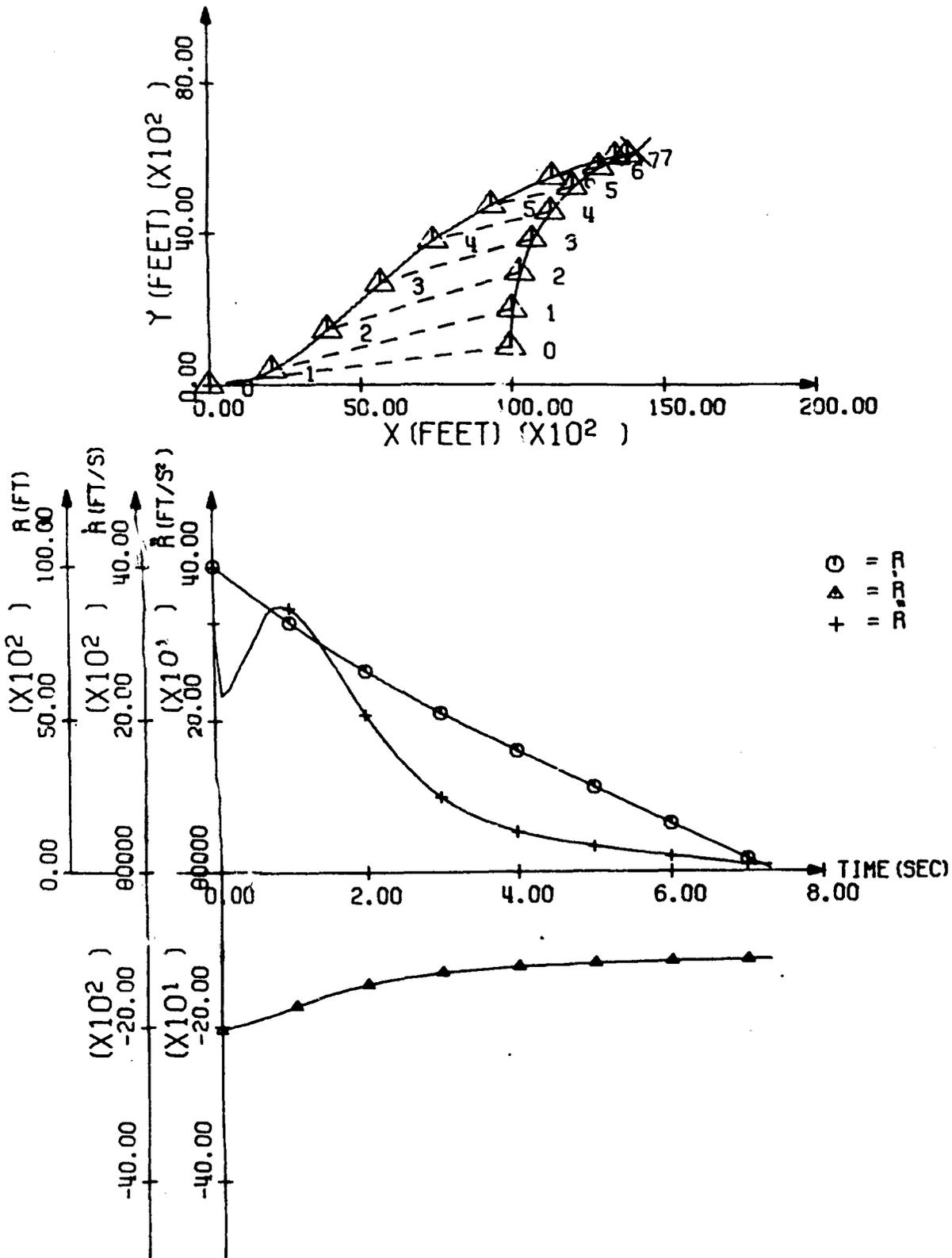
FIG. 4.3.1 DYNAMIC RANGING SIMULATION WITH
TARGET INITIAL CONDITIONS. $\dagger$=90 , Φ= -80 XT = 10000 ,
YT = 1000. PLOTS OF VARIABLES DEFINING GEOMETRY

31

FIGURE 4.3

Graph 1, the upper graph to the left, shows the plan view of the geometry of the missile chase. The target has an initial range of slightly more than 10,000 ft., and initially is traveling across the LOS. The target airplane undergoes a 5.7g constant right turn which is indicated by the bank angle $\phi_T = -80^\circ$.

Graph 2, bottom left, plots actual range, range-rate, and range-acceleration. One may note the decrease in magnitude of range-rate as the chase changes from a side attack to a tail chase.

Graphs 3 and 4, top and bottom immediate right on the facing foldout page, show the errors in the range estimate due to various error sources for the geometry described above.

Curve (a) represents no errors except those due to the computation process and shows the ability to track the target when perfect signals are used in the algorithm. Maximum error for range is approximately 5 ft. Curves (b) thru (j), on Graphs 3 and 4 represent the effects of the error sources specified in Section 4.3.

Graphs 5 and 6, on the far right of the facing page display the errors in range-rate from the error sources. Curves (a) thru (j) again correspond to the errors mentioned in Section 4.3. Curve (a) shows a maximum error of 3 ft/sec.

Curves (j) on Graphs 4 and 6 represent the largest errors, and appear reasonable since the basic assumption of the algorithm ($\dot{V}_T=0$) is violated. Curve (j) thus shows the error due to target airspeed changes, reading a maximum range-error of 350 feet.

For convenience, the labels a...j in the curves imply:

a. no error sources

b. 1% error in $\hat{r}(0)$

c. 1% error in $\hat{\dot{r}}(0)$

d. 0.5° bias in $\dot{\sigma}$

e. 0.1 g bias in a_{M_σ}

f. 0.1 g bias in $a_{M_{r'}}$

g. 0.1° bias in seeker gimbal angle

h. 20 ft/s bias in $\hat{V}_M$

i. 1° error in $\hat{\alpha}$

j. $\dot{V}_T = 1$ g

FIG. 4.3.2 DYNAMIC RANGING SIMULATION WITH
TARGET INITIAL CONDITIONS. ¥=90 , Φ= -80 XT = 10000 .
ΓΤ = 1000 . ERRORS IN RANGE ESTIMATE FROM VARIOUS
SOURCES

FIG. 4
TARGET I
YT = 100

FIG. 4.3.3 DYNAMIC RANGING SIMULATION WITH
TARGET INITIAL CONDITIONS. Ψ=90, Φ= -80 XT =10000,
YT =1000. ERRORS IN RANGE RATE ESTIMATE FROM
VARIOUS SOURCES

FIG. 4.4.1 DYNAMIC RANGING SIMULATION WITH
TARGET INITIAL CONDITIONS. ψ=90 , Φ= 0 , XT =10000 ,
YT = 1000 . PLOTS OF VARIABLES DEFINING GEOMETRY

FIGURE 4.4

This grouping of curves shows a non-maneuvering target, with initial heading $90°$ relative to the attacking missile's centerline. In this situation, the LOS rate approaches zero after the missile response to the guidance. As a result, one can say in general that errors in the estimates will tend to grow large after LOS rate gets small. This is somewhat apparent to the curves on the right. It is also noted that curves (a) are not small compared to the others, as was observed in Figure 3. This is explained by the same reason, namely, that when neither the target nor missile maneuver, the estimation of range and range rate is difficult and more sensitive to computation error. The algorithm exhibits moderate sensitivity to initial range error and to accelerometer biasses.

a. no error sources

b. 1% error in $\hat{r}$ (0)

c. 1% error in $\hat{\dot{r}}$ (0)

d. $0.5°$ bias in $\dot{\sigma}$

e. 0.1 g bias in a_{M_σ}

f. 0.1 g bias in a_{M_r}

g. $0.1°$ bias in seeker gimbal angle

h. 20 ft/s bias in $\hat{V}_M$

i. $1°$ error in $\hat{\alpha}$

j. $\dot{V}_T$ = 1 g

FIG. 4.4.2 DYNAMIC RANGING SIMULATION WITH
TARGET INITIAL CONDITIONS. Ψ=90 , Φ= 0 , XT = 10000 ,
YT = 1000. ERRORS IN RANGE ESTIMATE FROM VARIOUS
SOURCES

37

FIG. 4.4.3 DYNAMIC RANGING SIMULATION WITH
TARGET INITIAL CONDITIONS. $\psi = 90$, $\phi = 0$, $XT = 10000$,
$YT = 1000$. ERRORS IN RANGE RATE ESTIMATE FROM
VARIOUS SOURCES

37

FIG. 4 .4 .1 DYNAMIC RANGING SIMULATION WITH.
TARGET INITIAL CONDITIONS. ᵼ=90 , Φ= 0 , XT = 10000 ,
YT = 1000 . PLOTS OF VARIABLES DEFINING GEOMETRY

36

FIGURE 4.5

Figure 4.5 shows the target with an initial heading of 90° relative to the missile centerline, and a bank angle of 80°, implying a hard turn to the left. With this configuration, the aspect angle ξ_T is close to 90° at all times, in fact it passes through 90°. The error analysis equation predicts that the estimates would be extremely sensitive in this case. However, the nonlinearity in sensing the sign of V_{T_r}, which is not considered in the error analysis equation, prevents the estimates from becoming sensitive, and in fact the errors from all sources are only slight; this can be observed on the curves to the right.

a. no error sources   f. 0.1 g bias in a_{M_r}

b. 1% error in $\hat{r}$ (0)   g. 0.1° bias in seeker gimbal angle

c. 1% error in $\hat{\dot{r}}$ (0)   h. 20 ft/s bias in $\hat{V}_M$

d. 0.5° bias in $\dot{\sigma}$ i. 1° error in $\hat{\alpha}$

e. 0.1 g bias in a_{M_σ} j. $\dot{V}_T = 1$ g

Without the dead space in Block H of Fig. 4.1, the estimator would be unstable, see Fig. 4.5.4 below.

FIG. 4.5.4 DYNAMIC RANGING SIMULATION WITH
TARGET INITIAL CONDITIONS. Ψ=90 , Φ= 80 , XT = 10000 ,
YT = 1000 . ERRORS IN RANGE ESTIMATE & RANGE RATE ESTIMATE
FROM VARIOUS SOURCES

FIG. 4.5.2 DYNAMIC RANGING SIMULATION WITH
TARGET INITIAL CONDITIONS. $\Psi = 90$, $\Phi = 80$, XT = 10000.
YT = 1000. ERRORS IN RANGE ESTIMATE FROM VARIOUS
SOURCES

FIG. 4.5.3 DYNAMIC
TARGET INITIAL CONDITI
YT = 1000. ERRORS IN R

39

FIG. 4.5.3 DYNAMIC RANGING SIMULATION WITH
TARGET INITIAL CONDITIONS. $\psi = 90$, $\phi = 80$, $XT = 10000$,
$YT = 1000$. ERRORS IN RANGE RATE ESTIMATE FROM
VARIOUS SOURCES

FIG. 4.6.1 DYNAMIC RANGING SIMULATION WITH
TARGET INITIAL CONDITIONS. $\dot{\gamma}$=0 , Φ= 80, XT = 10000,
rT = 1000. PLOTS OF VARIABLES DEFINING GEOMETRY

FIGURE 4.6

This shows the target with an initial relative heading of $0°$, and a bank angle of $80°$. The largest error appears to occur for case (j), target airspeed change, in agreement with previously explained simulations. The other significant error source, (d), is LOS rate bias.

FIGURE 4.6.4, below, shows the errors when noise is added to the LOS rate, instead of the fixed bias present in curve (d). This random noise was constructed to have zero mean and standard deviation equal to 5.0/Range; thus the noise becomes quite large as range decreases.

a. no error sources   f. 0.1 g bias in a_{M_r}

b. 1% error in $\hat{r}$ (0)   g. $0.1°$ bias in seeker gimbal angle

c. 1% error in $\hat{\dot{r}}$ (0)   h. 20 ft/s bias in $\hat{V}_M$

d. $0.5°$ bias in $\dot{\sigma}$ i. $1°$ error in $\hat{\alpha}$

e. 0.1 g bias in a_{M_σ} j. $\dot{V}_T = 1$ g
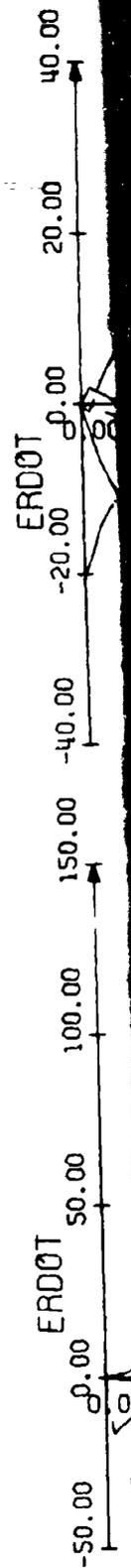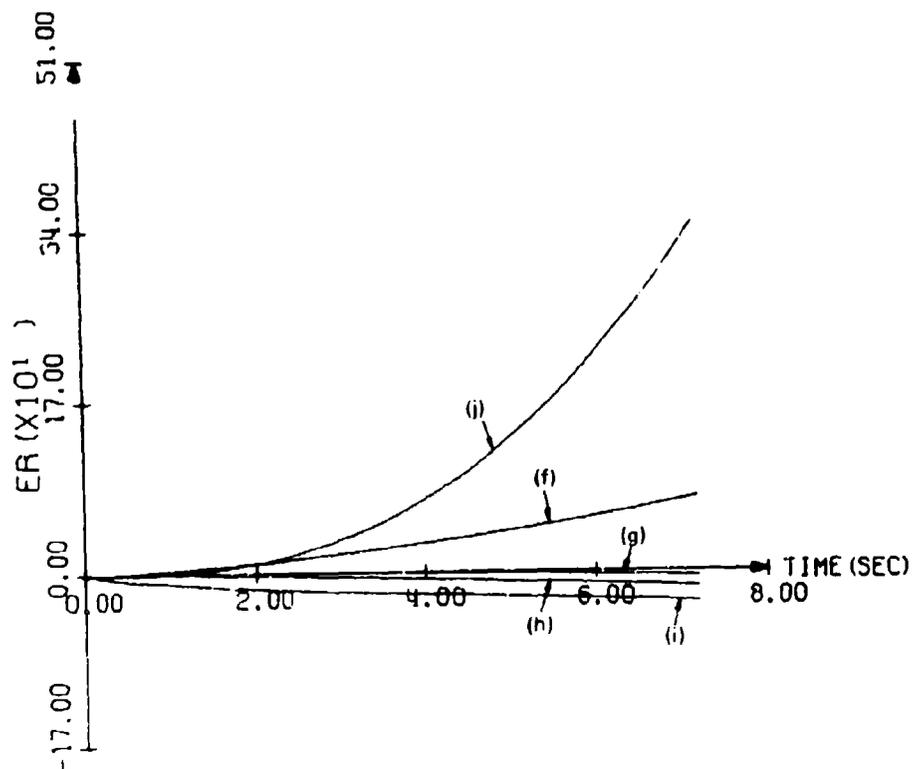

FIG. 4.6.4 DYNAMIC RANGING SIMULATION WITH TARGET INITIAL CONDITIONS. $\psi = 0$, $\phi = 80$,   XT = 10000, YT = 1000. ERRORS IN ESTIMATE WITH NOISE PRESENT IN LOS RATE.
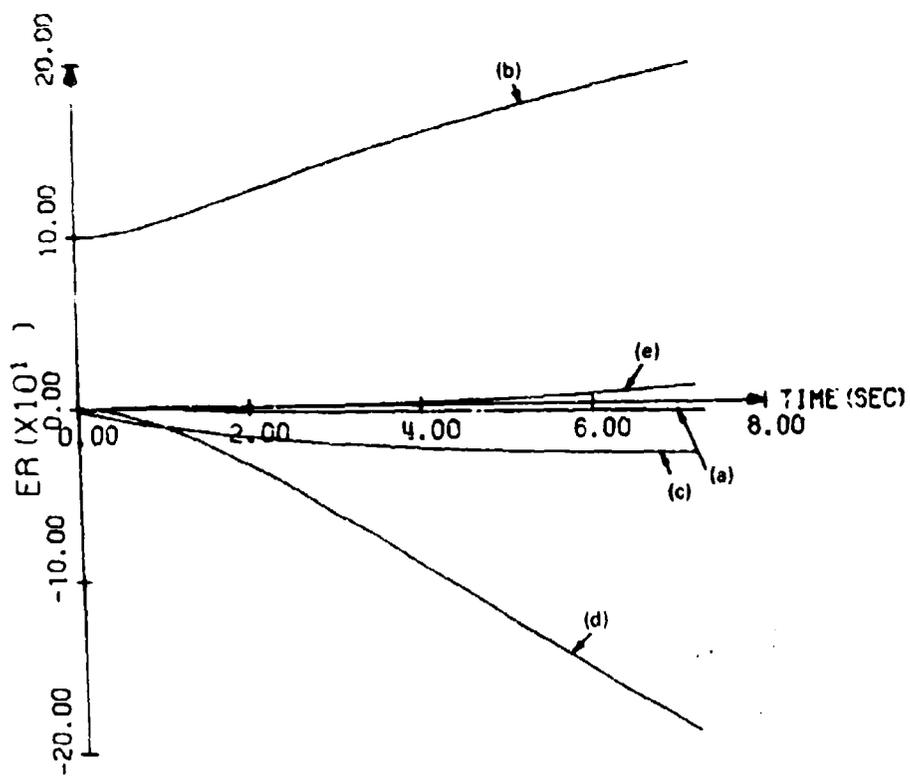
FIG. 4.6.2 DYNAMIC RANGING SIMULATION WITH
TARGET INITIAL CONDITIONS. ψ=0 , Φ= 80, XT = 10000 .
C = 1000. ERRORS IN RANGE ESTIMATE FROM VARIOUS
SOURCES
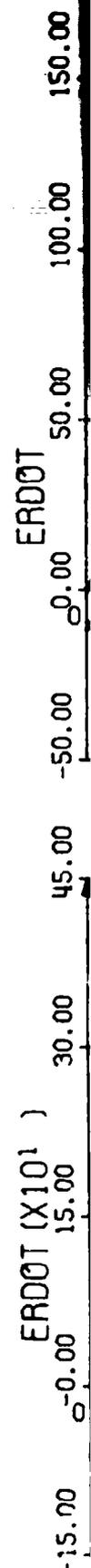
FIG.
TARGET
YT = 1

FIG. 4.6.3 DYNAMIC RANGING SIMULATION WITH
TARGET INITIAL CONDITIONS. ᵛ=0 , ᵠ= 80. XT = 10000 .
YT = 1000. ERRORS IN RANGE RATE ESTIMATE FROM
VARIOUS SOURCES
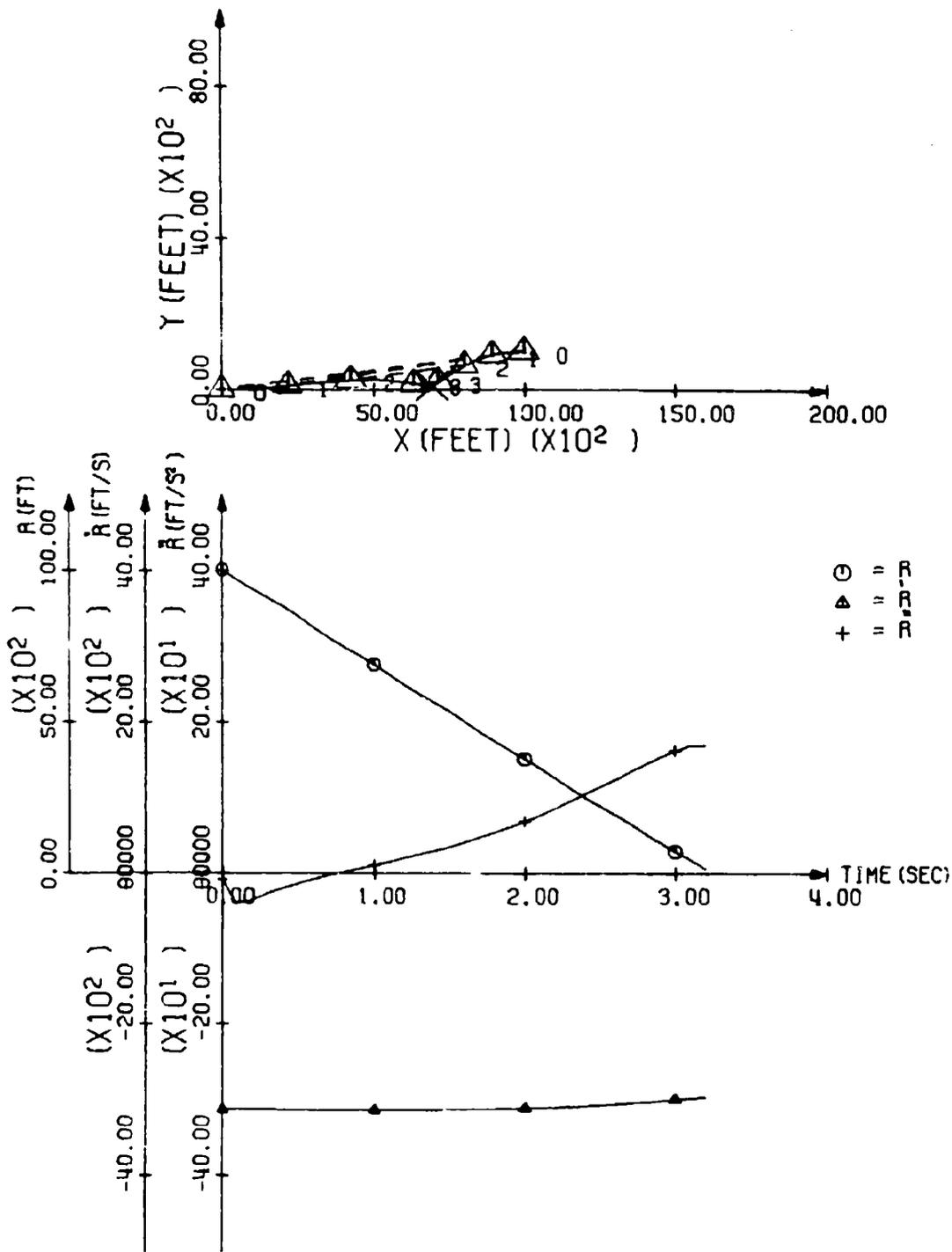
FIG. 4.7.1 DYNAMIC RANGING SIMULATION WITH
TARGET INITIAL CONDITIONS. ✦=180, Φ= 80, XT = 10000,
YT = 1000. PLOTS OF VARIABLES DEFINING GEOMETRY

targ
clos
rema
that
dive
that
rang
airs

42

FIGURE 4.7

This geometry displays a head-on situation where the target and missile are approaching each other with maximum closure rate. The target is turning left. Error curve (a) remains small. Curve (b) is worthy of note, as it demonstrates that an error in initial range estimate need not lead to divergence of the range-rate estimate. Curve (c) shows readily that an error in range-rate leads to an increasing error in range. Curve (j) again shows the largest errors, due to target airspeed change.

a. no error sources

b. 1% error in $\hat{r}$ (0)

c. 1% error in $\hat{\dot{r}}$ (0)

d. 0.5° bias in $\dot{\sigma}$

e. 0.1 g bias in a_{M_σ}

f. 0.1 g bias in a_{M_r}

g. 0.1° bias in seeker gimbal angle

h. 20 ft/s bias in $\hat{V}_M$

i. 1° error in $\hat{\alpha}$

j. $\dot{V}_T = 1$ g

FIG. 4.7.2 DYNAMIC RANGING SIMULATION WITH
TARGET INITIAL CONDITIONS. +=180, Φ= 80, XT = 10000 .
rt = 1000. ERRORS IN RANGE ESTIMATE FROM VARIOUS
SOURCES

43

FIG.
TARGET
YT = 1
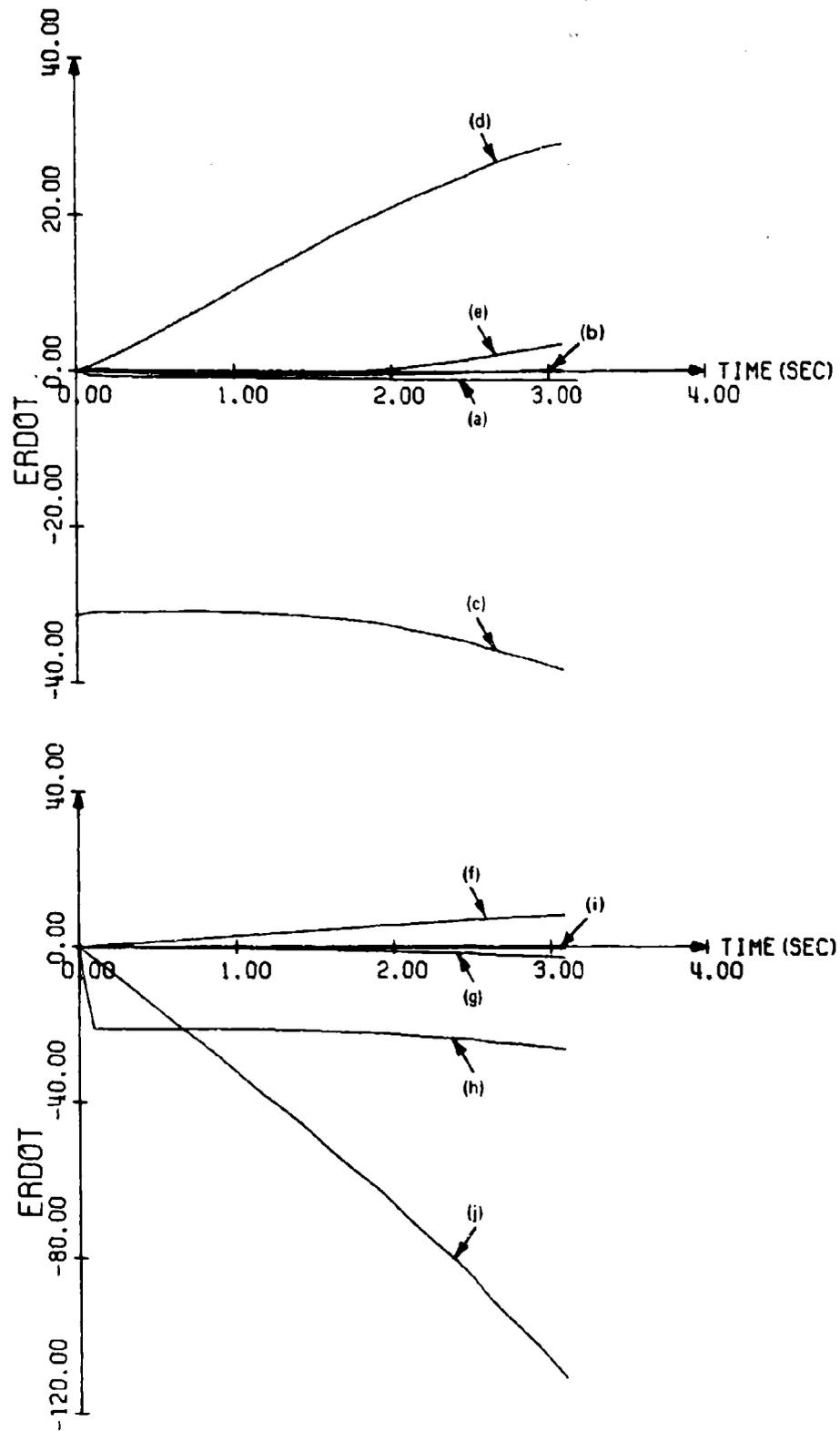
FIG. 4.7.3 DYNAMIC RANGING SIMULATION WITH
TARGET INITIAL CONDITIONS. $\Psi=180$, $\Phi=80$, XT = 10000,
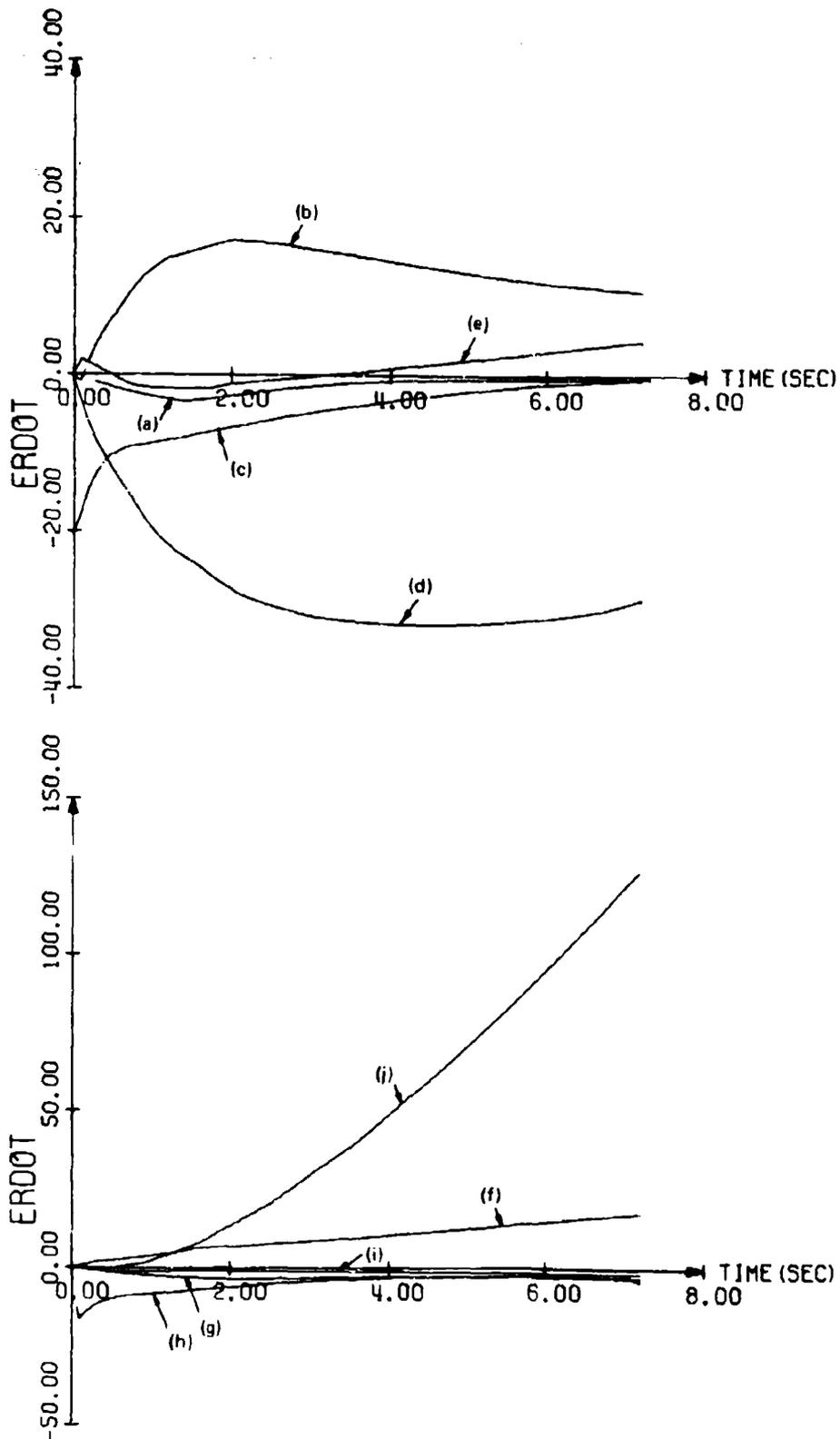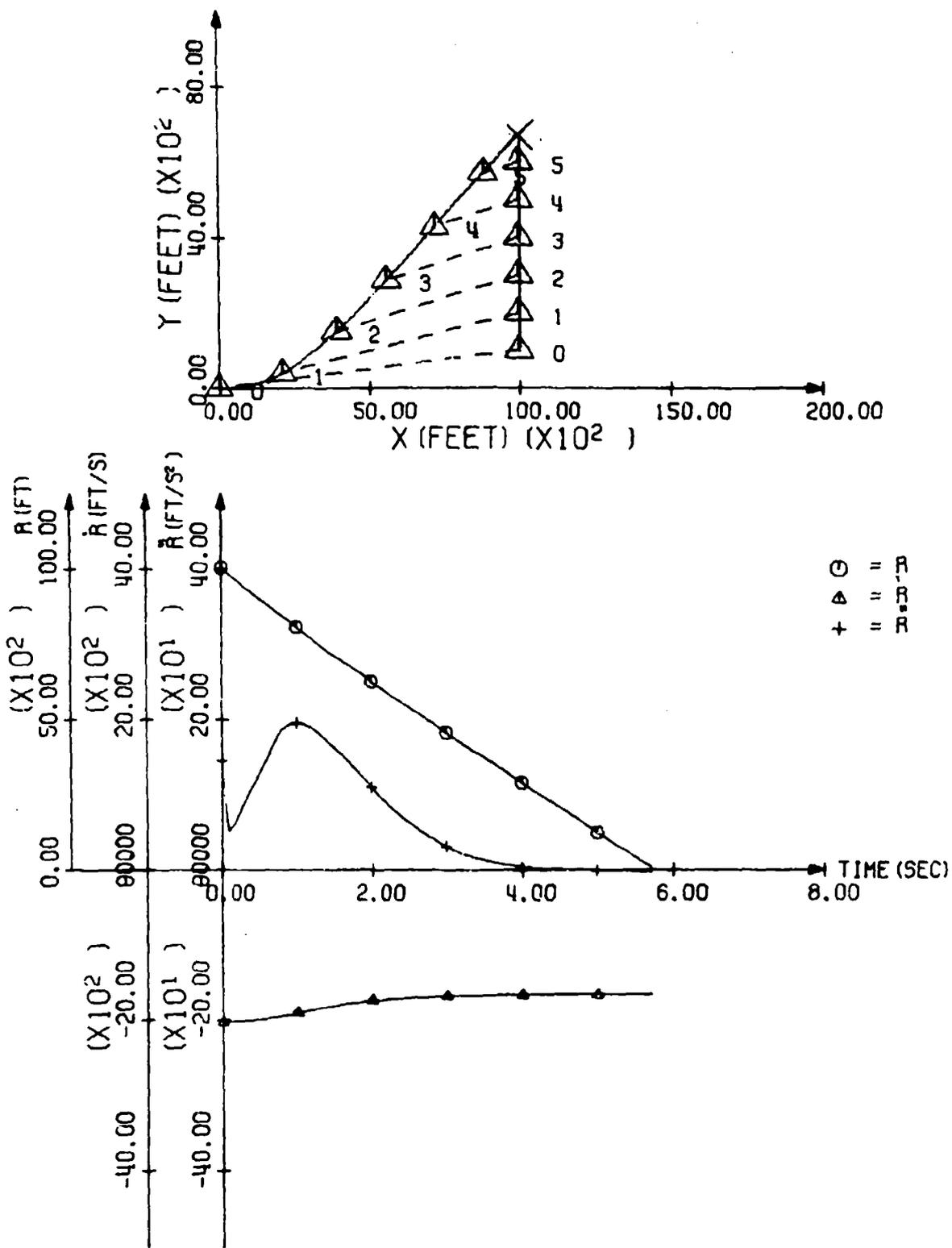YT = 1000. ERRORS IN RANGE RATE ESTIMATE FROM
VARIOUS SOURCES

43
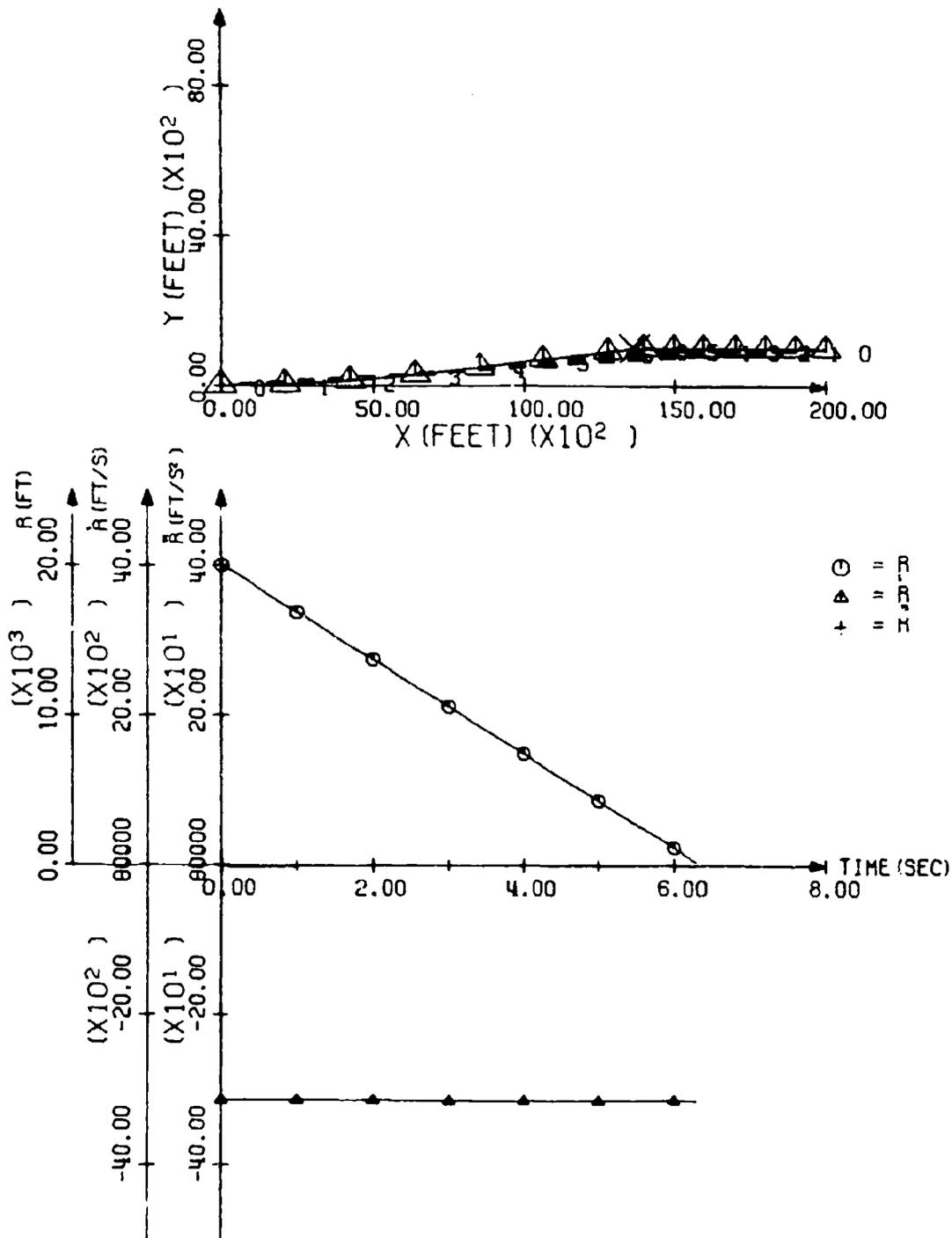
FIG. 4.8.1 DYNAMIC RANGING SIMULATION WITH
TARGET INITIAL CONDITIONS. ✦=180, Φ= 0 , XT = 20000,
YT = 1000. PLOTS OF VARIABLES DEFINING GEOMETRY

FIGURE 4.8

The figure shows a head-on situation, with the target
initially at slightly more than 20,000 feet range, flying
straight (no turn rate). Range-rate is quite constant, and
range acceleration is negligible and barely discernible
from the time axis. Errors in the estimates are very small
except for a few cases. Curve (c) again shows that a con-
stant range-rate error leads to an increasing range error.
Again, the range error in curve (b) does not lead to a range-
rate error. Curves (j) show the largest errors.

a. no error sources

b. 1% error in $\hat{r}$ (0)

c. 1% error in $\hat{\dot{r}}$ (0)

d. 0.5° bias in $\dot{\sigma}$

e. 0.1 g bias in a_{M_σ}

f. 0.1 g bias in a_{M_r}

g. 0.1° bias in seeker gimbal angle

h. 20 ft/s bias in $\hat{V}_M$

i. 1° error in $\hat{\alpha}$

j. $\dot{V}_T = 1$ g
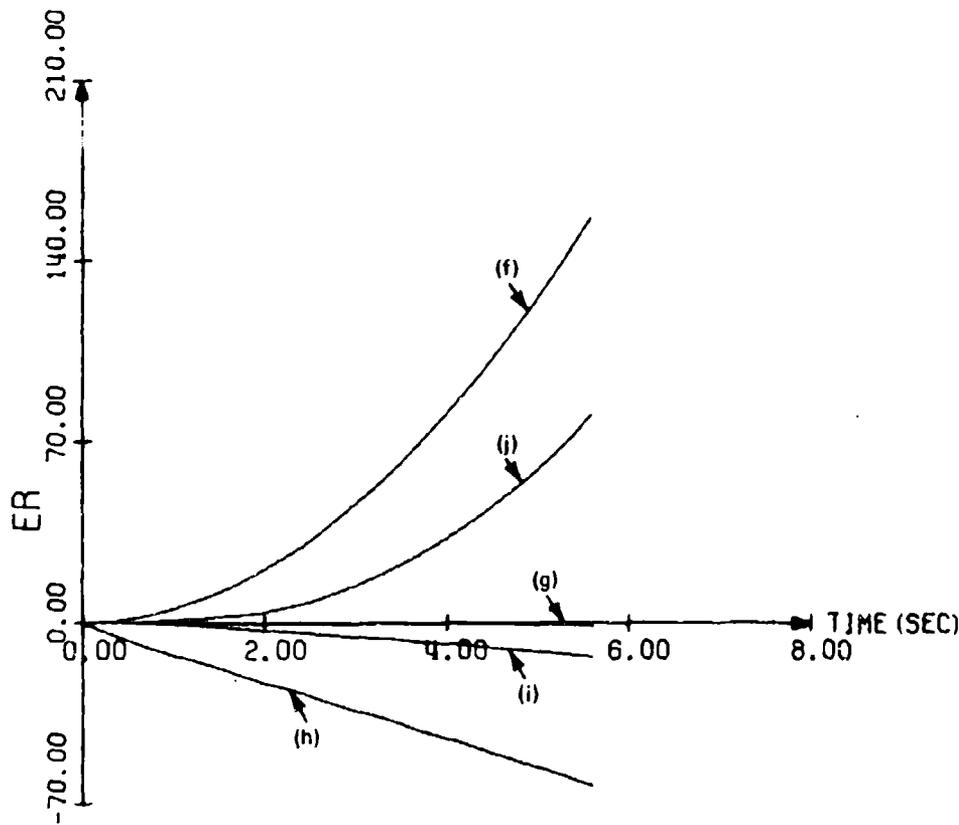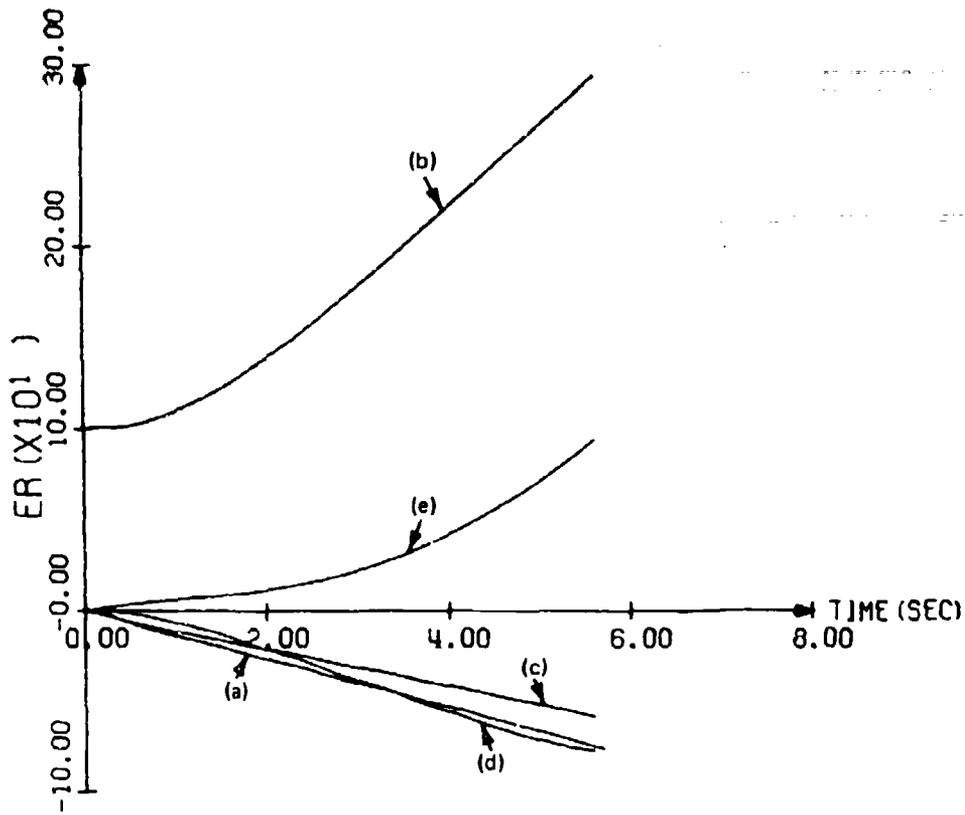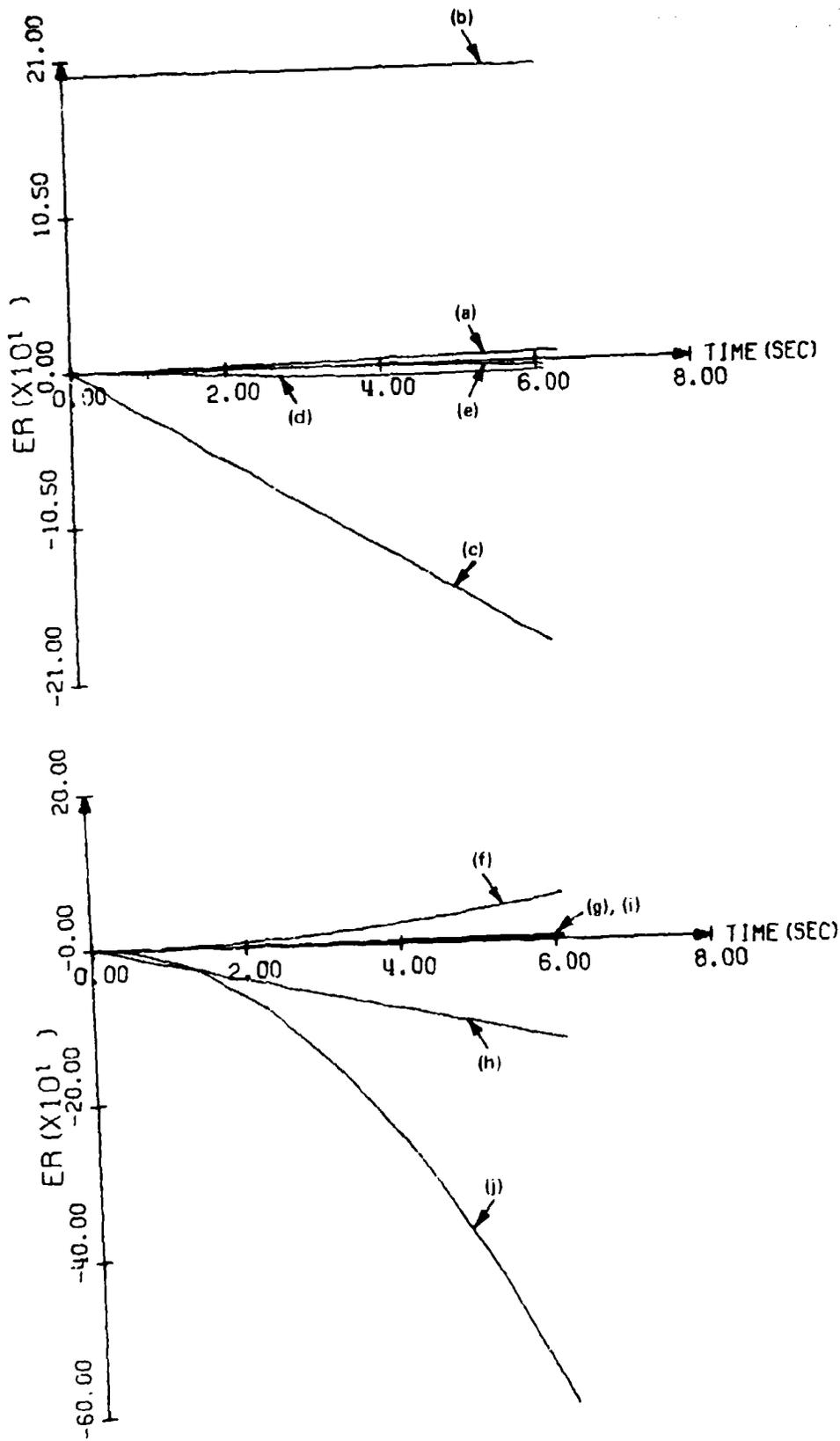
FIG. 4.8.2 DYNAMIC RANGING SIMULATION WITH
TARGET INITIAL CONDITIONS. ᵠ=180, Φ=0 , XT =20000,
YT = 1000. ERRORS IN RANGE ESTIMATE FROM VARIOUS
SOURCES

FIG. 4
TARGET
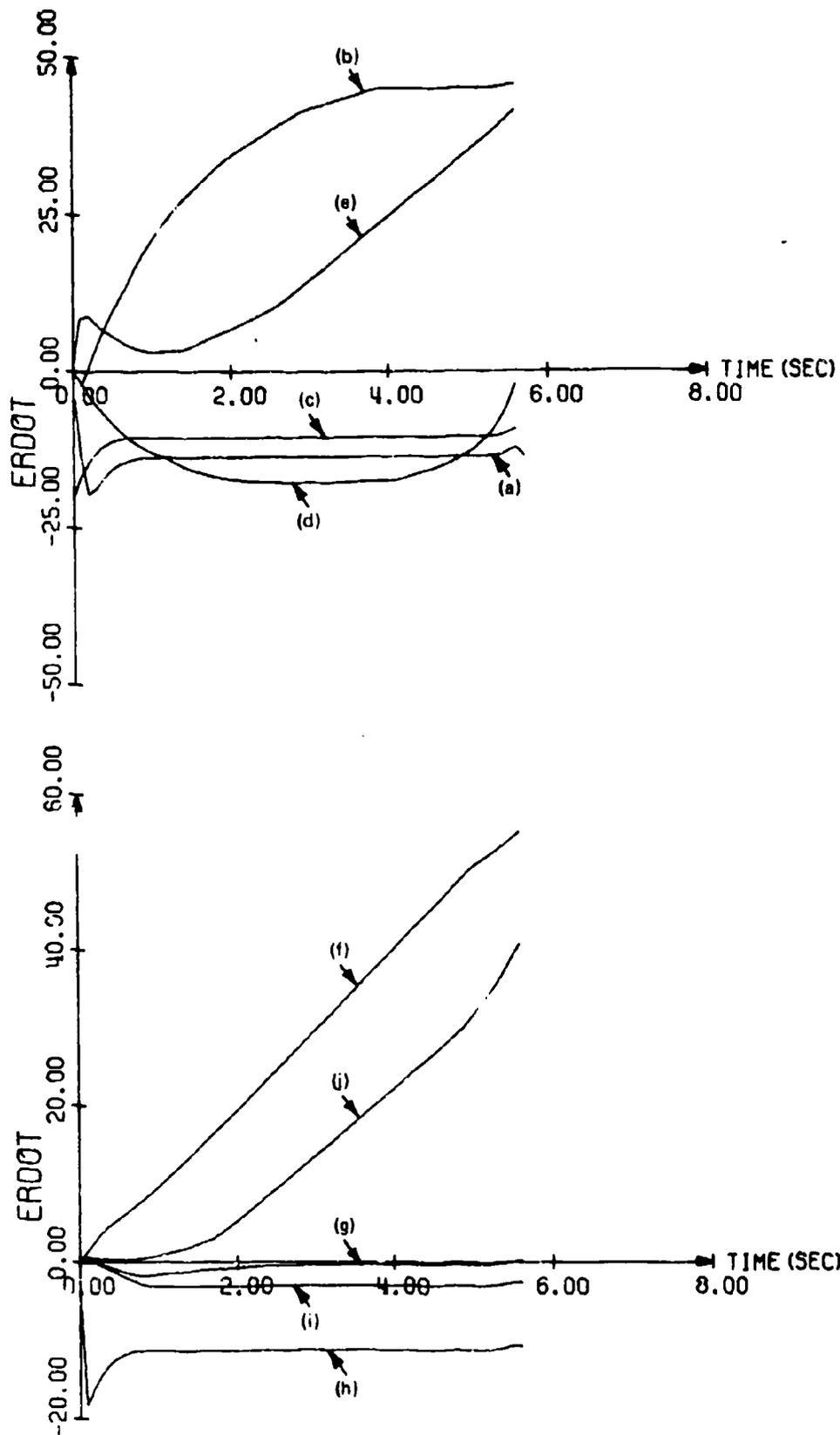YT = 100

45
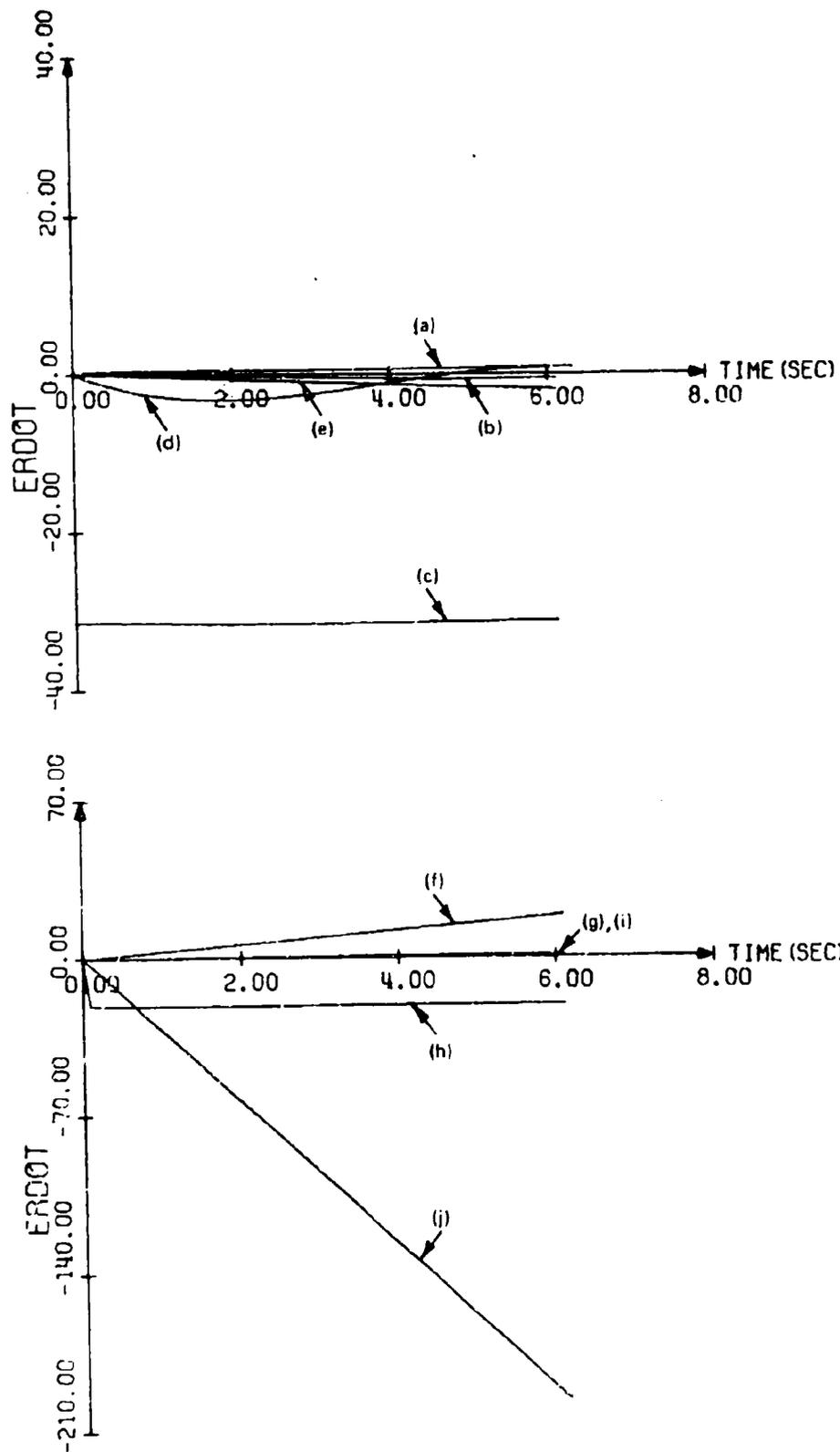
FIG. 4.8.3 DYNAMIC RANGING SIMULATION WITH TARGET INITIAL CONDITIONS. ⍦=180, ⏀= ⌐ . XT = 20000, YT = 1000. ERRORS IN RANGE RATE ESTIMATE FROM VARIOUS SOURCES
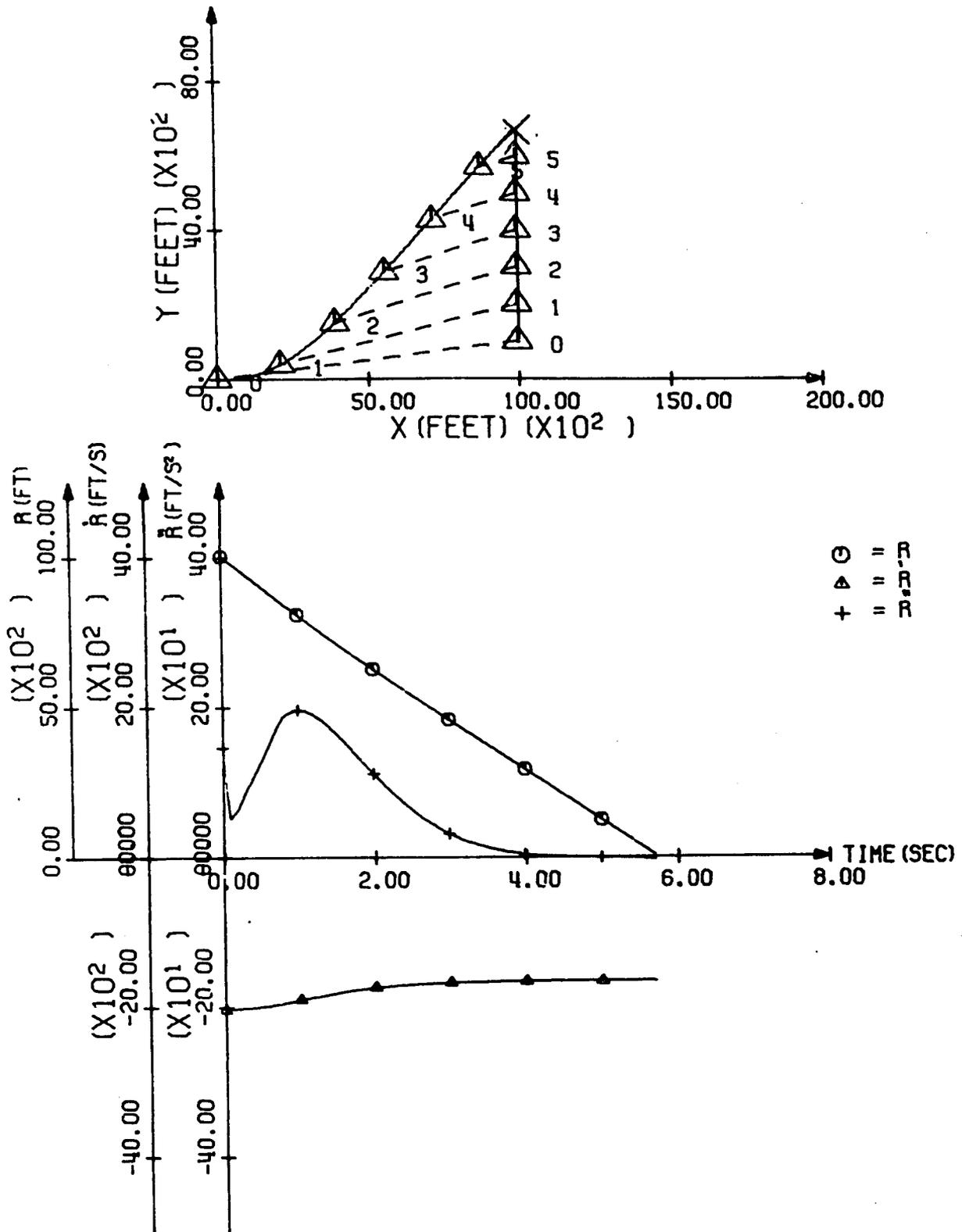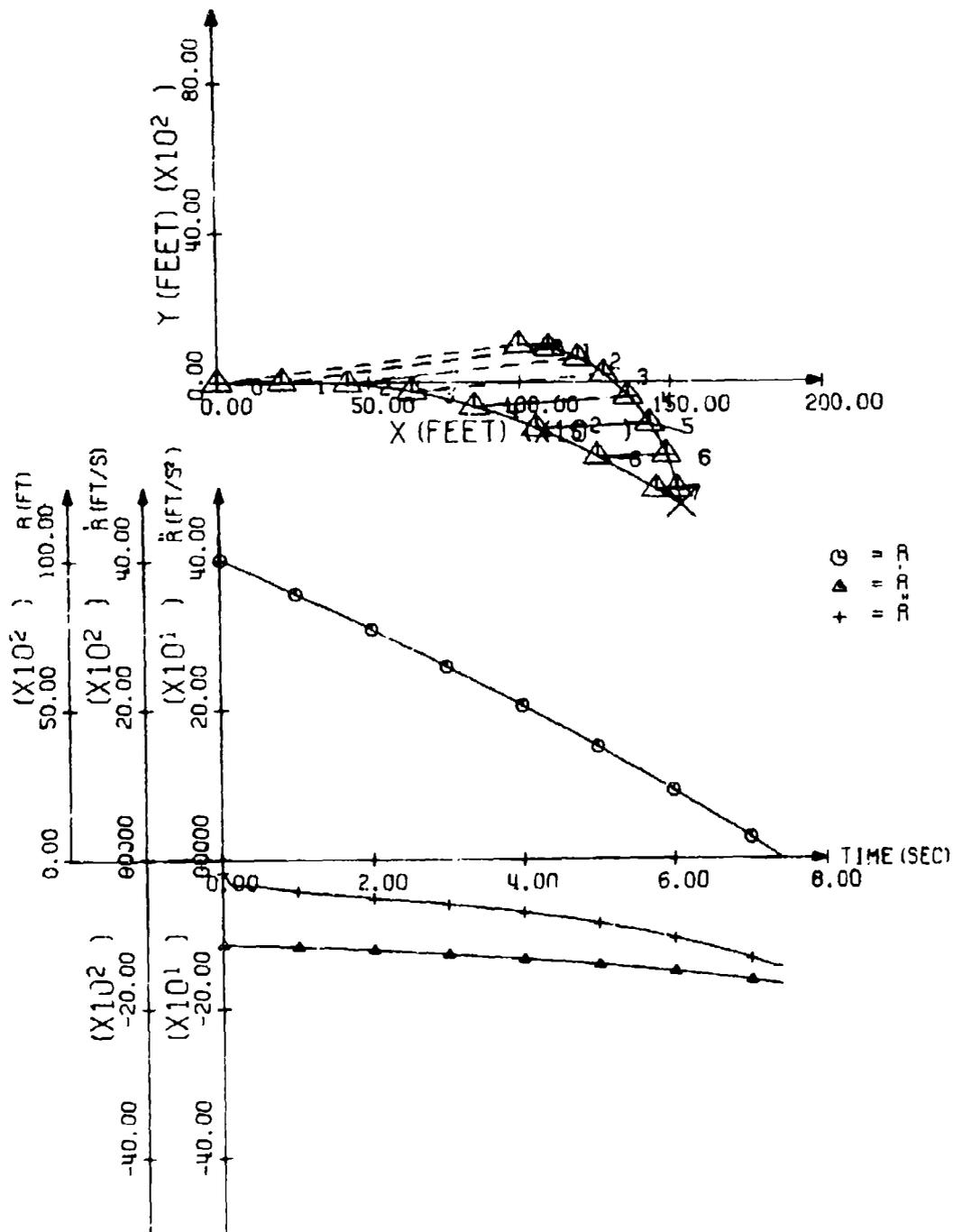
FIG. 4.9.1 DYNAMIC RANGING SIMULATION WITH
TARGET INITIAL CONDITIONS. ⊽=0 , ϕ=-80, XT = 10000 ,
YT = 1000. PLOTS OF VARIABLES DEFINING GEOMETRY

FIGURE 4.9

This figure has target heading 0°, and bank angle -80°.
Thus pursuit starts as a tail chase, and ends with a rear-side
attack. Target initial range is slightly more than 10,000 ft.
The estimate errors generally follow the same pattern established
in previous trajectories, with the largest error sources being
$\dot{\sigma}$ bias (d) and target airspeed change (j).

a. no error sources

b. 1% error in $\hat{r}$ (0)

c. 1% error in $\hat{\dot{r}}$ (0)

d. 0.5° bias in $\dot{\sigma}$

e. 0.1 g bias in a_{M_σ}

f. 0.1 g bias in a_{M_r}

g. 0.1° bias in seeker gimbal angle

h. 20 ft/s bias in $\hat{V}_M$

i. 1° error in $\hat{\alpha}$

j. $\dot{V}_T = 1$ g
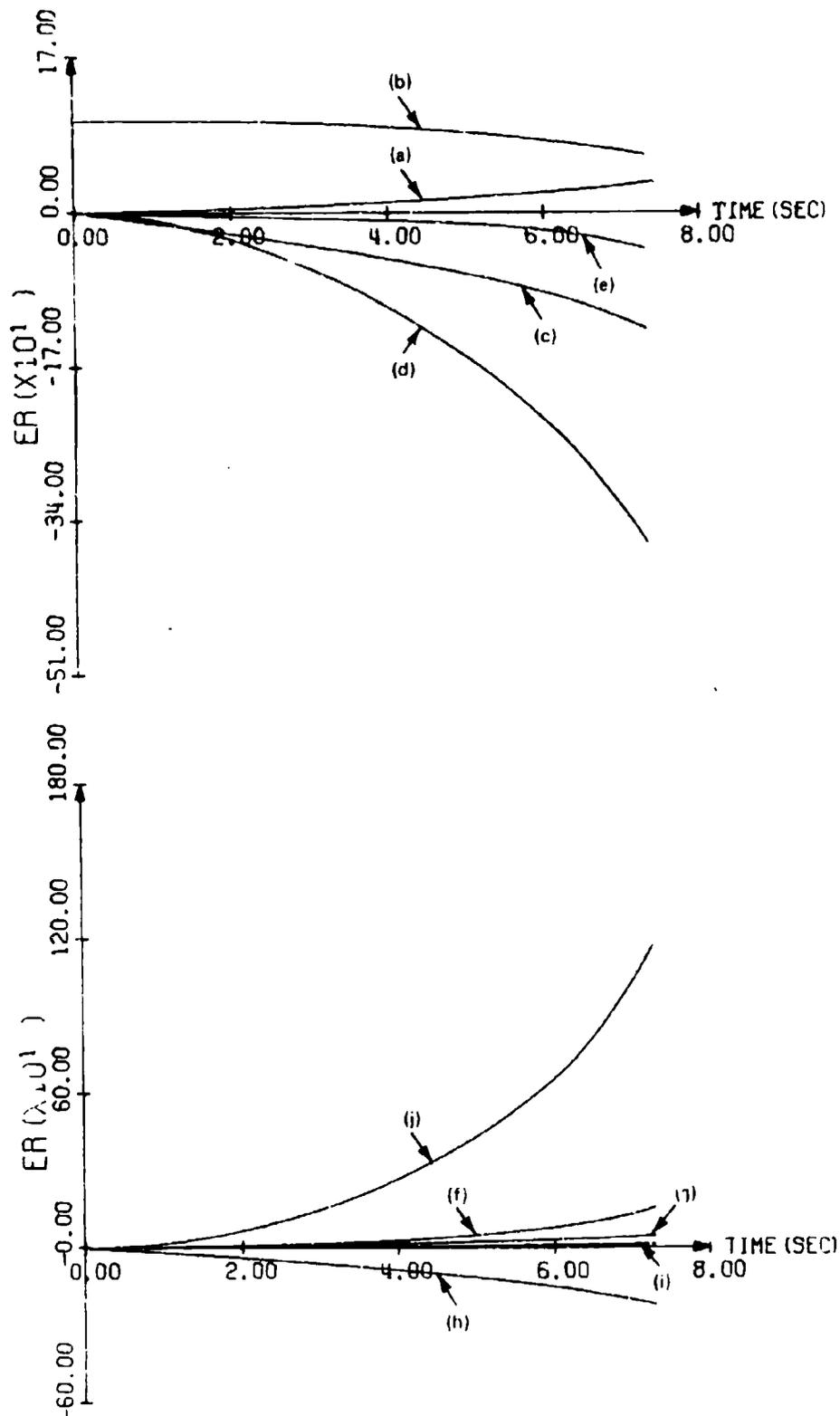
FIG. 4 .9 .2 DYNAMIC RANGING SIMULATION WITH
TARGET INITIAL CONDITIONS. $\psi = 0$, $\phi = -80$, $XT = 10000$.
$YT = 1000$. ERRORS IN RANGE ESTIMATE FROM VARIOUS
SOURCES
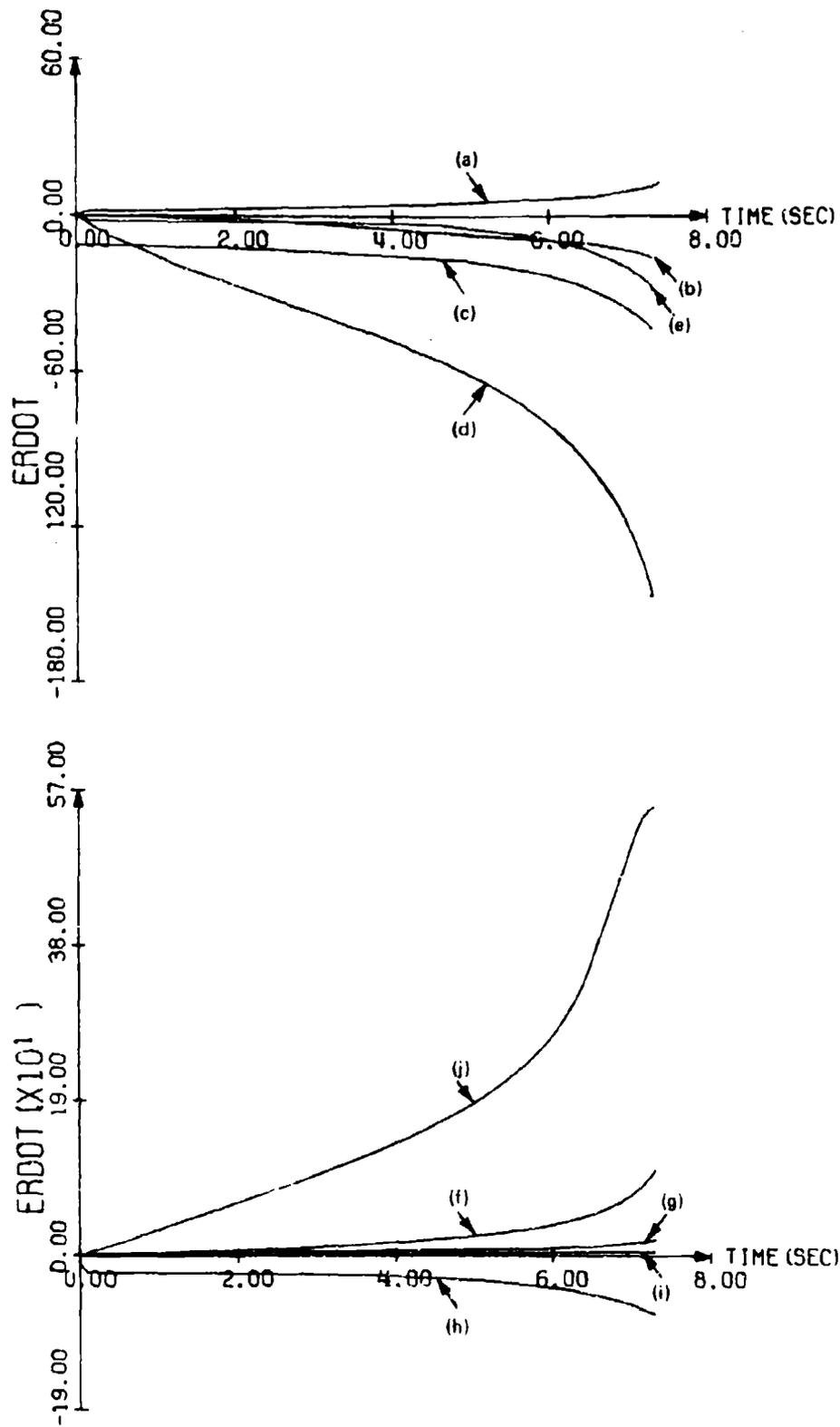
FIG. 4.9.3 DYNAMIC RANGING SIMULATION WITH
TARGET INITIAL CONDITIONS. $\Psi = 0$, $\Phi = -80$, XT $= 10000$,
YT $= 1000$. ERRORS IN RANGE RATE ESTIMATE FROM
VARIOUS SOURCES
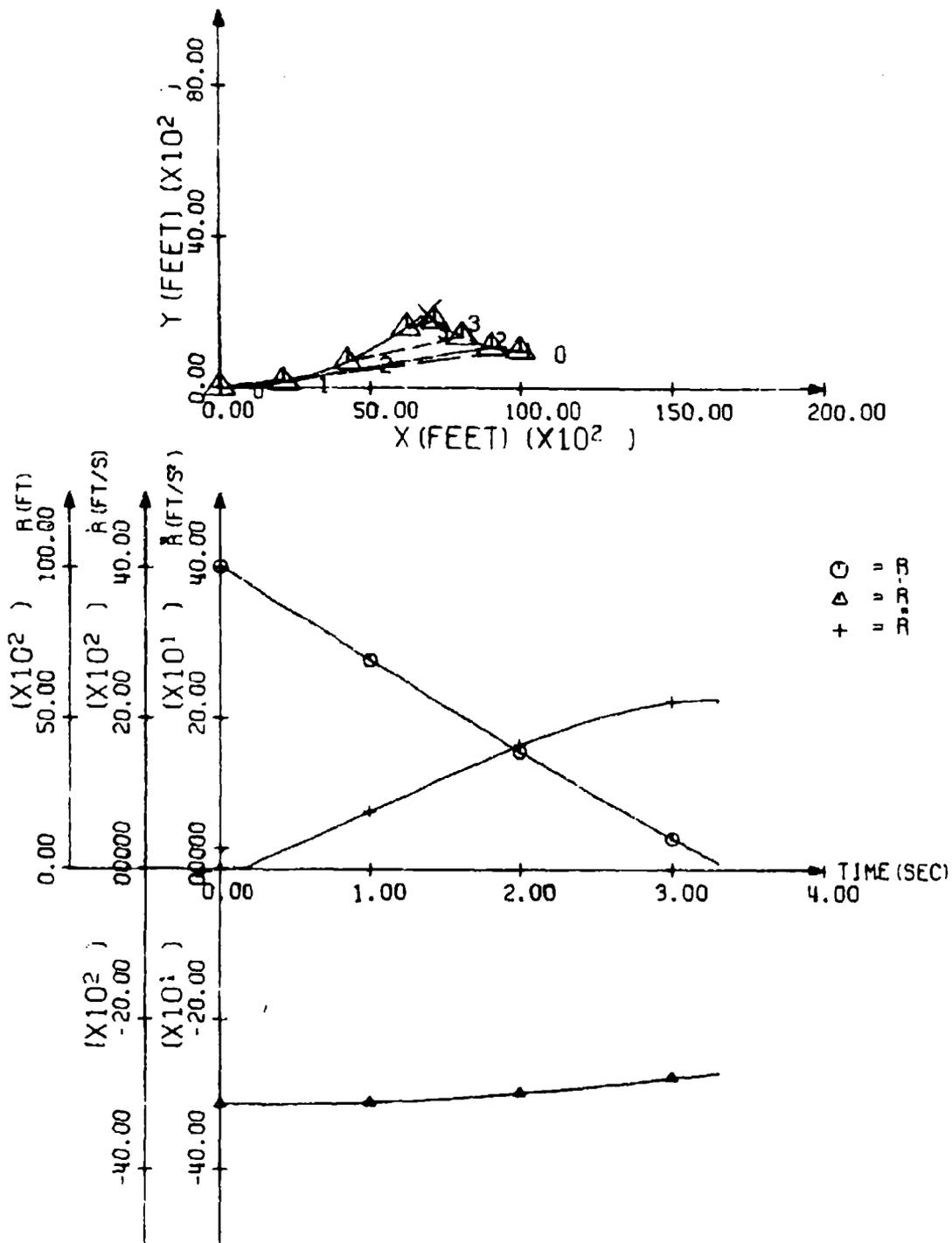
FIG. 4.10.1 DYNAMIC RANGING SIMULATION WITH
TARGET INITIAL CONDITIONS. +=180, Φ=-80, XT = 10000,
YT = 1000. PLOTS OF VARIABLES DEFINING GEOMETRY

Bell Aerospace Company

FIGURE 4.10

This trajectory displays a head-on trajectory with initial range around 10,000 ft. The target is executing a hard right turn. The estimate errors are somewhat related to the errors portrayed in Figure 4.7, where the turn was in the opposite direction.

a. no error sources

b. 1% error in $\hat{r}(0)$

c. 1% error in $\hat{\dot{r}}(0)$

d. 0.5° bias in $\dot{\sigma}$

e. 0.1 g bias in a_{M_σ}

f. 0.1 g bias in a_{M_r}

g. 0.1° bias in seeker gimbal angle

h. 20 ft/s bias in $\hat{V}_M$
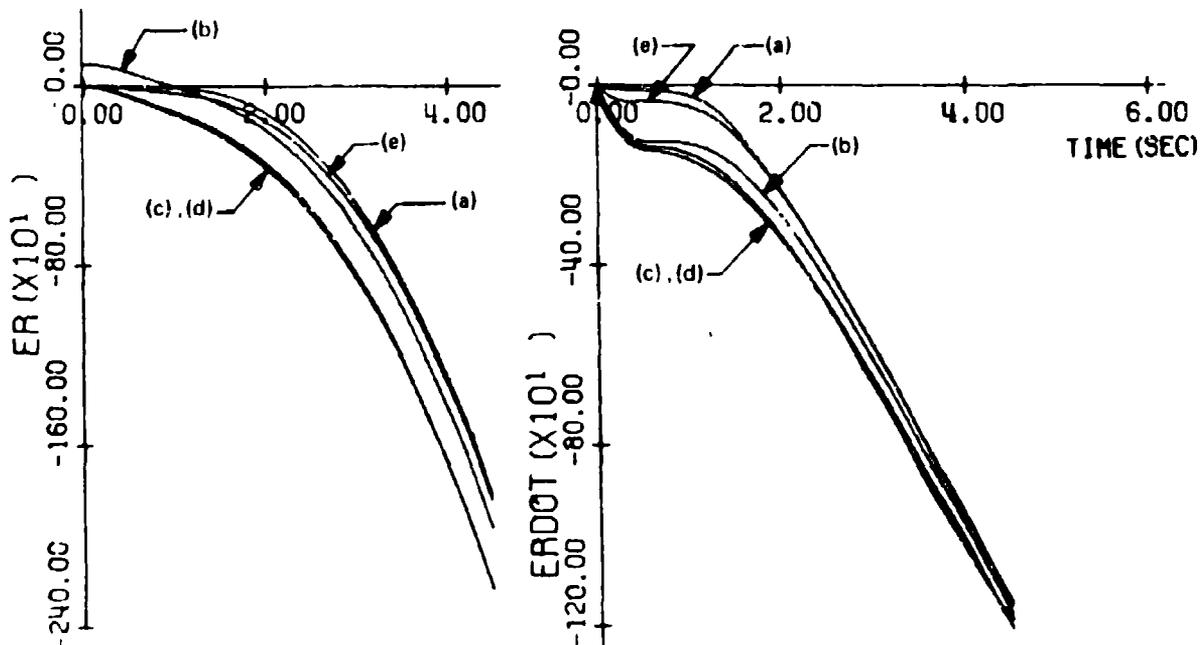
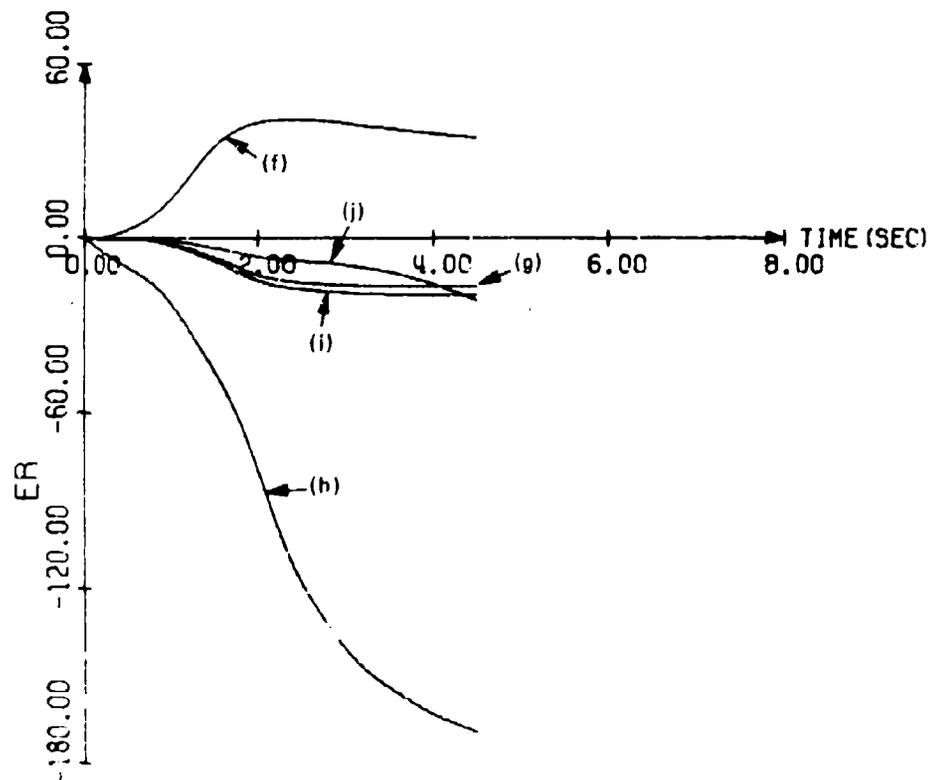i. 1° error in $\hat{\alpha}$

j. $\dot{V}_T = 1$ g
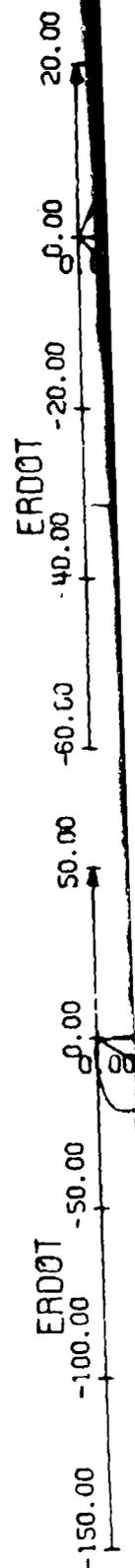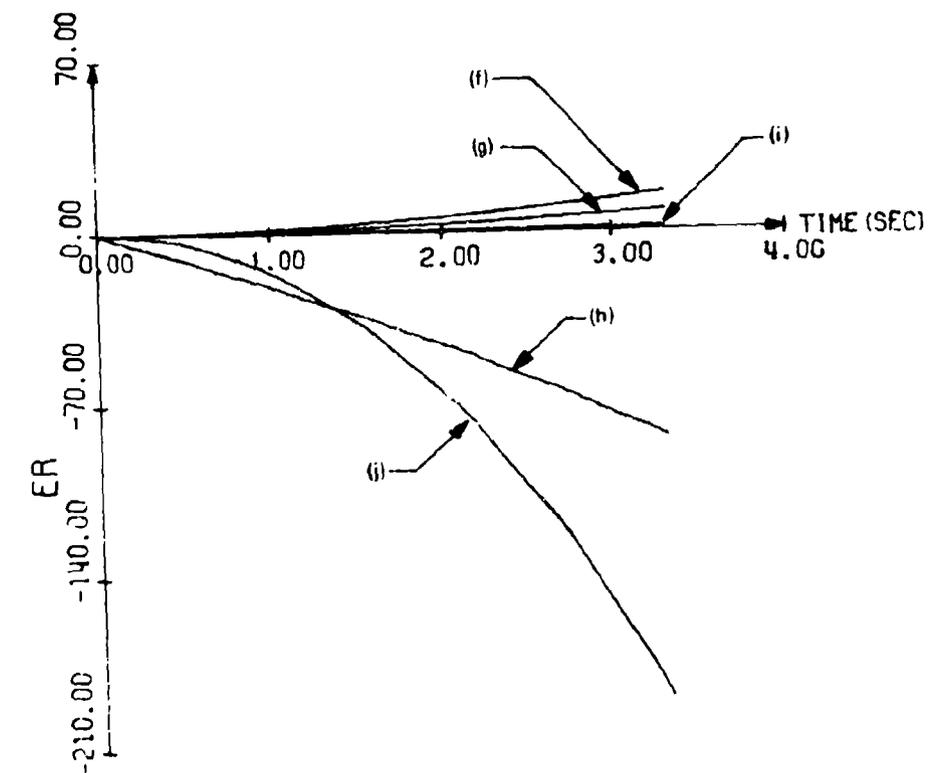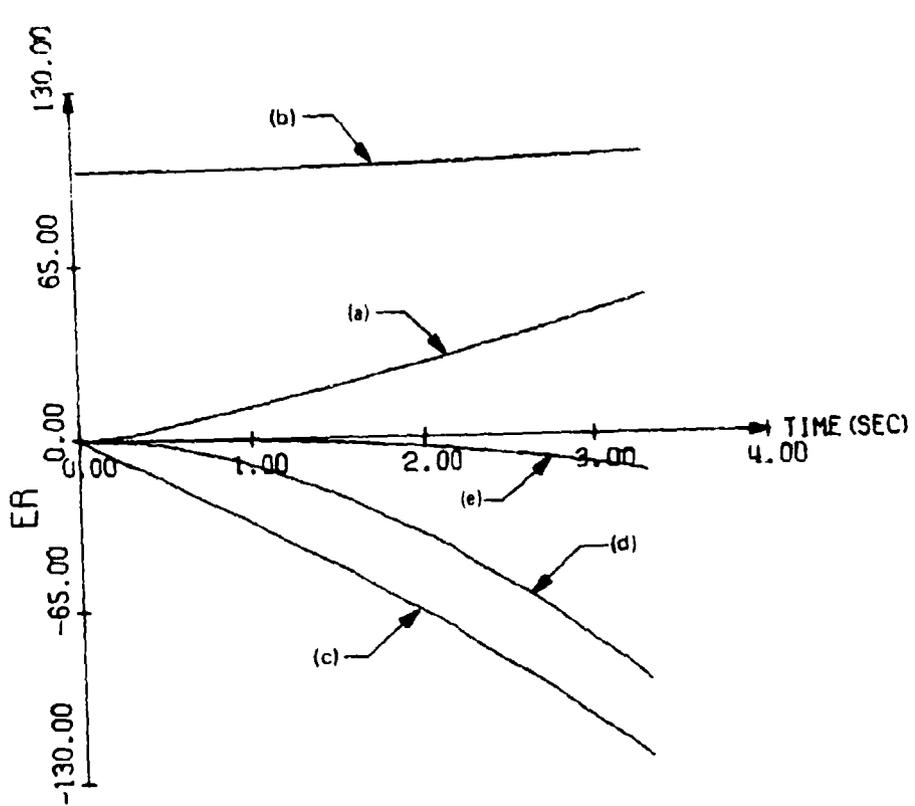
FIG. 4.10.2 DYNAMIC RANGING SIMULATION WITH
TARGET INITIAL CONDITIONS. $\psi = 180$, $\phi = -80$, $YT = 10000$,
$\dot{Y}T = .000$. ERRORS IN RANGE ESTIMATE FROM VARIOUS
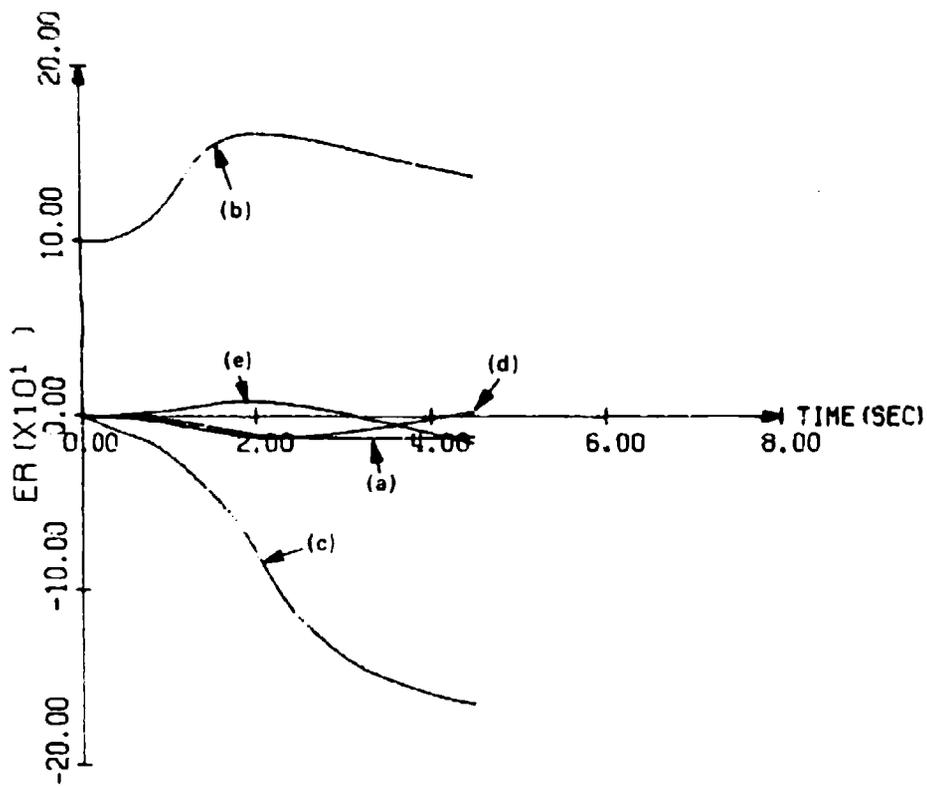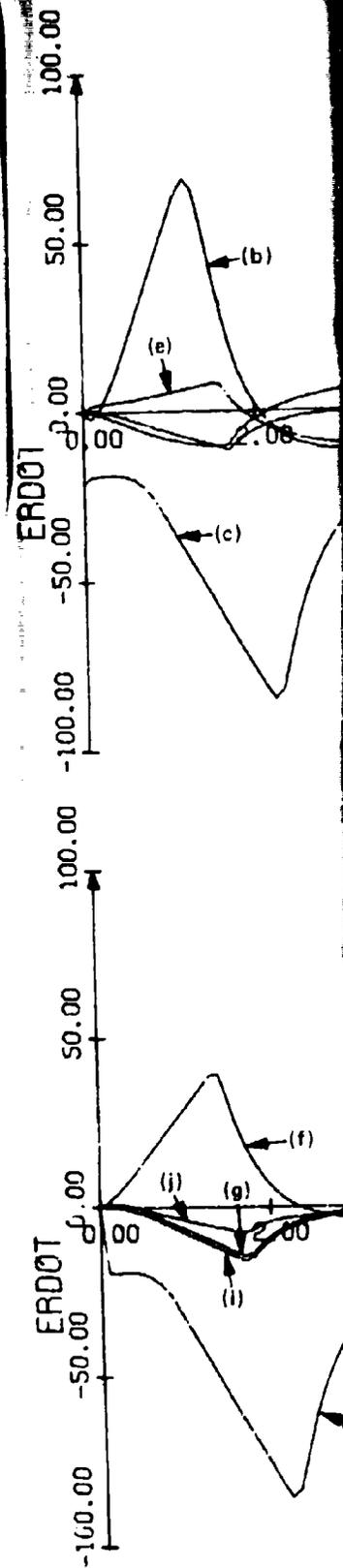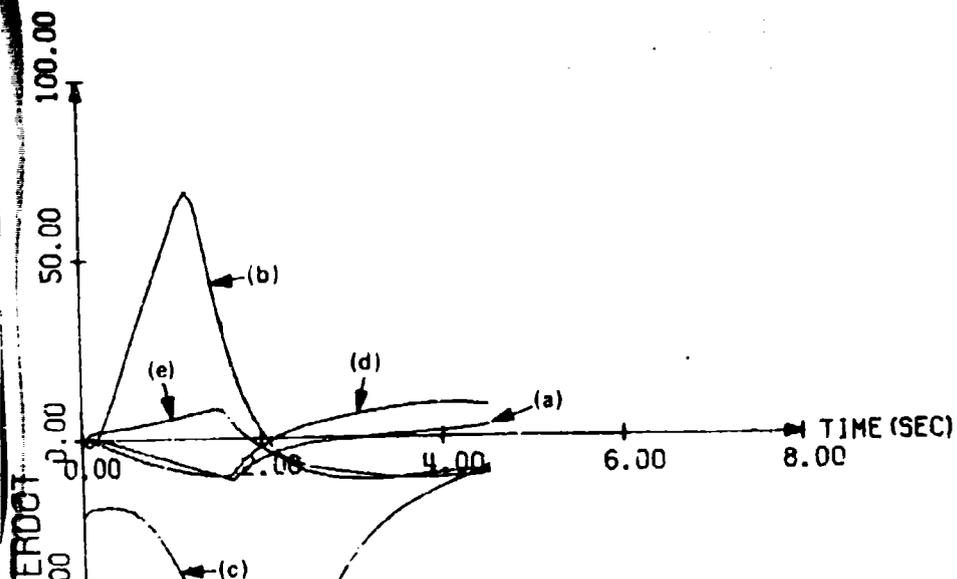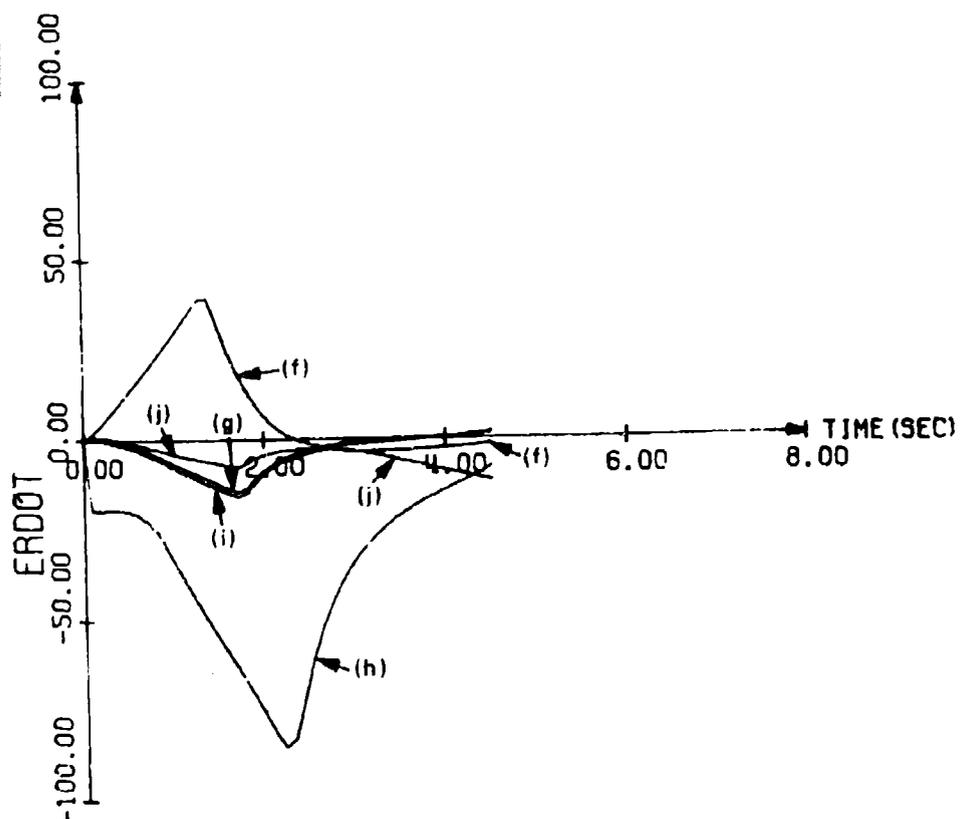SOURCES

FIG. 4
TARGET IN
YT = 1000

49
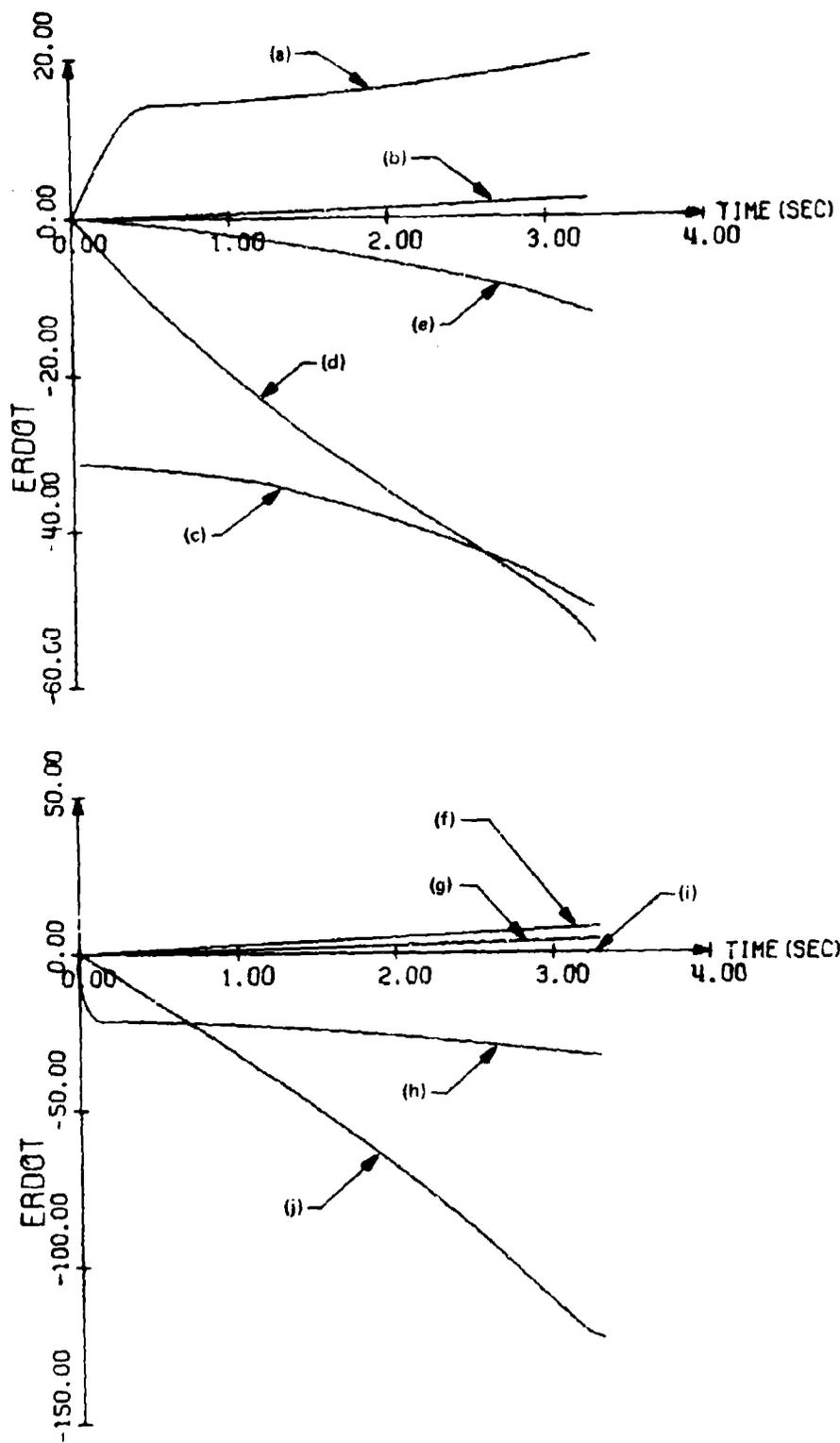
FIG. 4.10.3 DYNAMIC RANGING SIMULATION WITH
TARGET INITIAL CONDITIONS. $\psi = 180$, $\phi = -80$, $XT = 10000$,
$YT = 1000$. ERRORS IN RANGE RATE ESTIMATE FROM
VARIOUS SOURCES
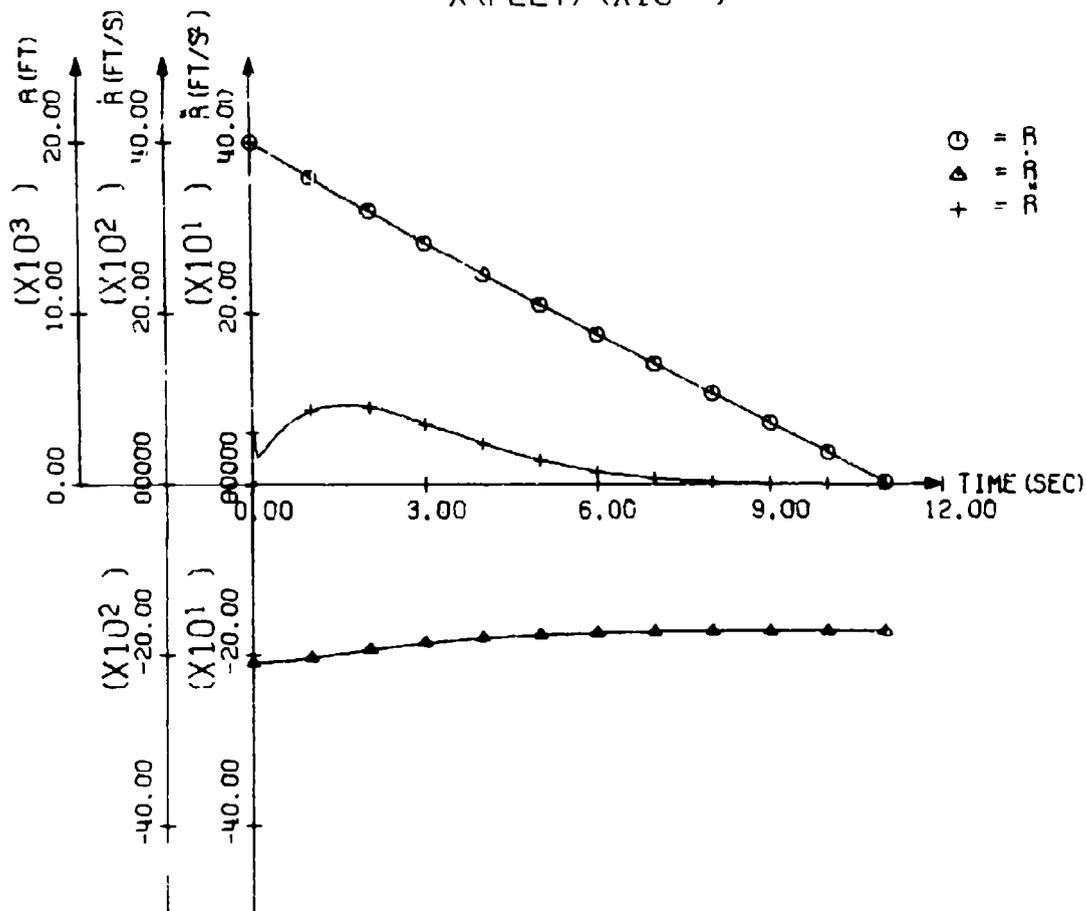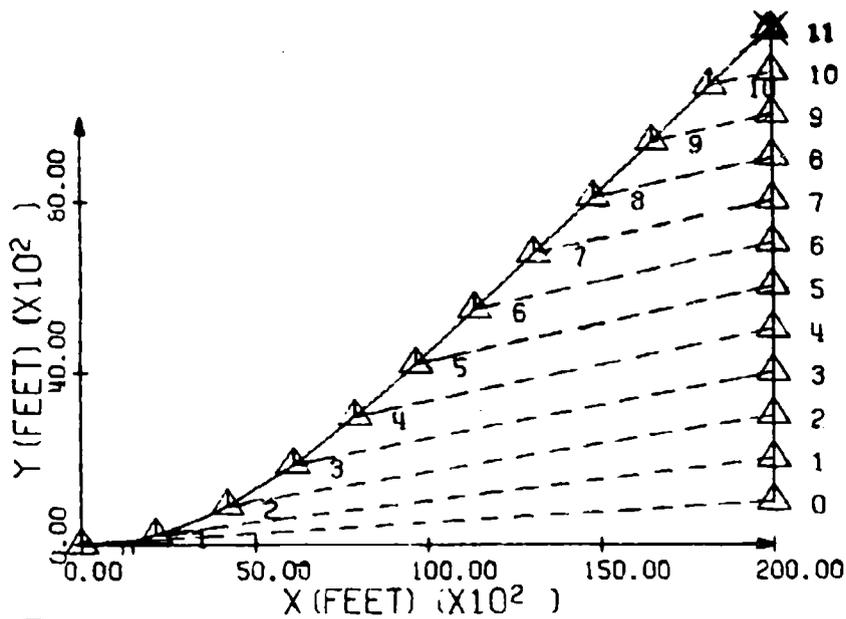
FIG. 4.11.1 DYNAMIC RANGING SIMULATION WITH
TARGET INITIAL CONDITIONS. ᵠ = 90 , Φ = 0 , XT = 20000 ,
YT = 1000, PLOTS OF VARIABLES DEFINING GEOMETRY

FIGURE 4.11

Figure 4.11 portrays a side attack. Initial range is slightly more than 20,000 ft., and the target is not maneuvering. As is evident, the guidance system has established an intercept course at around 3 seconds, and after this point, missile maneuvering is negligible. This results in the signals $\dot{\sigma}$ and consequently $\ddot{\sigma}$ approaching zero, and thus the main signals being used by the algorithm have little significance. Thus after 3 seconds it can be anticipated that if the algorithm is not set up properly at that point, then serious errors can and will result. This is evident in the curves to the right.

a. no error sources

b. 1% error in $\hat{r}$ (0)

c. 1% error in $\hat{\dot{r}}$ (0)

d. 0.5° bias in $\dot{\sigma}$

e. 0.1 g bias in a_{M_σ}

f. 0.1 g bias in a_{M_r}

g. 0.1° in seeker gimbal angle

h. 20 ft/s bias in $\hat{V}_M$

i. 1° error in $\hat{\alpha}$

j. $\dot{V}_T = 1$ g
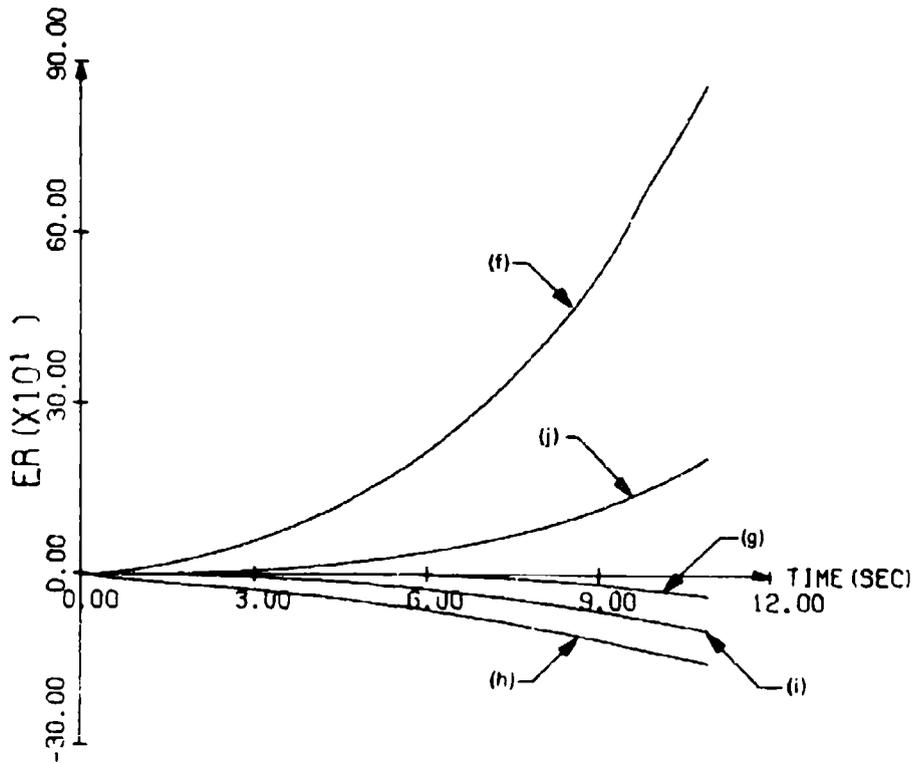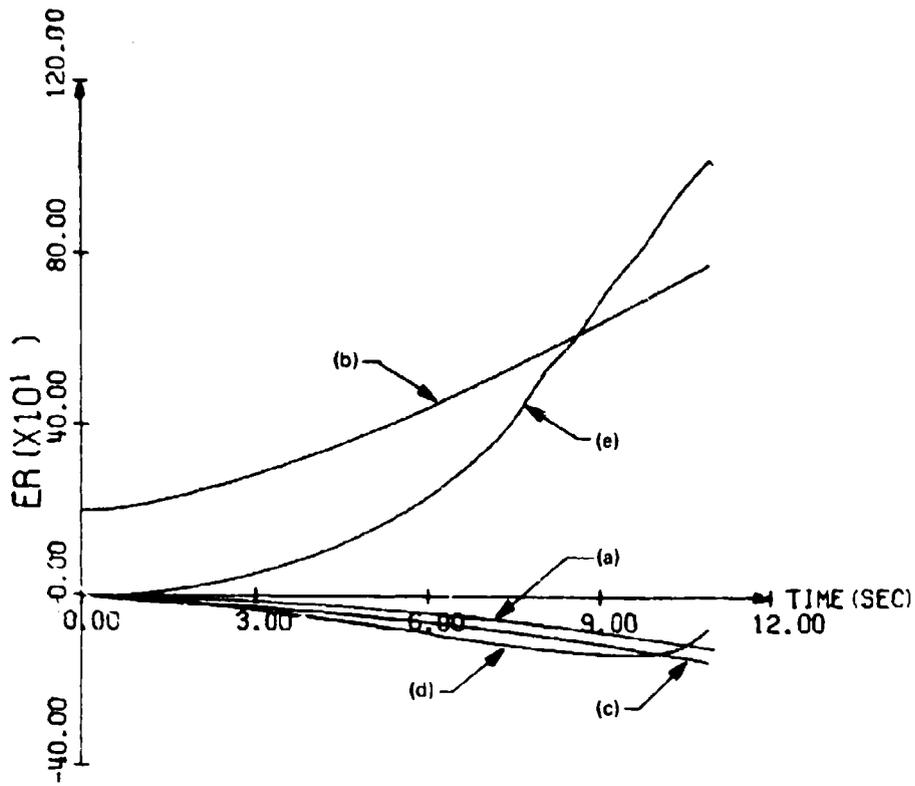
FIG. 4 .11.2 DYNAMIC RANGING SIMULATION WITH
TARGET INITIAL CONDITIONS. ↓= 90, Φ= 0 , XT = 20000 .
YT = 1000 . ERRORS IN RANGE ESTIMATE FROM VARIOUS
SOURCES

51

FIG. 4.11.3 DYNAMIC RANGING SIMULATION WITH
TARGET INITIAL CONDITIONS. $\gamma = 90$, $\Phi = 0$, $XT = 20000$,
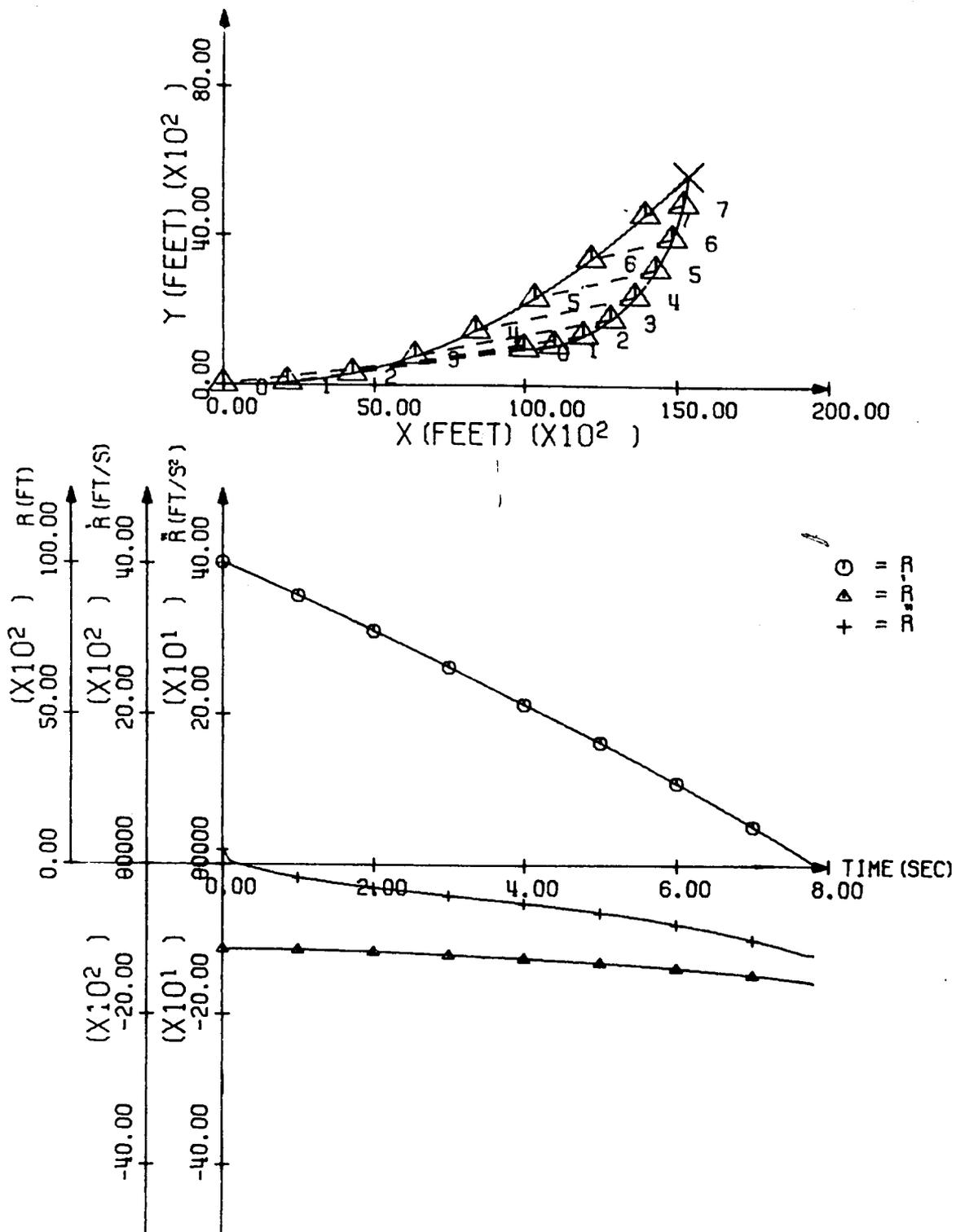$YT = 1000$. ERRORS IN RANGE RATE ESTIMATE FROM
VARIOUS SOURCES
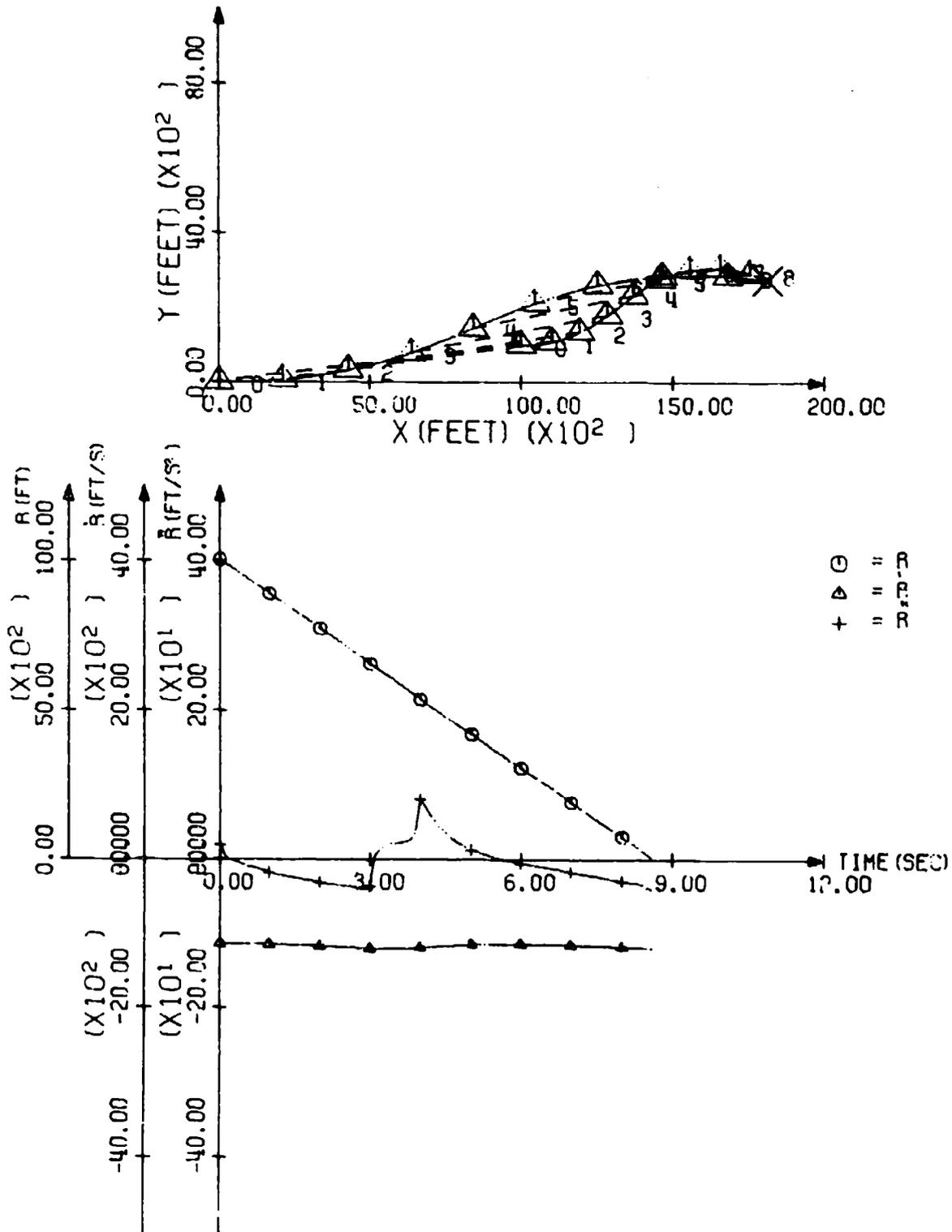
FIG. 4.121 DYNAMIC RANGING SIMULATION WITH
TARGET INITIAL CONDITIONS.$\dot{\phi}=0, \phi=80 \cdot -80$, XT = 10000,
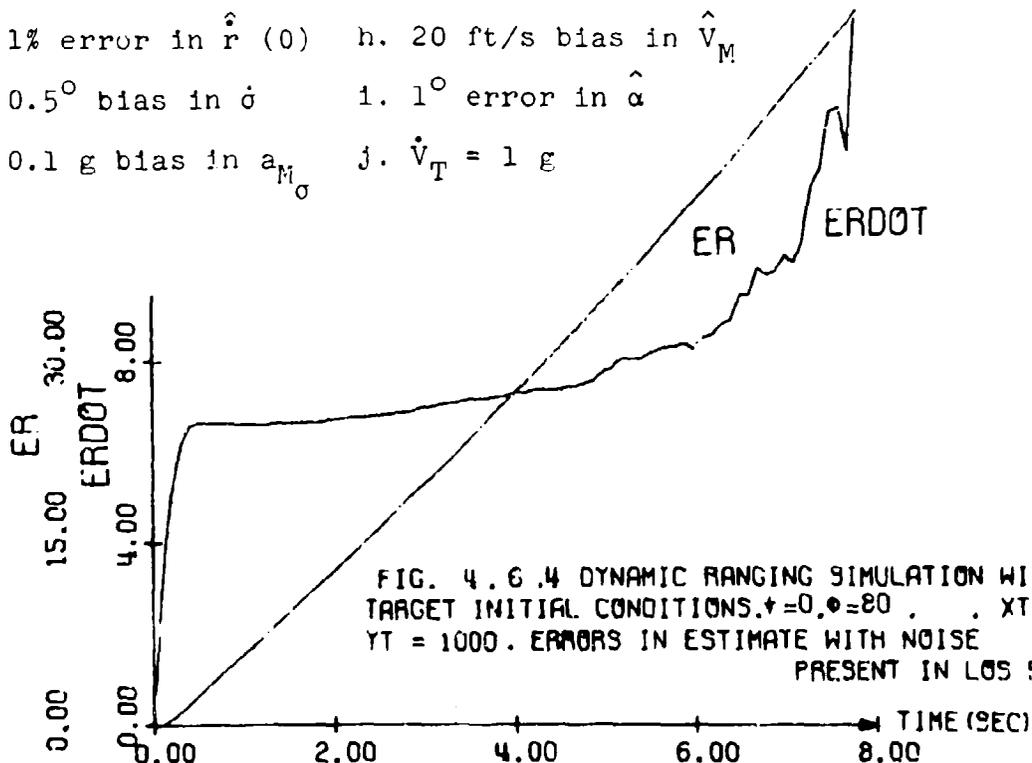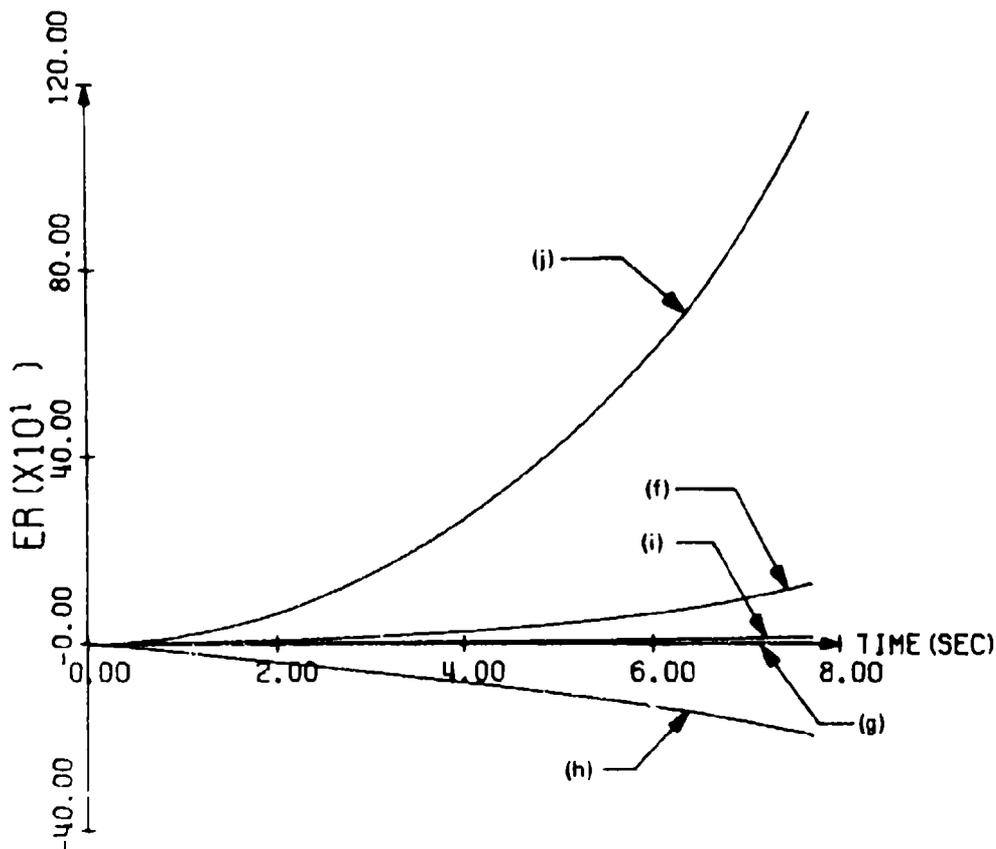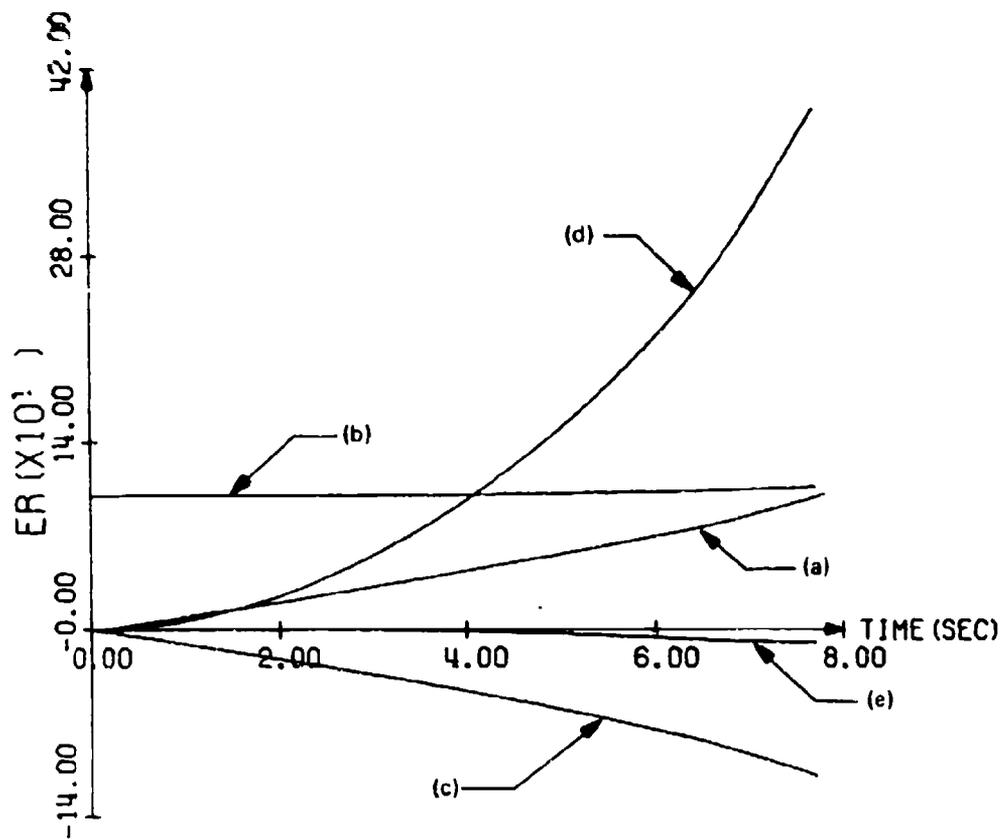YT = 1000. PLOTS OF VARIABLES DEFINING GEOMETRY
DUE TO CHANGE IN TARGET MANUEVER.

FIGURE 4.12

This figure displays a situation where the target performs a rapid change in acceleration by changing its turn from left to right. This trajectory is identical to that of Fig. 4.6 for the first three seconds; at t = 3, the target bank angle was changed from 80° left turn to 80° right turn, requiring one second to do so; the bank angle is 80° right turn for t>4. The algorithm which estimates range must therefore re-adapt to accommodate the change in target turn rate. The bank angle was changed in a linear fashion; however as acceleration is related to tan ϕ, the acceleration of the target changed in a nonlinear fashion. This is evident on inspection of the $\ddot{r}$ trace, on the left, at $3 \leq t \leq 4$ seconds. As the acceleration changed in a way which violates the estimator's assumptions, an error is formed while the maneuver change occurs. But there are many ways in which an airplane can change its maneuver, and any one is as likely as another. The estimator properties lie in the mid-range of the likely types of maneuver change methods. The curves on the facing page are the errors in the range and range-rate estimates with range error on the upper graph, and range-rate error on the lower. No additional curves representing sources of error were made.

The trace at the lower right shows the error of range-rate estimate. Notice that this error jumps from 4 ft/sec to 6 ft/sec at the time of impact at the end of the run. This change is due to imperfect tracking of the term($r\dot{\sigma}^2$) since $\dot{\sigma}$ is extremely large at impact while $\hat{r}$ is not exactly equal to r; in this connection see the discussion of the physical meaning of the term $(r\dot{\sigma}^2)$ on page 13. Notice also that the error of tracking the changing maneuver during $3 \leq t \leq 4$ seconds causes the range-rate estimate error to increase from 1 ft./sec at t = 3 to 4 ft./sec at t = 4; the increase of error of 3 ft./sec is considered to be minimal and demonstrates the surprising power of this nonlinear estimator.
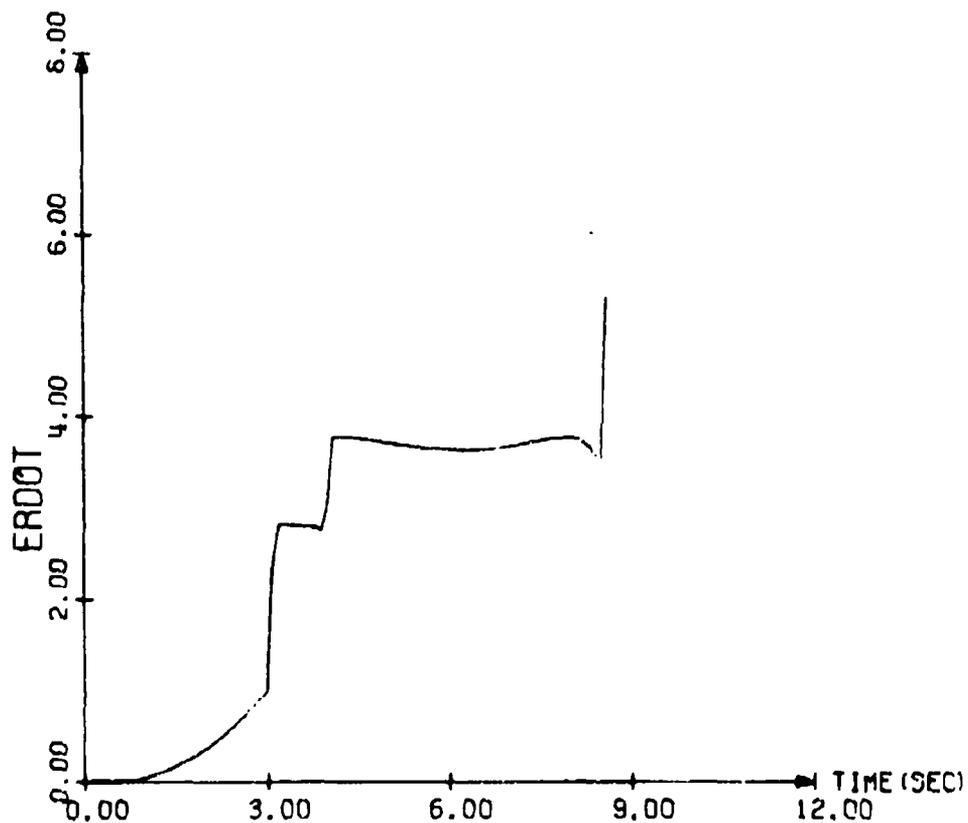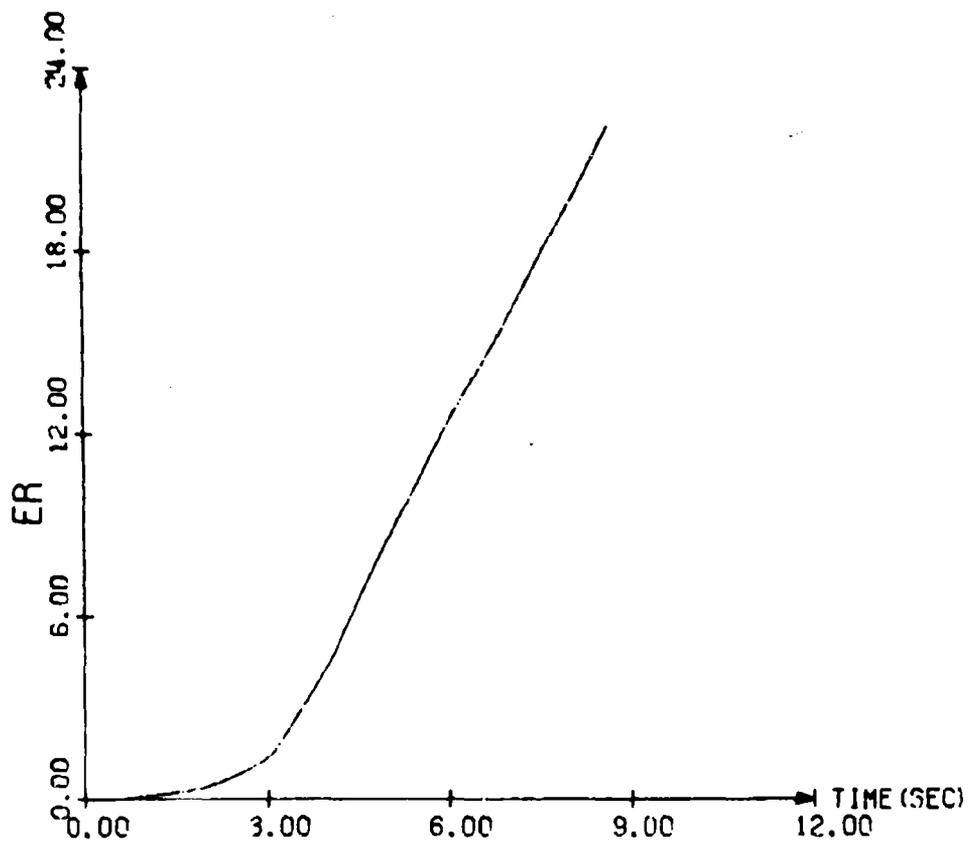
FIG. 4.12.2 DYNAMIC RANGING SIMULATION WITH
TARGET INITIAL CONDITIONS. $\psi = 0. \Phi = 90, -80$, XT $= 10000$,
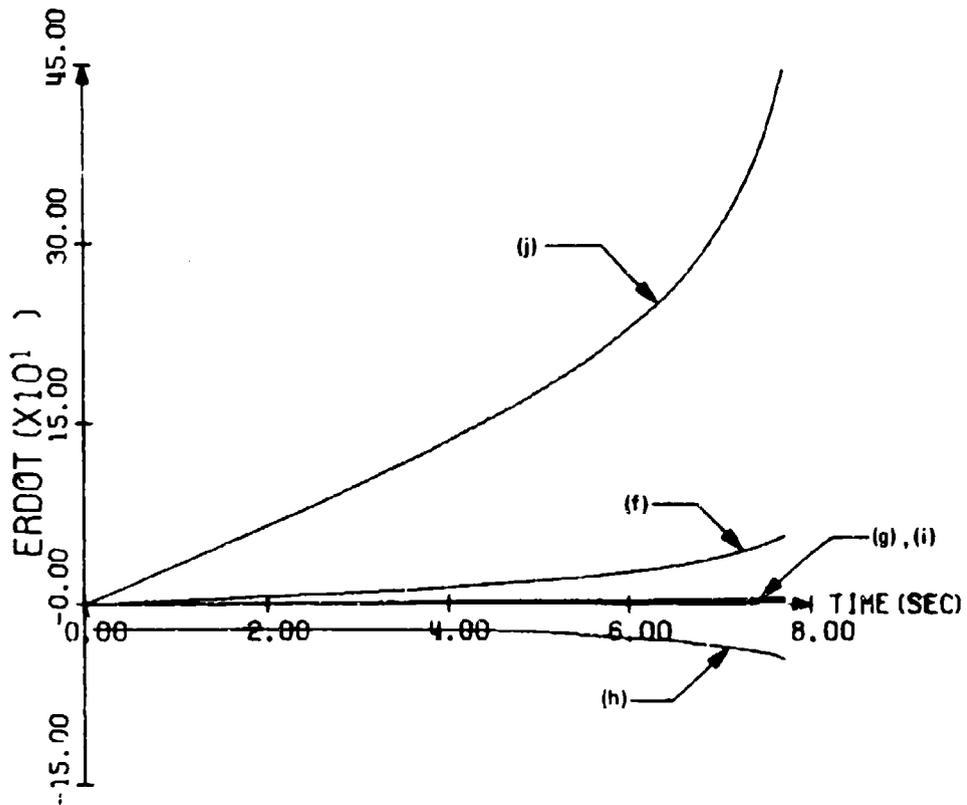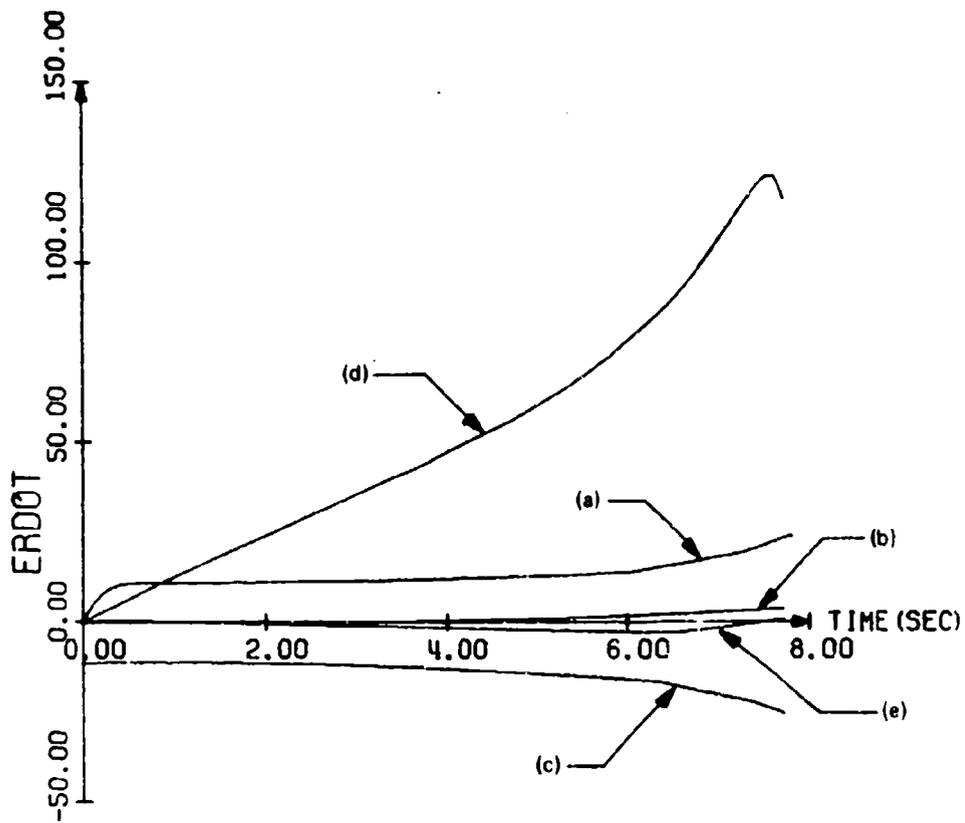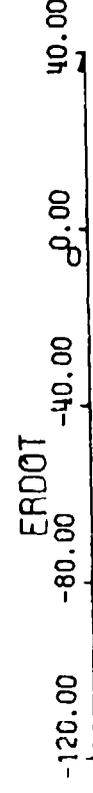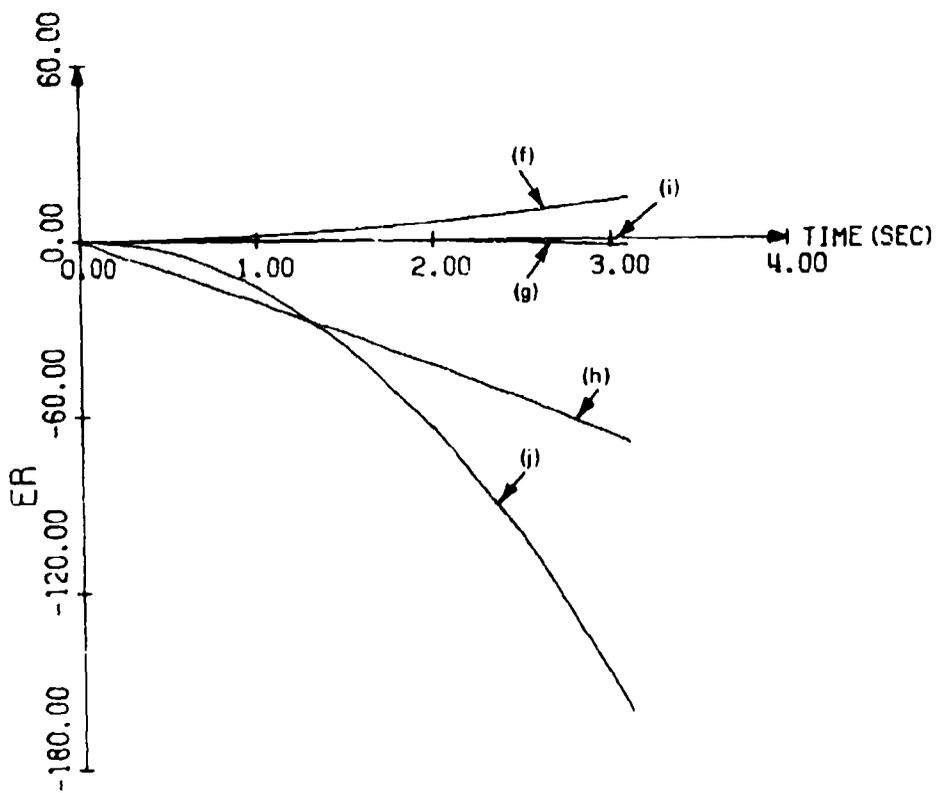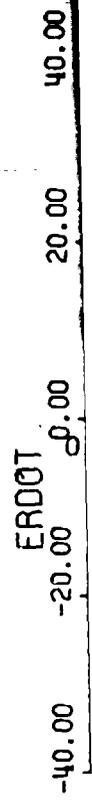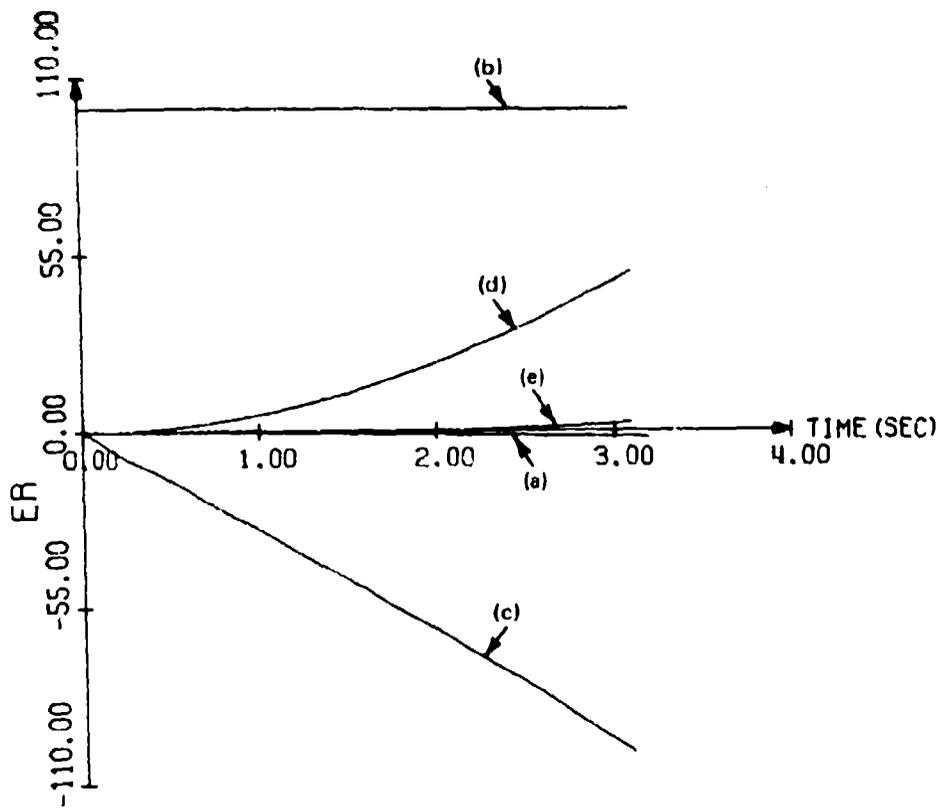YT $= 1000$. ERRORS IN RANGE AND RANGE RATE
ESTIMATE DUE TO CHANGE IN TARGET MANUEVER.

5. LINEAR ESTIMATORS

Linear estimators may, for the purpose of this dis-
cussion, be divided into two classes, depending on whether
a gradient technique is used to achieve convergence. We
term "adaptive" those methods which use a gradient technique
in some form. A matrix-inverse problem is always implicit
in the formation of an "adaptive" or gradient-seeking solu-
tion. In the "matrix-inverse" technique, that inverse
problem appears explicitly and must be treated explicitly.

The adaptive methods lead to simpler instrumentations
than the matrix-inverse methods and were therefore considered
first. The adaptive methods failed, whether with simple
single-error nets, or with multiple-error nets or Kalman
filters, principally due to target acceleration effects.
The mode of failure was that the estimated range-rate was as
much as 30% to 50% in error at the end of the major maneuvers
of the missile. The study then turned to matrix-inverse
methods; these failed to converge for some encounter geometries
and converged to erroneous solutions for other geometries. The
modes of failure were large errors of range-rate estimate or
a problem of ill-conditioning which precluded convergence. We
therefore tentatively concluded that fundamental questions of
mathematical observability were involved and then verified that
hypothesis.

This section presents a brief outline of the adaptive
methods, and of the matrix-inverse methods, with comments
on the physical reasons for their deficiencies, followed by
a discussion on mathematical observability, as applied to
this situation. The section concludes with some comments
on the possibilities available by combining the kinematic
ranging linear estimator with other linear devices, in
particular with a stadimetric ranging method.

5.1 Adaptive Estimators

Adaptive identifiers, as a class, share the use of the
gradient of the index of performance as the guide to improv-
ing the parameter estimates from one instant to the next.
The two principal well-known methods of forming parameter
identifying nets are known as the response-error[2] and equa-
tion error[1,3,5] methods. The response-error method is known to
be relatively slow, and relatively insensitive to noise, as
compared to the equation-error method. The air-air intercept
problem clearly requires rapid solution; efforts were therefore
concentrated on the equation-error method.

A brief analytical outline of the method is followed by
discussion of the representatives of the various adaptive
systems.

Assume that the output of the plant whose parameters are
to be identified is designated y, and that a set of signals v,

consisting of various functions of the plant's input and output, is available. If the true values of the unknown parameters are represented by the vector x^* then the plant output takes the form

$$y = v^T x^* . \tag{5.1}$$

Given the same set of signals, v, and a vector of estimates of the parameter values, x, we may form an estimate of the plant output

$$\hat{y} = v^T x . \tag{5.2}$$

Then we may form an error as $y - \hat{y} = y - v^T x = e$, (5.3)

and the error will become identically zero if and only if $x = x^*$. The common and simplest gradient algorithm for adjusting the parameter estimates, x, minimizing $J = \overline{e^2}$, is

$$\dot{x} = +k \, v e \tag{5.4}$$

which on substituting e from (5.3) yields

$$(Is + k \, v \, v^T) \, x = k \, v \, y .$$

The gain k must be positive definite; it may be a scalar or a matrix. If the value of k is chosen small enough to ensure averaging, and if the parameter x^* is constant, then the steady state is reached when

$$\overline{v \, v^T} \, x = \overline{v \, y}$$

with solution $x = (\dfrac{\overline{}}{\overline{v \, v^T}})^{-1} \dfrac{\overline{}}{\overline{v \, y}} .$ (5.5)

56

The covariance matrix $\overline{v\,v^T}$ is implicit in all adaptive techniques as they use the algorithm (5.4). The convergence properties and noise sensitivity of the solution are determined by the properties of that matrix.

Matrix-inverse methods, to be discussed in Section 5.2, find the solution vector x directly from (5.5). The covariance matrix $\overline{v\,v^T}$ is obviously involved explicitly.

If the parameters x^* are known a priori to be variable or to be related, the known properties may advantageously be used in a modified algorithm. Assume that it is known that $\dot{x}_1^* = x_2^*$ and $\dot{x}_2^* = bt$, or in general, $\dot{x}^* = Ax^* + B(t)$, then an algorithm equivalent to (5.4) is

$$\dot{x} = Ax + B(t) + k\,v\,e,$$

$$(5.6)$$

and the term $k\,v\,e$ is required only to correct for the unknown errors in the parameter estimates.

Our initial approach was to use the identity

$$r\dot{\sigma} + \dot{r}\sigma = \dot{y}_T - \dot{y}_M \tag{5.7}$$

as a starting point for an adaptive algorithm. This equation results from the inertial space geometry

57
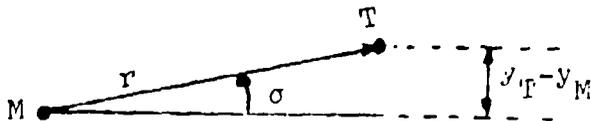
which shows

$$r \sin \sigma = y_T - y_M$$

For small σ, this equation has the approximate form

$$r \sigma = y_T - y_M$$

with first derivative (5.7). Taking current estimates for range and range rate, which in general are different from the actual values, the equation error is

$$x_1 v_1 + x_2 v_2 + x_3 v_3 + \dot{y}_M = e_1$$

(5.8)

where $x_1 = \hat{r}_1, x_2 = \hat{\dot{r}}_1, x_3 = \dot{y}_T$, $v_1 = \dot{\sigma}_1, v_2 = \sigma$, $v_3 = -1$ and $\dot{x}_1 = x_2$,

or $\dot{x} = AX$, $A = \begin{pmatrix} 0 & 1 & 0 \\ 0 & 0 & 0 \\ 0 & 0 & 0 \end{pmatrix}$,

where $\dot{\sigma}$, σ and $\dot{y}_M$ are known. The index of error is defined as

$$J = \overline{e_1^2}.$$

The algorithm for updating the estimate $x = (\hat{r}, \hat{\dot{r}}_1 \hat{\dot{y}}_T)^T$ is $\dot{x} = Ax - k \, v \, e_1$, which is then readily implemented for a suitable choice of $k > 0$. Using this method assumes that the variables $\hat{r}$ and $\hat{\dot{y}}_T$ are constant. But in an actual dogfight situation, both target and missile are accelerating, and the assumption is too optimistic. This approach therefore failed and was abandoned.

58

A second approach, consistent with the mathematical model of Section 3, was taken. In this development, the frame of reference is polar coordinates centered at the missile, with the instantaneous radius vector parallel to the line of sight. The error equation which holds in this case is

$$\hat{r}\ddot{\sigma} + 2\,\hat{\dot{r}}\,\dot{\sigma} - \hat{a}_{T_\sigma} + a_{M_\sigma} = e_2,$$

and the error index is then chosen as $J = \overline{e_2^2}$.
Again, let $x_1 = \hat{r}$, $x_2 = \hat{\dot{r}}$, $x_3 = \hat{a}_{T_\sigma}$ and let $v_1 = \ddot{\sigma}$, $v_2 = \dot{\sigma}$, $v_3 = -1$. Then that error equation can be put into the form

$$v^T x + a_{M_\sigma} = e_2. \tag{5.9}$$

The complete statement of the components of acceleration is from, Section 3,

Accelerations
perpendicular $r\ddot{\sigma} + 2\,\dot{r}\,\dot{\sigma} - a_{T_\sigma} + a_{M_\sigma} = 0$
to the LOS

$$\tag{5.10}$$

Accelerations
parallel $\ddot{r} - r\,\dot{\sigma}^2 - a_{T_r} + a_{M_r} = 0.$
to the LOS

$$\tag{5.11}$$

The first of these may be used to form the "observation equation", or, in adaptive terminology, the equation error.

But the second expression provides a statement of the value of $\ddot{r}$ which has previously been lacking. Let us define $x_1 = \hat{r}$, $x_2 = \hat{\dot{r}}$, $x_3 = \hat{a}_{T_\sigma}$ and $x_4 = \hat{a}_{T_r}$. We can directly sense the LOS angular rate and acceleration and the unit gains $v_3 = -1$, $v_4 = +1$, and also the missile accelerations a_{M_σ} and a_{M_r}. Then the equation error to be minimized is again in the form

$$v^T x + a_{M_\sigma} = e_3 \tag{5.12}$$

and the algorithm which minimizes $J = \overline{e_3^2}$, is

$$\dot{x} = Ax + B(t) - k \, v \, e_3 \tag{5.13}$$

where

$$A = \begin{pmatrix} 0 & 1 & 0 & 0 \\ \dot{\sigma}^2 & 0 & 0 & 1 \\ 0 & 0 & 0 & 0 \\ 0 & 0 & 0 & 0 \end{pmatrix} \quad , \quad B = \begin{pmatrix} 0 \\ -a_{M_r} \\ 0 \\ 0 \end{pmatrix} \quad . \tag{5.14}$$

The matrix A expresses the differential relationship between range and range-rate on the first line; it expresses the definition of $\ddot{r}$ from (5.11) on the second line, and on the third and last lines expresses the assumption that the target accelerations with respect to the LOS are quasi-constant.

The term $r\dot{\sigma}^2$ in (5.11) can easily be as large as 100 ft/sec^2, e.g., when in the initial geometry the target at a range of 10,000 feet has 1,000 ft/sec velocity and is flying perpendicular to the LOS. This is not negligible.

The kinematic ranging estimation method expressed by equations (5.13) and (5.14) was examined for a variety of geometrical conditions.

The simple adaptive schemes following (5.13) and (5.14), with the adaption-rate parameter k as a scalar constant, were quite unsatisfactory as there was no single constant value of k which worked well for all combat geometries or throughout any single trajectory. The difficulty is that a large value of k is required to find the correct values of $\hat{r}$ and $\hat{\dot{r}}$ at the start of the trajectory, while a low value is required to prevent undue sensitivity to noise in later parts of the trajectory. Further, the rate parameter k should ideally be proportional to $(\frac{1}{\dot{\sigma}^2})$ so as to accommodate both to large and small maneuver geometries. The gain k must thus vary with time and also with geometry to achieve satisfactory results.

It was therefore necessary to replace the scalar adaption-rate parameter k by a Kalman Filter type matrix, K, where the values of K are time-varying, according to the well-known[8] rule

$$\dot{K} = -K \, v \, N^{-1} \, v^T \, K$$

(5.15)

where N is the noise covariance. Even so, while this approach would generate good estimates of $\hat{r}$ and $\hat{\dot{r}}$ for

61

some trajectories, it failed when the trajectory was such
that $a_{T_r} \neq 0$.

In the geometrical conditions in which this Kalman-
filter type algorithm works well, i.e., when the target
acceleration along the LOS, a_{T_r}, is negligible, a signifi-
cant simplification is possible. Consider (5.11) and
"transform-differentiate-integrate"[6] by premultiplying by

$$\frac{T_i s}{T_i s+1} \quad , \quad i = 1,2,\ldots, T_i \neq T_j, \text{ yielding, if } \ddot{r} \approx 0,$$

$$\frac{T_i s}{T_i s+1} \left(r\, \ddot{\sigma}+2\dot{r}\dot{\sigma} - a_{T_\sigma} + a_{M_\sigma} \right) = r \left(\frac{T_i s}{T_i s+1}\, \ddot{\sigma} \right) + \dot{r} \left(\frac{2 T_i s}{T_i s+1}\, \dot{\sigma} + \right.$$

$$\left. \frac{T_i}{(T_i s+1)^2}\, \ddot{\sigma} \right) - \left(\frac{T_i s}{T_i s+1} \right) a_{T_\sigma} + \left(\frac{T_i}{T_i s+1} \right) a_{M_\sigma} .$$

$$(5.16)$$

For these geometries, it is a reasonably good assumption
that a_{T_σ} is quasi-constant. It therefore follows that

$$\frac{T_i s}{T_i s+1}\, a_{T_\sigma} \approx 0 \text{ is valid. The result is that the estimating}$$

variable $x_3 = \hat{a}_{T_\sigma}$ may be omitted, and there is one less un-
known parameter. Equation (5.16) may be put into the equation
error form

$$v_i^T x + y_i = e_{4_i}$$

where $\quad x = (\hat{r}, \hat{\dot{r}})^T,$

$$v_i = \{(\frac{T_i s}{T_i s + 1})\, \ddot{\sigma}\ , [(\frac{2T_i s}{T_i s + 1}) + \frac{T_i s}{(T_i s + 1)^2}]\, \dot{\sigma}\}^T$$

and $\quad y_i = \frac{T_i s}{T_i s + 1}\, a_{m_c}.$ $\hfill$ (5.17)

If this transform-integration, (5.16), is instrumented for several different values of T_i, a vector of errors $(e_{4_1}, e_{4_2}, \ldots)$ may be generated. This is one of the several multiple-error techniques[5],[6] This technique did not work in an adaptive approach although it was better than single-error techniques. The solution usually involved an ill-conditioned $\overline{v\ v}^T$ covariance matrix and was therefore noise-sensitive. When averaging over a sufficiently large interval was used, the unknown acceleration a_{T_r} caused $\hat{\dot{r}}$ to be as much as 30% to 50% in error in 1 to 2 seconds.

The difficulty is that if the filter time-constants T_i are small, then the several vectors v_i are almost parallel resulting in an ill-conditioning problem and a poorly defined solution. On the other hand, if T_i are large enough to avoid ill-conditioning then the invalid assumption that $\ddot{r} \approx \hat{a}_{T_r} = 0$ caused excessive error in the range-rate estimate.

63

The difficulty common to all the methods is that
whenever the averaging time must exceed 1/4 to 1/2 second,
to enable the vectors which carry the information to be
linearly independent, then it is essential to take into
account the target acceleration along the LOS. On the
other hand an averaging time of 1/2 second or less is
not sufficient as the LOS does not rotate sufficiently in
that interval to permit determining a solution in the
presence of noise, and also to correct the initial estimates.
For these reasons, the various adaptive gradient-seeking
methods of parameter estimation were abandoned.

5.2 Matrix-Inverse Methods

Several schemes were derived from the classical[7] point
of view of least mean square estimation. The general theory
of this method can be explained quite briefly, as follows.
Consider the linear homogeneous vector differential system

$$\dot{\underline{x}} = A(t)\underline{x} \ .$$

$$(5.18)$$

Assume the observed output of the system is the vector

$$\underline{y} = H(t)\ \underline{x} + \underline{v}$$

$$(5.19)$$

where $H(t)$ is known and $\underline{v}$ represents additive random noise.
It is desired to estimate $\underline{x}$ knowing only $A(t)$, $\underline{y}(t)$ and the
statistics of $\underline{v}$.

Knowing $A(t)$, generate the state transition matrix $,\Phi,$ for the system so that the state at any time can be written as a function of the state at another time. Thus,

$$\underline{x}\,(t+\zeta) = \Phi\,(t+\zeta,t)\,\underline{x}\,(t).$$

$$(5.20)$$

Many estimates can be constructed. The one which is usually considered the most desirable, however, has the property that it is an "unbiased" estimate of $\underline{x}$ and furthermore, it minimizes the variance of the expected error in the estimate. This estimate is found[7] by computing

$$\hat{\underline{x}} = (T_n^T T_n)^{-1} T_n^T Y_{(n)}$$

$$(5.21)$$

where
$$Y_{(n)} = \begin{pmatrix} y(t_n) \\ \hline y(t_{n-1}) \\ \hline \vdots \\ \hline \underline{y_1}(t_1) \end{pmatrix}$$

$$(5.22)$$

$$T_n \triangleq \begin{pmatrix} H(t_{n-L})\Phi(t_{n-L},tn) \\ \hline \vdots \\ \hline H(t_{n-1})\Phi(t_{n-1},t_n) \\ \hline H(t_n) \end{pmatrix}.$$

$$(5.23)$$

The matrix T_n is thus a "continuously updated observation matrix" and the vector $Y_{(n)}$ is a "series of output observations". The expression (5.21) is valid provided the noise $\underline{v}$ is independent from computing instant to instant and has zero mean. The construction of the matrix T_n is often a formidable task as it requires keeping in storage a large amount of past data $H(t_i)$ so that it can be updated by the state transition matrix $\Phi(t_i, t_j)$ which is at times also difficult to obtain.

Apply this theory to, typically, the reduced dimensionality problem defined by (5.16) and (5.17); assume that $\dot{r}$ is constant, thus x_2 is constant after convergence. But $x_1 = r$ and is not constant. Now we have, at some specific instant, and with only one value of $i = 1$,

$$v_1(t_1)x_1 + v_2(t_1)x_2 + y_1 = e_5.$$

(5.24)

At the next instant we have

$$v_1(t_2)x_1 + v_2(t_2) x_2 + y_2 = e_5.$$

(5.25)

But while the value of x_2 is ideally the same at these two instants, the value of x_1 changes continuously, for $x_1 = r$, and r is the integral of $\dot{r}$. We may modify (5.24) so that x_1 is the same for the two instants. If Δt

66

is the time between samples, we may rewrite (5.24) as

$$v_1(t_1) (x_1(t_2) + x_2 \Delta t) + v_2 (t_1) x_2 + y_1 = e_5 \text{ ,}$$

which may be rearranged as

$$v_1(x_1) x_1(t_2) + (v_2 (t_1) + v_1 (t_1) \Delta t) x_2 + y_1 = e_5.$$

(5.26)

Now Eqns. (5.25) and (5.26) represent two measurements referred to the same instant, and may be solved jointly. More generally, a larger sequence of such instants may be gathered in the more general form of (5.23).

This method exhibited several modes of failure. Whenever any two of:

the missile velocity vector

the target velocity vector

'ıe LOS

become col ʼar, or $\dot{\sigma} = 0$, the matrix $(T_n^T T_n)$ became ill-conditioned ʼ indeterminate, yielding inaccurate and noise-s ;itive ɛ utions. In geometries when this mode of failure di ᵐʳ ʼ ɔur, this algorithm has a different mode of failure. If the duration of the stored memory exceeds 1/2 second, the neglected target acceleration parallel to the LOS, a_{T_r} , causes the estimate of $\dot{r}$ to be 30% to 50% in error within 1 to 2 seconds, as the assumption that $\ddot{r} = 0$ is too incorrect. On the other hand, a shorter duration memory results in high noise sensitivity. But these algorithms work

well (Range-Rate errors of 1%) if $a_{T_r} = 0$.

In any case the computational complexity and memory storage requirements of this algorithm are excessive. An alternate was therefore examined. If

$$\hat{r} = \hat{r}_0 + \int \hat{\dot{r}} \, dt$$

$$(5.27)$$

and $\qquad x_1 = \hat{r}_0, \ x_2 = \hat{\dot{r}}$, etc.,

then a much simpler algorithm results. At a number of successive instants we have

$$
\begin{pmatrix}
v_1 (1) & v_2 (1) \\
v_1 (2) & v_2 (2) + v_1 \, \Delta t \\
\vdots & \vdots \\
\vdots & \vdots \\
\vdots & \vdots
\end{pmatrix}
\begin{pmatrix}
x_1 \\
x_2
\end{pmatrix}
=
\begin{pmatrix}
y_1 \\
y_2 \\
\vdots \\
\vdots \\
\vdots
\end{pmatrix}
$$

$$(5.28)$$

and both x_1 and x_2 may be assumed constant. If the nth row of the left of (5.28) is

$$v_1(n) \quad v_2(n) + \Delta t \, v_1 \, (n-1) \quad ,$$

then the matrix $(T_n^T T_n)$ may be recursively formed as

$$(T_n^T \ T_n) = (T_{n-1}^T \ T_{n-1}) \ + \ v_n \ v_n^T \ .$$

$$(5.29)$$

Although sufficiently simple to be feasible for
an air-air missile, this approach to range estimation
also failed for the same reasons:

(a) Ill-conditioned matrix for some
geometries,

(b) High noise-sensitivity for short
averaging times,

(c) Large errors in range-rate estimates
for longer averaging times due to
the invalid assumption that $a_{T_r} = 0$.

When failure-mode (a) did not occur, and $a_{T_r} = 0$ was
valid, the algorithm yields estimate errors of the order
of 1%.

No attempt at estimating a_{T_r}, target acceleration
parallel to the LOS, by linear methods was successful.
Any algorithm which neglected $a_{T_r} \neq 0$ when it was signifi-
cant operated unsuccessfully; either excessive noise sensi-
tivity became a problem, or the neglected acceleration
caused excessive errors in the estimation of Range-Rate, $\hat{r}$.

In summary, except for encounter geometries which
yield ill-conditioned matrices, the matrix-inverse algorithms
work well with long-filtering times which eliminate noise
effects if the assumption that $a_{T_r} = 0$ is valid. If that

69

assumption is invalid, the matrix-inverse schemes fail due to the bias in range-rate estimate caused by target acceleration, or due to noise.

5.3 Observability

The failure of these various adaptive and matrix-inverse parameter identification methods, whether continuous or discrete, is fundamentally due to the existence of target acceleration in the radial direction, parallel to the line of flight. That acceleration component cannot be estimated by linear techniques because it is "unobservable" in the mathematical sense. This section relates the concept of "observability" to this application and problem.

The state of a linear system with constant coefficents in the dynamics and constant coefficients in the output relation can be e;timated from knowledge of the output provided the system is mathematically observable. For this discussion, we view the quantities of range, range-rate, etc., as states which are to be determined and consider the signals of LOS-rate and missile acceleration as time-varying parameters. In state-variable notation a plant may be described as

$$\text{Plant Dynamics:} \quad \dot{x} = Ax + Bu$$

$$\text{Output:} \quad y = Hx + v$$

(5.30)

where v is zero-mean Gaussian white noise, and x is an N-component vector.

The observability of the system is specified by a relationship between the A matrix, specifying the dynamics, and the H matrix, relating the state to the output. If the order of the system is N, then the matrix

$$O_N = [\ H^T\ \vdots\ A^T\ H^T\ \vdots\ (A^T)^2 H^T\ \vdots\ \ldots\ \vdots\ (A^T)^{N-1} H^T\ ]$$

(5.31)

must have full rank for the system to be observable. Let us now apply this to one of the possible formulations of the problem. For the system definition, use the acceleration-component equations from Section 2

accelerations
parallel to the
LOS

$$\ddot{r} - r\ \dot{\sigma}^2 - a_{T_r} + a_{M_r} = 0$$

(5.32)

Perpendicular to
the LOS

$$r\ \ddot{\sigma} + 2\ \dot{r}\ \dot{\sigma} - a_{T_\sigma} + a_{M_\sigma} = 0.$$

(5.33)

In order to cast this into the standard form of (5.30), define state variables

$$
\begin{aligned}
x_1 &= \hat{r}\\
x_2 &= \hat{\dot{r}}\\
x_3 &= \hat{a}_{T_r}\\
x_4 &= \hat{a}_{T_\sigma}
\end{aligned}
\Bigg\}
$$

(5.34)

71

i.e. the variables x are the estimates of the unknown parameters. The last two lines of (5.34) express the fact that the two components of target acceleration must be estimated and are assumed to be unknown constants.

The state variable expression of the relationships among the several variables may be found from (5.32) and (5.34) as

$$
\begin{pmatrix} \dot{x}_1 \\ \dot{x}_2 \\ \dot{x}_3 \\ \dot{x}_4 \end{pmatrix} = \begin{pmatrix} 0 & 1 & 0 & 0 \\ \dot{\sigma}^2 & 0 & 1 & 0 \\ 0 & 0 & 0 & 0 \\ 0 & 0 & 0 & 0 \end{pmatrix} \begin{pmatrix} x_1 \\ x_2 \\ x_3 \\ x_4 \end{pmatrix} + \begin{pmatrix} 0 \\ -a_{m_r} \\ 0 \\ 0 \end{pmatrix} .
$$

$$(5.35)$$

The first row of (5.35) expresses the differential equation relating range and range-rate estimates. The second row consists of (5.34) while the third and fourth rows express the assumption that the target's unknown accelerations a_{T_r} and a_{T_σ} are constant. From (5.35), the matrix A is

$$
A_n = \begin{pmatrix} 0 & 1 & 0 & 0 \\ \dot{\sigma}^2 & 0 & 1 & 0 \\ 0 & 0 & 0 & 0 \\ 0 & 0 & 0 & 0 \end{pmatrix}
$$

$$(5.36)$$

and N=4.

Equation (5.33) yields the output relationship

$$(-\ddot{\sigma} \quad -2\dot{\sigma} \quad 0 \quad 1) \begin{pmatrix} x_1 \\ x_2 \\ x_3 \\ x_4 \end{pmatrix} = \hat{a}_{M_\sigma} ;$$

(5.37)

comparison of the estimate, $\hat{a}_{M_\sigma}$, with the measured acceleration a_{M_σ} yields an error whose minimization will presumably yield optimal estimates of the range, x_1, and range-rate, x_2. From (5.37),

$$H = (-\ddot{\sigma} \quad -2\dot{\sigma} \quad 0 \quad 1).$$

(5.38)

Combining (5.36) with (5.38) in the format of (5.35) yields the observability matrix

$$O_4 = \begin{pmatrix} -\ddot{\sigma} & -2\dot{\sigma}^3 & -\dot{\sigma}^2 & -2\dot{\sigma}^5 \\ 2\dot{\sigma} & -\ddot{\sigma} & -2\dot{\sigma}^3 & -\dot{\sigma}^2\ddot{\sigma} \\ 0 & -2\dot{\sigma} & -\ddot{\sigma} & -2\dot{\sigma}^3 \\ 1 & 0 & 0 & 0 \end{pmatrix} .$$

(5.39)

The fourth column of (5.39) is exactly equal to $\dot{\sigma}^2$ times the second column, and the rank is less than the order. This system is unobservable; experiment confirmed this result.

73

In realistic combat trajectories it is generally erroneous to assume that a_{T_r}, target acceleration in the range-direction, is zero. If, however, that assumption is valid for some situation, then we can simplify (5.35) by omitting the third row and column and similarly simplify H, so that if $a_{T_r} \equiv 0$, a priori, then

$$A_{31} = \begin{pmatrix} 0 & 1 & 0 \\ \dot{\sigma}^2 & 0 & 0 \\ 0 & 0 & 0 \end{pmatrix} \quad , \quad H_{31} = (-\ddot{\sigma} \quad -2\dot{\sigma} \quad 1)$$

and

$$0_{31} = \begin{pmatrix} -\ddot{\sigma} & -2\dot{\sigma}^3 & -\ddot{\sigma}\,\dot{\sigma}^2 \\ -2\dot{\sigma} & -\ddot{\sigma} & -2\dot{\sigma}^3 \\ 1 & 0 & 0 \end{pmatrix} .$$

$$(5.40)$$

In this case rank equals order and the system is observable if $\ddot{\sigma} \neq 0$ and $\dot{\sigma} \neq 0$. This result was experimentally confirmed.

Returning to (5.35), assume that the target acceleration perpendicular to the LOS, a_{T_σ}, is identically zero, i.e., $x_4 = \hat{a}_{T_\sigma} \equiv 0$, a priori, but the other component, $x_3 = \hat{a}_{T_r}$, is a non-zero constant. Then, making the appropriate changes in A and H, we have

$$A_{32} = \begin{pmatrix} 0 & 1 & 0 \\ \dot{\sigma}^2 & 0 & 1 \\ 0 & 0 & 0 \end{pmatrix} \quad , \quad H_{32} = (-\ddot{\sigma} \quad -2\dot{\sigma} \quad 0)$$

74

and

$$O_{32} = \begin{pmatrix} -\ddot{\sigma} & -2\dot{\sigma}^3 & -\dot{\sigma}^2\ddot{\sigma} \\ -2\dot{\sigma} & -\ddot{\sigma} & -2\dot{\sigma}^3 \\ 0 & -2\dot{\sigma} & 0 \end{pmatrix} \quad .$$

(5.41)

In this case the third column equals $\dot{\sigma}^2$ times the first; therefore the system is unobservable.

The result may now be stated: If the target has significant acceleration parallel to the line of sight, $(a_{T_r} \neq 0)$, it is not possible to estimate range and range-rate; the system is unobservable. If the target acceleration a_{T_r} is known to be zero, a priori; then the system is observable, and it may be reduced to a problem in the three states, $x_1 = \hat{r}$, $x_2 = \hat{\dot{r}}$ and $x_4 = \hat{a}_{T_\sigma}$. In this case, Equation (5.32) can be exactly instrumented. If $x_4 = \hat{a}_{T_\sigma}$ = constant is a reasonable assumption, it is possible to reduce the problem from three states to two by differentiating the output expression (5.37) and eliminating $x_4 = \hat{a}_{T_\sigma}$, as in (5.16).

It is, however, an important restriction that the theorems on observability do not apply perfectly to systems whose coefficients are time-varying. In our case the system dynamics are constant, while the observation matrix is not. Intuitively, it seemed possible that if

75

the coefficients of the output equation vary sufficiently in the observation interval, then a result might be obtained which is of value. Many variations of the above development, using different models of the system dynamics and output equations were therefore examined to pursue this question. The results were disappointing whenever $a_{T_r} \neq 0$, or $\dot{\sigma}$ was small. The system is unobservable, despite the uncertainty of the theory on this question, whenever $a_{T_r} \neq 0$.

5.4   Other Linear Systems

It is advantageous to unify the results of the above discussions on kinematic linear parameter identification systems in order to form a basis for considering other possible linear systems. We therefore re-present the problem from a geometrical viewpoint and then consider possible extensions beyond the scope of this contract.

Consider the equation of acceleration components perpendicular to the LOS, from the kinematics,

$$r \ddot{\sigma} + 2 \dot{r} \dot{\sigma} - a_{T_\sigma} + a_{m_\sigma} = 0.$$

$$(5.41)$$

Assume that the range acceleration, $\ddot{r}$, is zero, and may therefore be neglected. Assume further that a_{T_σ} is quasi-constant, i.e., cannot change significantly in less than 1/2 second. Then differentiation of (5.41) with a high pass filter such as $\dfrac{T_1}{T_1 s + 1}$, where T_1 is of the order of 1/2 second or less, reduces (5.41) to

$$r v_1 + \dot{r} v_2 + v_o = 0$$

$$(5.42)$$

where $v_1 = \left(\dfrac{T_1 s}{T_1 s + 1}\right) \ddot{\sigma}$; $v_2 = \left(\dfrac{2 T_1 s \dot{\sigma}}{T_1 s + 1} + \dfrac{T_1 \ddot{\sigma}}{(T_1 s + 1)^2}\right)$, $v_o = \left(\dfrac{T_1 s}{T_1 s + 1}\right) a_{m_\sigma}$.

If in (5.42) we replace r and $\dot{r}$ by the estimates $\hat{r}$ and $\hat{\dot{r}}$, (5.42) may be expressed as $\hat{r} v_1 + \hat{\dot{r}} v_2 + v_o = e_6$; then the solution for $\hat{r}$ and $\hat{\dot{r}}$ lies on a locus such that $e_6 = 0$. In this

$$(5.43)$$

77

case (5.43) forms a straight line, as shown in the
sketch below for some particular instant.
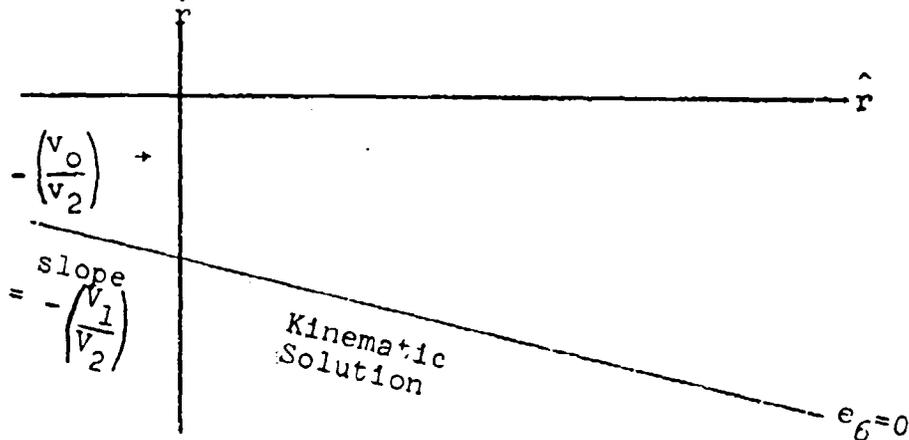
Fig. 5.1
Geometrical View of Equation Error.

The entire problem of estimation is based on the ne-
cessity of finding another line in the $(\hat{r}, \hat{\dot{r}})$ space:

(a) The multiple-error [4,6] adaptive process, by
using a variety of values of T_1 generates a
number of other lines which are, more or less,
linearly independent. This approach may be
categorized as achieving distribution in the
T_1-lag space at one instant of true time.

(b) The various single-error adaptive nets and the
Kalman net take advantage of the fact that, at
some other instant than that shown in Fig. 5.1,
the line of zero error in the $(\hat{r}, \hat{\dot{r}})$ space is

78

differently oriented, if $\dot{\sigma} \neq 0$, and is therefore

linearly independent.   These approaches thus

use the idea of distribution in true time, t,

rather than in the T_1 space.

(c) The matrix inverse schemes gather all lines

over the computing interval, thus achieving

distribution in time, and then find the solution.

A physically different approach to finding a second

linearly independent line in the $(\hat{r}, \hat{\dot{r}})$ space is obviously

preferable if possible.   Stadimetric ranging provides such

an approach.   Seekers which enable measurement of some

function of the target size, or area, such as mosaic IR,

TV, area, or correlation, have this capability.   In a

single plane we have the geometrical relationship

$$r\theta = D$$

(5.44)

where r Range

θ Angle Subtended by Target, assumed a small angle

D Target Size

as shown in the sketch below.

Assume that D is constant; this assumption is fair if D is the diameter of the least circle which contains the target as viewed from the seeker in both the maneuver and cross maneuver planes. From (5.44), by differentiating,

$$r\dot{\theta} + \dot{r}\,\theta = 0$$

and

$$\hat{r}\dot{\theta} + \hat{\dot{r}}\theta = e_7.$$

<div style="text-align:right">(5.45)</div>

The choices of $\hat{r}$ and $\hat{\dot{r}}$ for which $e_7 = 0$ lie on a straight line which passes through the origin of the $(\hat{r}, \hat{\dot{r}})$ space at every instant. Combining this with the kinematic ranging sketch, Fig. 5.1, yields the sketch below.

Fig. 5.2
Combining Kinematic and Stadimetric Ranging.

If we solve (5.44) and (5.45 simultaneously, we get one equation for $\hat{r}$ and one for $\hat{\dot{r}}$. These are independent and their joint solution may therefore be determined. It is usually better to solve the two equations in a decoupled format as the solution can always be accomplished more rapidly, more simply and more accurately. A Least Magnitude algorithm may be used. They are analytically valid in such cases and are attractive for they estimate a moving parameter with smaller lag than quadratic algorithms, and thereby decrease the effect of target accelerations.

However, this argument rests on the rather uncertain base of the assumptions. One assumption is that the target cross-track acceleration (a_{T_σ}) is quasi-constant, i.e., changes negligibly within two time-constants of the high-pass filter $\dfrac{T_1 s}{T_1 s+1}$, in (5.42). The other assumption is that $\ddot{r} \simeq 0$, or at least the unknown portion (a_{T_r}) thereof. In fact, in any maneuver of the target, a_{T_σ} and a_{T_r} change continuously and can change rapidly. This scheme is therefore less powerful than appears at first.

However, stadimetric data can be valuable in reducing the difficulty of range estimation. Equation (5.41) states one relationship between three of the unknowns in the kinematic ranging problem. Stadimetric data provides another relationship, so that the effective total number of unknowns may be reduced by one. The possibility therefore exists that linear estimation of range and range rate could be accomplished with acceptably small error, due to the unobservability of a_{T_r}, by combining kinematic and stadimetric methods.

It should be observed that stadimetric ranging has an advantage over kinematic ranging. In stadimetry, the subtended angle θ is positive-definite, and its rate $\dot{\theta}$ is zero if and only if $\dot{r} = 0$; this almost never occurs. On the other hand, in kinematic ranging, the objective of a proportional navigation homing system is to keep $\dot{\sigma} \approx 0$ at all times; consequently an ill-conditioned covariance matrix must result at least occasionally.

This observation leads to describing the possible weakness in the idea of combining kinematic and stadimetric ranging principles. In both schemes, express $\hat{\dot{r}}$ as a function of $\hat{r}$, and assume $\ddot{r} \approx 0$. Then, using (5.42) and (5.45)

Kinematic:
$$\hat{\dot{r}} = \frac{v_0}{v_2} - \frac{v_1}{v_2}\,\hat{r}$$

$$(5.46)$$

Stadimetric:
$$\hat{\dot{r}} = -\left(\dot{\theta}/\theta\right)\hat{r},$$

$$(5.47)$$

under the simplifying assumption that $a_{T_\sigma} = 0$.

As previously observed for the stadimetric method, in (5.47) θ is always positive, and $\dot{\theta}$ is almost always positive. Neglecting the rare and anomalous case of $\dot{\theta} \approx 0$, implying increasing range, $\dot{\theta}/\theta$ is positive and the solution for $\hat{\dot{r}}$ as a function of $\hat{r}$ passes through the origin with a time-varying negative slope which is a quotient of non-zero finite quantities. In the kinematic approach (5.46), the

coefficient of $\hat{r}$ will normally have a negative value but is
a quotient in which the numerator and denominator rapidly
approach small values and ultimately zero, in favorable
geometries, and start and remain at small values in unfavorable
geometries. The slope of (5.46) and the joint solution of
(5.46) and (5.47), therefore are increasingly sensitive to
instrument and computation noise as the maneuver becomes
small. In geometric terms, the two lines in the $(\hat{r}, \dot{\hat{r}})$
space of Figure 5.2 become parallel as the maneuver becomes
small.

In consequence, it is evident that the stadimetric/linear-
kinematic method outlined above could be improved by use of the
nonlinear kinematic method described in Section 4.

6. TECHNOLOGY ASSESSMENT

It appears that linear methods of kinematic ranging can work effectively only for favorable combat geometries and if the sensor noise levels are quite low. This implies high accuracy sensors, and frequent ineffectivity.

The nonlinear filter described in Section 4 estimates the target velocity-vector components and therefore can be used to deduce the target velocity and aspect angle. The filter also estimates the target's acceleration components, the turn-rate, and its derivative. It therefore estimates the entire specification of the target dynamics, and can be used to estimate the target future trajectory, and time to go. This may be useful not only to the air-air missile terminal-control guidance problem but also to a variety of terminal fire control systems in aircraft or helicopters instead of missiles. This nonlinear filter can also be used to eliminate impossible target accelerations from data provided by other tracking systems such as radar or laser rangers.

Many of the newer seekers of TV or IR types provide some indication of the target size or shape. Target size data can be used as a partial basis for a ranging system, as outlined in Section 5. In addition, information on the target shape or its aspect-angle can be used to provide clues enabling nonlinear filtering. For example, if the target is viewed from a head-on or tail-chase aspect it is clearly

difficult for the target to accelerate parallel to the
Line of Sight; it can accelerate across the line of sight
with relative ease.

Linear stadimetric ranging cannot by itself estimate
range and range-rate, but only their ratio. However, com-
bing linear stadimetry and kinematic schemes has the effect
of reducing the number of unknown variables to be determined
simultaneously. The parameter identification problem may in
fact be reduced to a problem in 2-space, without using the
poor assumptions that $\ddot{r}$, a_{T_r}, and a_{T_σ} are quasi-constant.

In this situation, two or (preferably) more independent
measurement instants enable an unique solution. The problem
of updating the hyperplane of Figs. 5.1 or 5.2 to another
instant is then reduced.   It is not eliminated, therefore
the solution is not rigorously observable; however, the
combination may be useful.

In a review of the present technology and an estimate of
the trends and potentials,the interaction of cost with systems
technology is perhaps most important in the air-air missile
problem. These points stand out:

a) Seekers of all kinds are very expensive; a
   small radar seeker is very costly in weight,
   space and dollars. A TV seeker may be less
   expensive in each sense, but is not cheap. The
   various sophisticated IR seekers are cheaper but
   are still quite costly compared to the simplest
   IR seekers.

(b) Sensors such as rate gyros are an order
    of magnitude less costly than simple seekers.

85

c) The introduction of medium or large scale integrated digital and analog chips has at once improved the reliability of the computation process and reduced the cost by orders of magnitude.

Taken together, these elements suggest that cost/effectivity considerations lead to improving missile system performance by combining a wide range of the inexpensive sensors with a relatively sophisticated computation capability. This may enable use of a relatively unsophisticated seeker of relatively low cost.

The nonlinear range/range rate estimator shown in Fig. 4.1 requires a considerable computation capability, and requires input signals from a pair of accelerometers. It also requires the missile airspeed components which may be obtained from relatively inexpensive sensors or may be estimated from accelerometer and rate-gyro data. But the least sophisticated seeker is sufficient. Our approach was to maximize the information which could be extracted from an inexpensive seeker by combining several inexpensive sensors with a relatively sophisticated yet inexpensive computer which will soon be available.

7. <u>REFERENCES</u>

1. Eyckhoff, P., "Aspects of Process Parameter Estimation," IEEE Transactions on Automatic Control, October, 1963.

2. Narendra, T. S., and L. E. McBride, "Multi-Parameter Self-Optimizing System Using Correlation Techniques," IEEE Transactions on Automatic Control, January, 1962.

3. Young, P. C., "The Use of Linear Regression and Related Procedures for the Identification of Dynamic Processes," IEEE Proceedings of the Seventh Symposium on Adaptive Processes, UCLA, December, 1968.

4. Lion, P. M., "Rapid Identification of Linear and Nonlinear Systems," AIAA Journal, Vol. 5, No. 10, October, 1967.

5. Bell Aerospace Company Report 9500-920183, "Adaptive Modeling and Control," F. D. Powell, June, 1970, Final Report on Office of Naval Research Contract Nonr-4864(00), NR049-207.

6. NASA Report 68-11-7, "Use of Integral Transforms in Parameter Estimation." H. C. Lessing and D. F. Crane, 1968.

7. Morrison, N., "Introduction to Sequential Smoothing and Prediction," McGraw-Hill Book Company, New York 1969.

8. Kalman, R. E., "A New Approach to Linear Filtering and Prediction Problems, " Transactions of the A.S.M.E., Journal of Basic Engineering, Vol. 82, PP 35-45, March, 1960.

APPENDICES

APPENDIX A

The Nonlinear Estimator; Derivation and Instrumentation

It is possible, due to the particular form of the equations and constraints of the Mathematical Model of the system, to develop a nonlinear range and range-rate identifier. This type of identifier is discussed in this section.

A.1 Analysis

The key elements cf the Mathematical Model are quoted from Section 3:

Velocity component equations parallel to the Line-of-Sight:

$$\dot{r} - V_T \cos(\gamma_T - \sigma) + V_M \cos(\gamma_M - \sigma) = 0,$$

or

$$\dot{r} - V_{T_r} + V_{M_r} = 0.$$

(A.1)

Velocity component equations perpendicular to the LOS

$$r\dot{\sigma} - V_T \sin(\gamma_T - \sigma) + V_M \sin(\gamma_M - \sigma) = 0,$$

or

$$r\dot{\sigma} - V_{T_\sigma} + V_{M_\sigma} = 0.$$

(A.2)

We also demonstrated that the acceleration component equations parallel and perpendicular to the LOS are, respectively:

$$\ddot{r} - r\dot{\sigma}^2 - a_{T_r} + a_{M_r} = 0$$

(A.3)

and

$$r\ddot{\sigma} + 2\dot{r}\dot{\sigma} - a_{T_\sigma} + a_{M_\sigma} = 0.$$

(A.4)

The target and missile velocity and acceleration components parallel and perpendicular to the LOS are:

Velocities:

Parallel: $V_{T_r} = V_T \cos \xi_T$

$$V_{M_r} = V_M \cos \xi_M$$

Perpendicular: $V_{T_\sigma} = V_T \sin \xi_T$

$$V_{M_\sigma} = V_M \sin \xi_M.$$

(A.5)

Accelerations:

Parallel: $a_{T_r} = \dot{V}_T \cos \xi_T - V_T\dot{\gamma}_T \sin \xi_T$

$$a_{M_r} = \dot{V}_M \cos \xi_M - V_M\dot{\gamma}_M \sin \xi_T$$

Perpendicular: $a_{T_\sigma} = \dot{V}_T \sin \xi_T + V_T \dot{\gamma}_T \cos \xi_T$

(A.6)

$$a_{M_\sigma} = \dot{V}_T \sin \xi_T + V_M\dot{\gamma}_M \cos \xi_T$$

where

89

Angles: $\quad \xi_T = \gamma_T - \sigma$

$\qquad\quad \xi_M = \gamma_M - \sigma.$ $\qquad\qquad\qquad\qquad\qquad$ (A.7)

The principle of this approach is simply to solve A.3 for $\ddot{r}$ as

$$\ddot{r} = r\dot{\sigma}^2 + a_{M_r} - a_{T_r}. \qquad\qquad (A.8)$$

Integration of $\ddot{r}$ will yield $\dot{r}$ and r if the terms on the right of (A.8) are available.

The term $r\dot{\sigma}^2$ can be computed easily while a_{M_r}, the missile acceleration parallel to the LOS, can be measured directly The problem therefore is now to estimate a_{T_r} in some way. It is assumed that initial values of $\hat{r}$ and $\hat{\dot{r}}$ are provided.

It was shown that the target acceleration in the range direction, a_{T_r}, can be determined from available data. The procedure is first to calculate V_T, the target airspeed, by use of (A.1) and (A.2) as

$$(\dot{r} + V_M \cos \xi_M)^2 + (r\dot{\sigma} + V_M \sin \xi_M)^2 =$$

$$V_T^2 \cos^2 \xi_T + V_T^2 \sin^2 \xi_T = V_{T_r}^2 + V_{T_\sigma}^2 = V_T^2. \qquad (A.9)$$

It was stated in Section (4.1) that this expression may be differentiated to yield $\quad V_{T_r} a_{T_r} + V_{T_\sigma} a_{T_\sigma} = V_T \dot{V}_T;$ This is demonstrated below. Therefore, let us differentiate (A.9) with respect to time, yielding

$$2\{(\dot{r} + V_M \cos \xi_M)[\ddot{r} + (\dot{V}_M \cos \xi_M - V_M \dot{\gamma}_M \sin \xi_M) + V_M \dot{\sigma} \sin \xi_M]$$

$$+ (r\dot{\sigma} + V_M \sin \xi_M)[r\ddot{\sigma} + \dot{r}\dot{\sigma} + (\dot{V}_M \sin \xi_M + V_M \dot{\gamma}_M \cos \xi_M) -$$

$$V_M \dot{\sigma} \cos \xi_M]\} = 2 V_T \dot{V}_T.$$

90

Substitute from (A.5) the simplifying notation for the acceleration components of the missile, a_{M_r} and a_{M_σ}, parallel and perpendicular to the LOS, respectively; these accelerations are gathered in parenthesis within the same brackets in the expression above [( )].

This yields

$$(\dot{r} + V_M \cos \xi_M)(\ddot{r} + a_{M_r} + V_M \dot{\sigma} \sin \xi_M)$$
$$+ (r\dot{\sigma} + V_M \sin \xi_M)(r\ddot{\sigma} + \dot{r}\dot{\sigma} + a_{M_\sigma} - V_M \dot{\sigma} \cos \xi_M) =$$
$$V_T \dot{V}_T. \qquad (A.10)$$

Now solve (A.2) for $V_M \sin \xi_M$, multiply by $\dot{\sigma}$ and replace the term $(V_M \dot{\sigma} \sin \xi_M)$ on the first line of (A.10) by the term thus formed. Similarly, solve (A.1) for $V_M \cos \xi_M$, multiply by $\dot{\sigma}$ and eliminate the term $(V_M \dot{\sigma} \cos \xi_M)$ from the second line of (A.10). These substitutions yield

$$(\dot{r} + V_M \cos \xi_M)(\ddot{r} - r\dot{\sigma}^2 + a_{M_r} + \dot{\sigma}V_T \sin \xi_T) +$$
$$(r\dot{\sigma} + V_M \sin \xi_M)(r\ddot{\sigma} + 2\dot{r}\dot{\sigma} + a_{M_\sigma} - \dot{\sigma}V_T \cos \xi_T) =$$
$$V_T \dot{V}_T.$$

Keeping the right side of this expression, gather the coefficients of V_T on the left; this reduces to

$$(\dot{r}+V_M \cos \xi_M)(\ddot{r} - r\dot{\sigma}^2 + a_{M_r}) + (r\dot{\sigma} + V_M \sin \xi_M)$$
$$(r\ddot{\sigma} + 2\dot{r}\dot{\sigma} + a_{M_\sigma}) + \dot{\sigma}\{(\dot{r}+V_M \cos \xi_M)(V_T \sin \xi_T) -$$
$$-(r\dot{\sigma} + V_M \sin \xi_M)(V_T \cos \xi_T)\} = V_T \dot{V}_T \qquad (A.11)$$

The term in curly braces { } in (A.11) is identically zero. This follows from (A.1), $\dot{r} + V_M \cos \xi_M = V_T \cos \xi_T$, while from (A.2), $r\dot{\sigma} + V_M \sin \xi_M = V_T \sin \xi_T$, so that the brace has the value $\{V_T \cos \xi_T (V_T \sin \xi_T) - V_T \sin \xi_T (V_T \cos \xi_T)\} = 0$.

As a consequence, (A.11) takes the simpler form

$$(\dot{r} + V_M \cos \xi_M)(\ddot{r} - r\dot{\sigma}^2 + a_{M_r}) + (r\dot{\sigma} + V_M \sin \xi_M)$$

$$(r\ddot{\sigma} + 2\dot{r}\dot{\sigma} + a_{M_r}) = V_T \dot{V}_T. \tag{A.12}$$

By use of (A.1) through (A.6), this may be expressed in the intuitively satisfying form $V_{T_r} a_{T_r} + V_{T_\sigma} a_{T_\sigma} = V_T \dot{V}_T$, (A.13) which is the form used in the discussion in Section 4, where we use the simplifying notation, from (A.5),

$$V_{T_r} = V_T \cos \xi_T$$

$$V_{T_\sigma} = V_T \sin \xi_T$$

to express the target velocity components parallel and perpendicular to the LOS.

The exact solution for a_{T_r} is thus

$$a_{T_r} = \frac{V_T \dot{V}_T - V_{T_\sigma} a_{T_\sigma}}{V_{T_r}} . \tag{A.14}$$

and

$$\ddot{r} = r\dot{\sigma}^2 - a_{M_r} + \frac{V_T \dot{V}_T - V_{T_\sigma} a_{T_\sigma}}{V_{T_r}} , \tag{A.15}$$

while a_{T_σ}

$$\frac{a_{T_\sigma}}{V_{T_r}} = \dot{\gamma}_T \quad \text{if} \quad \dot{V}_T = 0.$$

Usually $\dot{V}_T$ is small and can be neglected, and all other terms on the right of (A.15) can be estimated.

The mechanization of this algorithm is discussed in Section (A.2), following.

A.2 Mechanization of the Signals for the Ideal Algorithm

The range acceleration is given by (A.15); it may be integrated to yield $\dot{r}$ and r. The term $r\dot{\sigma}^2$ can then be formed, while the missile acceleration component, a_{M_r}, can be directly sensed.

The mechanization of (A.15) requires that missile airspeed V_M, the missile acceleration components a_{M_r} and a_{M_σ}, and the angle ξ_M be available as signals or be estimated. It will now be shown that this can be accomplished.

(a) Acceleration Components

The accelerometer components, a_{M_r}, and a_{M_σ}, are a special case; two easy solutions are available:

(1) Mount the accelerometers on the seeker; then one yields a_{M_r} and the other yields a_{M_σ} directly.

(2) Mount the accelerometers on the missile body; then their signals are a_{M_x}, and a_{M_y}, fore – aft and cross-body, respectively; and resolution of the signals from the accelerometer through

93

the "look-angle," λ, yields

$$\begin{pmatrix} a_{M_r} \\ a_{M_\sigma} \end{pmatrix} = \begin{pmatrix} \cos \lambda & -\sin \lambda \\ \sin \lambda & \cos \lambda \end{pmatrix} \begin{pmatrix} a_{M_x} \\ a_{M_y} \end{pmatrix}. \qquad (A.16)$$

As the "look-angle," λ, between the missile centerline and the LOS can easily be made physically available in a seeker gimbal, the resolution of the acceleration components is easily accomplished.

(b) <u>Velocity Estimation</u>

If the missile body pitch rate, q, or equivalent, is an available signal, and further, if the cross-body acceleration of the missile, a_{M_y}, is also available as a signal, it is relatively easy to estimate missile velocity, V_M.

The pertinent equations of motion of the missile are,

$$\dot{\alpha} = q - \frac{a_{M_y}}{V_M} \qquad (A.17)$$

$$a_{M_y} = N\alpha + G\delta$$

where α angle of attack

$\qquad a_{M_y}$ cross-body acceleration

$\qquad \delta$ control displacement

$\qquad q$ body pitch rate

$\qquad V_M$ airspeed

N, G   cross-body accelerations per

radian, due to angle of attack

and control displacements,

respectively

Assuming quasi-constant conditions, the transfer
function defining acceleration is

$$a_{M_y} = \frac{N\ q + Gs\delta}{s+N/V_M} \ .$$ (A.18)

The acceleration due to control displacement may
usually be neglected so that

$$a_{M_y} \simeq \frac{N\ q}{s+N/V_M} = V_M \left(\frac{N/V_M}{s+N/V_M} \right) \ q$$

$$= V_M \ \frac{q}{Ts+1}$$ (A.19)

where $T = V_M/N$. Then V_M may be estimated by the algorithms

$$\hat{\dot{V}}_M = k\ a_{M_y}\ (a_{M_y} - \hat{V}_M\ q)$$

(A.20)

or $$\hat{\dot{V}}_M = k\ (\ |a_{M_y}| - \hat{V}_M\ |q|\ )$$ (A.21)

where $k > 0$ has the appropriate value.

Somewhat superior algorithms which will lag less
are achieved by biassing the algorithms given by the missile
longitudinal acceleration component a_{M_x}.

Algorithm (A.21) is obviously simple to instrument, requiring only one multiplication.

(c) Estimation of the Angle ξ_M

The angle ξ_M is defined as $\xi_M = \gamma_M - \sigma$. But as $\gamma_M = \theta_M - \alpha$, where θ_M is the centerline attitude, then $\xi_M = \theta_M - \alpha - \sigma$, and as the angle from missile centerline to the seeker LOS is

$$\lambda = \sigma - \theta_M$$

we have $\xi_M = -\lambda - \alpha$ (A.22)

where α is the angle of attack between the missile centerline and the velocity vector. But this can easily be estimated as

$$\hat{\alpha} \simeq \frac{q}{Ts+1}$$

(A.23)

where T was defined above.

The missile velocity components V_{M_r} and V_{M_σ} can then be computed as $V_{M_r} = V_M \cos \xi_M$ and $V_{M_\sigma} = V_M \sin \xi_M$.

APPENDIX B

Error Analysis Coefficients

The numerical data presented in this appendix represent the time varying coefficients of the error equation. As discussed in Chapter 4, the error equation is of the form

$$\ddot{x} + a_1 \dot{x} + a_2 x = \sum_{i=1}^{7} b_i N_i,$$

and the data here represent the coefficients a_i and b_i tabulated for every 0.25 seconds. There are six tables, representing a selection of six choices of initial geometry configuration. They are ordered, and correspond respectively to Figures 4.3 through 4.8 inclusive; however, each graph is labelled to show the initial geometry. These data permit more general stochastic analyses of the effects on the estimates due to errors in the several signals which are used in the algorithm. The coefficients a_1 and a_2 are:

$$a_1 = 2\dot{\sigma} \tan \xi_T - \dot{\gamma}_T \tan \xi_T , \text{ and}$$

$$a_2 = -\dot{\sigma}^2 + \dot{\gamma}_T \dot{\sigma} + \ddot{\sigma} \tan \xi_T.$$

The coefficients b_i and error sources N_i are:

$b_1 = -1$ $\qquad\qquad N_1 \quad a_{M_r}$, accel⊥LOS error

$b_2 = \sec \xi_T$ $\qquad\qquad N_2 \quad \dot{V}_T$, target airspeed change

$b_3 = -\dot{\gamma}_T \sec \xi_T \sin (\gamma_M - \gamma_T)$ $\qquad N_3 \quad \hat{V}_M$, missile airspeed error

$b_4 = -r\dot{\gamma}_T - 2\dot{r}\tan \xi_T + 2r\dot{\sigma}$ N_4 $\dot{\sigma}$, LOS rate error

$b_5 = -V_M\dot{\gamma}_T \sec \xi_T \cos (\gamma_M - \gamma_T)$ N_5 $\hat{\xi}_M$, error of estimating $\hat{\alpha}$

$b_6 = -r\tan \xi_T$ N_6 $\ddot{\sigma}$ LOS acceleration error

$b_7 = -\tan \xi_T$ N_7 a_{M_σ} , accel. $\perp$ LOS, error

All angles are in radian measure unless specifically stated otherwise.

The data of this appendix are presented in a conventional "exponential format" for digital output data. Thus the tabulated item 0.422E 01 is interpreted as $(0.422)10^{+1} = 4.22$, while $-0.244E-01$ is interpreted as $(-0.244)10^{-1} = -0.0244$.

TIME	a1	A2	A1	B2	B3	b4	b5	B6	B7
0.0	0.422E 01	0.451E 00	-0.100E 01	0.100E 02	-0.153E 01	0.445E 05	0.454E 03	-0.100E 06	-0.954E 06
0.250E 00	0.232E 01	-0.330E 00	-0.100E 01	0.572E 01	-0.104E 01	0.261E 05	0.275E 03	-0.535E 05	-0.663E 05
0.500E 00	0.150E 01	-0.285E 00	-0.100E 01	0.407E 01	-0.714E 00	0.194E 05	0.442E 03	-0.358E 05	-0.355E 05
0.750E 00	0.105E 01	-0.256E 00	-0.100E 01	0.322E 01	-0.531E 00	0.140E 05	0.536E 03	-0.263E 05	-0.366E 05
0.100E 01	0.704E 00	-0.128E 00	-0.100E 01	0.270E 01	-0.412E 00	0.112E 05	0.591E 03	-0.205E 05	-0.251E 05
0.125E 01	0.562E 00	-0.130E 00	-0.100E 01	0.236E 01	-0.329E 00	0.914E 04	0.595E 03	-0.165E 05	-0.213E 05
0.150E 01	0.450E 00	-0.455E-01	-0.100E 01	0.211E 01	-0.266E 00	0.765E 04	0.593E 03	-0.134E 05	-0.186E 05
0.175E 01	0.369E 00	-0.692E-01	-0.100E 01	0.193E 01	-0.223E 00	0.651E 04	0.583E 03	-0.115E 05	-0.165E 05
0.200E 01	0.304E 00	-0.501E-01	-0.100E 01	0.178E 01	-0.189E 00	0.563E 04	0.569E 03	-0.972E 04	-0.146E 05
0.225E 01	0.255E 00	-0.356E-01	-0.100E 01	0.167E 01	-0.162E 00	0.493E 04	0.553E 03	-0.831E 04	-0.134E 05
0.250E 01	0.213E 00	-0.251E-01	-0.100E 01	0.157E 01	-0.140E 00	0.436E 04	0.537E 03	-0.714E 04	-0.121E 05
0.275E 01	0.189E 00	-0.170E-01	-0.100E 01	0.149E 01	-0.123E 00	0.339E 04	0.522E 03	-0.615E 04	-0.111E 05
0.300E 01	0.166E 00	-0.110E-01	-0.100E 01	0.143E 01	-0.108E 00	0.350E 04	0.507E 03	-0.530E 04	-0.102E 05
0.325E 01	0.147E 00	-0.654E-02	-0.100E 01	0.137E 01	-0.955E-01	0.316E 04	0.49?E 03	-0.457E 04	-0.933E 03
0.350E 01	0.131E 00	-0.333E-02	-0.100E 01	0.132E 01	-0.863E-01	0.286E 04	0.481E 03	-0.392E 04	-0.857E 03
0.375E 01	0.119E 00	-0.104E-02	-0.100E 01	0.127E 01	-0.776E-01	0.260E 04	0.495E 03	-0.335E 04	-0.787E 03
0.400E 01	0.107E 00	0.557E-03	-0.100E 01	0.123E 01	-0.699E-01	0.236E 04	0.459E 03	-0.285E 04	-0.722E 03
0.425E 01	0.965E-01	0.166E-02	-0.100E 01	0.120E 01	-0.630E-01	0.215E 04	0.444E 03	-0.241E 04	-0.641E 03
0.450E 01	0.874E-01	0.241E-02	-0.100E 01	0.117E 01	-0.567E-01	0.194E 04	0.441E 03	-0.202E 04	-0.604E 03
0.475E 01	0.790E-01	0.292E-02	-0.100E 01	0.114E 01	-0.510E-01	0.175E 04	0.433E 03	-0.167E 04	-0.549E 03
0.500E 01	0.711E-01	0.328E-02	-0.100E 01	0.112E 01	-0.458E-01	0.158E 04	0.426E 03	-0.137E 04	-0.492E 03
0.525E 01	0.637E-01	0.354E-02	-0.100E 01	0.110E 01	-0.409E-01	0.141E 04	0.420E 03	-0.110E 04	-0.445E 03
0.550E 01	0.565E-01	0.373E-02	-0.100E 01	0.109E 01	-0.363E-01	0.125E 04	0.414E 03	-0.862E 03	-0.400E 03
0.575E 01	0.499E-01	0.391E-02	-0.100E 01	0.106E 01	-0.319E-01	0.109E 04	0.409E 03	-0.655E 03	-0.354E 03
0.600E 01	0.434E-01	0.403E-02	-0.100E 01	0.105E 01	-0.278E-01	0.939E 03	0.405E 03	-0.485E 03	-0.305E 03
0.625E 01	0.370E-01	0.415E-02	-0.100E 01	0.103E 01	-0.238E-01	0.793E 03	0.402E 03	-0.340E 03	-0.265E 03
0.650E 01	0.308E-01	0.426E-02	-0.100E 01	0.102E 01	-0.200E-01	0.651E 03	0.399E 03	-0.220E 03	-0.223E 03
0.675E 01	0.246E-01	0.435E-02	-0.100E 01	0.102E 01	-0.163E-01	0.511E 03	0.396E 03	-0.127E 03	-0.180E 03
0.700E 01	0.185E-01	0.435E-02	-0.100E 01	0.101E 01	-0.127E-01	0.373E 03	0.394E 03	-0.573E 02	-0.133E 02
0.725E 01	0.244E-01	0.180E-01	-0.100E 01	0.100E 01	-0.939E-02	0.244E 03	0.392E 03	-0.117E 02	-0.916E-01

TABLE B-1

Error Equation Coefficients a_1 and b_1 as functions of the time for the trajectory of Fig. 4.3 with initial conditions $\psi = 90°$, $\phi = 0°$, $x_T = 10{,}000$, $y_T = 1{,}000$.

Time	A1	A2	B1	B2	B3	B4	B5	B6	B7
0.0	0.240E 01	0.501E 00	-0.100E 01	0.100E 02	0.0	0.430E 05	0.0	-0.100E 06	-0.559E 01
0.250E 00	0.177E 01	-0.367E 01	-0.100E 01	0.771E 01	0.0	0.329E 05	0.0	-0.729E 05	-0.764E 01
0.500E 00	0.126E 01	-0.343E 01	-0.100E 01	0.538E 01	0.0	0.269E 05	0.0	-0.572E 05	-0.636E 01
0.750E 00	0.924E 00	-0.404E 00	-0.100E 01	0.557E 01	0.0	0.228E 05	0.0	-0.468E 05	-0.544E 01
0.100E 01	0.663E 00	-0.308E 00	-0.100E 01	0.505E 01	0.0	0.199E 05	0.0	-0.399E 05	-0.455E 01
0.125E 01	0.484E 00	-0.238E 00	-0.100E 01	0.470E 01	0.0	0.178E 05	0.0	-0.349E 05	-0.459E 01
0.150E 01	0.355E 00	-0.185E 00	-0.100E 01	0.446E 01	0.0	0.163E 05	0.0	-0.311E 05	-0.435E 01
0.175E 01	0.260E 00	-0.144E 00	-0.100E 01	0.430E 01	0.0	0.152E 05	0.0	-0.280E 05	-0.419E 01
0.200E 01	0.189E 00	-0.112E 00	-0.100E 01	0.418E 01	0.0	0.144E 05	0.0	-0.254E 05	-0.406E 01
0.225E 01	0.136E 00	-0.870E-01	-0.100E 01	0.409E 01	0.0	0.138E 05	0.0	-0.231E 05	-0.397E 01
0.250E 01	0.956E-01	-0.666E-01	-0.100E 01	0.404E 01	0.0	0.134E 05	0.0	-0.211E 05	-0.391E 01
0.275E 01	0.656E-01	-0.501E-01	-0.100E 01	0.400E 01	0.0	0.131E 05	0.0	-0.193E 05	-0.387E 01
0.300E 01	0.435E-01	-0.365E-01	-0.100E 01	0.397E 01	0.0	0.129E 05	0.0	-0.175E 05	-0.384E 01
0.325E 01	0.276E-01	-0.263E-01	-0.100E 01	0.395E 01	0.0	0.128E 05	0.0	-0.158E 05	-0.382E 01
0.350E 01	0.164E-01	-0.164E-01	-0.100E 01	0.394E 01	0.0	0.127E 05	0.0	-0.142E 05	-0.381E 01
0.375E 01	0.891E-02	-0.116E-01	-0.100E 01	0.394E 01	0.0	0.127E 05	0.0	-0.126E 05	-0.381E 01
0.400E 01	0.417E-02	-0.689E-02	-0.100E 01	0.394E 01	0.0	0.126E 05	0.0	-0.110E 05	-0.380E 01
0.425E 01	0.133E-02	-0.374E-02	-0.100E 01	0.393E 01	0.0	0.126E 05	0.0	-0.943E 04	-0.360E 01
0.450E 01	-0.375E-03	-0.176E-02	-0.100E 01	0.393E 01	0.0	0.126E 05	0.0	-0.785E 04	-0.380E 01
0.475E 01	-0.155E-02	-0.113E-02	-0.100E 01	0.393E 01	0.0	0.126E 05	0.0	-0.628E 04	-0.380E 01
0.500E 01	-0.336E-02	-0.172E-02	-0.100E 01	0.394E 01	0.0	0.126E 05	0.0	-0.470E 04	-0.381E 01
0.525E 01	-0.730E-02	-0.454E-02	-0.100E 01	0.394E 01	0.0	0.126E 05	0.0	-0.312E 04	-0.381E 01
0.550E 01	-0.202E-01	-0.408E-01	-0.100E 01	0.394E 01	0.0	0.126E 05	0.0	-0.154E 04	-0.381E 01

TABLE B-2

Error Equation Coefficients a_i and b_i as functions of the time for the trajectory of Fig. 4.4 with initial conditions $\psi = 90°$, $\phi = 0°$, $x_T = 10,000$, $y_T = 1,000$.

$a_1 = 2\dot{\sigma} \tan \xi_T - \dot{\gamma}_T \tan \xi_T$

$a_2 = -\dot{\sigma}^2 + \dot{\gamma}_T \ddot{\sigma} + \ddot{\sigma} \tan \xi_T$

$b_1 = -1$

$b_2 = \sec \xi_T$

$b_3 = -\dot{\gamma}_T \sec \xi_T \sin (\gamma_M - \gamma_T)$

$b_4 = -\dot{r}\dot{\gamma}_T - 2\dot{r} \tan \xi_T + 2r\dot{\sigma}$

$b_5 = -V_M \dot{\gamma}_T \sec \xi_T \cos (\gamma_M - \gamma_T)$

$b_6 = -r \tan \xi_T$

$b_7 = -\tan \xi_T$

N_1 a_{M_r}, accel ∥ LOS error

N_2 $\dot{V}_T$, target airspeed change

N_3 $\hat{V}_M$, missile airspeed error

N_4 $\dot{\sigma}$, LOS rate error

N_5 ξ_M, error of estimating $\hat{a}$

N_6 $\ddot{\sigma}$ LOS acceleration error

N_7 a_{M_σ}, accel ⊥ LOS error

100

TIME	A1	A2	B1	B2	B3	B4	B5	B6	B7
0.0	0.579E 00	0.541E 00	-0.100E 01	0.100E 02	0.193E 01	0.412E 05	-0.454E 05	-0.100E 06	-0.955E 01
0.250E 00	0.591E 00	-0.549E 00	-0.100E 01	0.118E 02	0.216E 01	0.490E 05	-0.147E 05	-0.112E 06	-0.118E 02
0.500E 00	0.351E 00	-0.250E 00	-0.100E 01	0.151E 02	0.274E 01	0.626E 05	-0.581E 05	-0.136E 06	-0.150E 02
0.750E 00	-0.192E 00	-0.150E 00	-0.100E 01	0.224E 02	0.403E 01	0.932E 05	-0.145E 05	-0.198E 06	-0.224E 02
0.100E 01	-0.230E 01	-0.335E 01	-0.100E 01	0.539E 02	0.958E 01	0.224E 06	-0.473E 06	-0.430E 06	-0.539E 02
0.125E 01	0.620E 01	0.464E 01	-0.100E 01	-0.875E 02	-0.154E 02	-0.364E 06	0.898E 06	0.653E 06	0.875E 02
0.150E 01	0.214E 01	0.100E 01	-0.100E 01	-0.224E 02	-0.392E 01	-0.933E 05	0.248E 05	0.155E 06	0.223E 02
0.175E 01	0.144E 01	0.471E 01	-0.100E 01	-0.124E 02	-0.216E 01	-0.520E 05	0.140E 05	0.793E 05	0.123E 02
0.200E 01	0.111E 01	0.271E 01	-0.100E 01	-0.841E 01	-0.147E 01	-0.356E 05	0.933E 05	0.453E 05	0.835E 01
0.225E 01	0.921E 00	0.173E 00	-0.100E 01	-0.629E 01	-0.111E 01	-0.270E 05	0.659E 05	0.334E 05	0.621E 01
0.250E 01	0.787E 00	0.117E 00	-0.100E 01	-0.499E 01	-0.683E 00	-0.216E 05	0.474E 05	0.237E 05	0.489E 01
0.275E 01	0.687E 00	0.832E-01	-0.100E 01	-0.411E 01	-0.734E 00	-0.180E 05	0.339E 05	0.172E 05	0.359E 01
0.300E 01	0.608E 00	0.613E-01	-0.100E 01	-0.349E 01	-0.628E 00	-0.154E 05	0.234E 05	0.126E 05	0.335E 01
0.325E 01	0.544E 00	0.465E-01	-0.100E 01	-0.303E 01	-0.548E 00	-0.135E 05	0.149E 05	0.918E 04	0.286E 01
0.350E 01	0.492E 00	0.364E-01	-0.100E 01	-0.267E 01	-0.486E 00	-0.119E 05	0.779E 04	0.655E 04	0.248E 01
0.375E 01	0.447E 00	0.294E-01	-0.100E 01	-0.239E 01	-0.436E 00	-0.106E 05	0.170E 04	0.448E 04	0.217E 01
0.400E 01	0.409E 00	0.252E-01	-0.100E 01	-0.216E 01	-0.394E 00	-0.953E 04	-0.362E 04	0.281E 04	0.192E 01
0.425E 01	0.378E 00	0.271E-01	-0.100E 01	-0.198E 01	-0.359E 00	-0.858E 04	-0.834E 04	0.147E 04	0.170E 01
0.450E 01	0.367E 00	0.185E 00	-0.100E 01	-0.182E 01	-0.327E 00	-0.773E 04	-0.126E 05	0.361E 03	0.152E 01

TABLE B-3

Error Equation Coefficients a_i and b_i as functions of the time for the trajectory of Fig. 4.5 with initial conditions $\psi=90°$, $\phi=80°$, $x_T = 10,000$, $y_T = 1,000$.

$a_1 = 2\dot{\sigma} \tan \xi_T - \dot{\gamma}_T \tan \xi_T$

$a_2 = -\dot{\sigma}^2 + \dot{\gamma}_T \dot{\sigma} + \ddot{\sigma} \tan \xi_T$

$b_1 = -1$

$b_2 = \sec \xi_T$

$b_3 = -\dot{\gamma}_T \sec \xi_T \sin(\gamma_M - \gamma_T)$

$b_4 = -r\dot{\gamma}_T - 2\dot{r} \tan \xi_T + 2r\dot{\sigma}$

$b_5 = -V_M \dot{\gamma}_T \sec \xi_T \cos(\gamma_M - \gamma_T)$

$b_6 = -r \tan \xi_T$

$b_7 = -\tan \xi_T$

N_1 a_{M_r}, accel|| LOS error

N_2 $\dot{V}_T$, target airspeed change

N_3 $\dot{V}_M$, missile airspeed error

N_4 $\dot{\sigma}$, LOS rate error

N_5 $\hat{\xi}_M$, error of estimating $\hat{\alpha}$

N_6 $\ddot{\sigma}$ LOS acceleration error

N_7 a_{M_σ}, accel. $\perp$ LOS, error

101

The matrix T_n is thus a "continuously updated observation matrix" and the vector $Y_{(n)}$ is a "series of output observations". The expression (5.21) is valid provided the noise $\underline{v}$ is independent from computing instant to instant and has zero mean. The construction of the matrix T_n is often a formidable task as it requires keeping in storage a large amount of past data $H(t_i)$ so that it can be updated by the state transition matrix $\Phi(t_i, t_j)$ which is at times also difficult to obtain.

Apply this theory to, typically, the reduced dimensionality problem defined by (5.16) and (5.17); assume that $\dot{r}$ is constant, thus x_2 is constant after convergence. But $x_1 = r$ and is not constant. Now we have, at some specific instant, and with only one value of $i = 1$,

$$v_1(t_1)x_1 + v_2(t_1)x_2 + y_1 = e_5.$$

$$(5.24)$$

At the next instant we have

$$v_1(t_2)x_1 + v_2(t_2)x_2 + y_2 = e_5.$$

$$(5.25)$$

But while the value of x_2 is ideally the same at these two instants, the value of x_1 changes continuously, for $x_1 = r$, and r is the integral of $\dot{r}$. We may modify (5.24) so that x_1 is the same for the two instants. If Δt

66

is the time between samples, we may rewrite (5.24) as

$$v_1(t_1) \, (x_1(t_2) + x_2 \, \Delta t) + v_2 \, (t_1) \, x_2 + y_1 = e_5 \, ,$$

which may be rearranged as

$$v_1(x_1) \, x_1(t_2) + \left(v_2 \, (t_1) + v_1 \, (t_1) \, \Delta t\right) x_2 + y_1 = e_5.$$

$$(5.26)$$

Now Eqns. (5.25) and (5.26) represent two measurements referred to the same instant, and may be solved jointly. More generally, a larger sequence of such instants may be gathered in the more general form of (5.23).

This method exhibited several modes of failure. Whenever any two of:

the missile velocity vector

the target velocity vector

the LOS

become colinear, or $\dot{\sigma} = 0$, the matrix $(T_n^T T_n)$ became ill-conditioned or indeterminate, yielding inaccurate and noise-sensitive solutions. In geometries when this mode of failure does not occur, this algorithm has a different mode of failure. If the duration of the stored memory exceeds 1/2 second, the neglected target acceleration parallel to the LOS, a_{m_r}, causes the estimate of $\dot{r}$ to be 30% to 50% in error within 1 to 2 seconds, as the assumption that $\ddot{r} = 0$ is too incorrect. On the other hand, a shorter duration memory results in high noise sensitivity. But these algorithms work

well (Range-Rate errors of 1%) if $a_{T_r} = 0$.

In any case the computational complexity and memory storage requirements of this algorithm are excessive. An alternate was therefore examined. If

$$\hat{r} = \hat{r}_0 + \int \hat{\dot{r}} \, dt$$

(5.27)

and $\quad x_1 = \hat{r}_0, \; x_2 = \hat{\dot{r}}, \;$ etc.,

then a much simpler algorithm results. At a number of successive instants we have

$$\begin{pmatrix} v_1(1) & v_2(1) \\ v_1(2) & v_2(2) + v_1 \Delta t \\ \vdots & \vdots \end{pmatrix} \begin{pmatrix} x_1 \\ x_2 \end{pmatrix} = \begin{pmatrix} y_1 \\ y_2 \\ \vdots \end{pmatrix}$$

(5.28)

and both x_1 and x_2 may be assumed constant. If the nth row of the left of (5.28) is

$$v_1(n) \quad v_2(n) + \Delta t \, v_1(n-1) \quad ,$$

then the matrix $(T_n^T T_n)$ may be recursively formed as

$$(T_n^T \, T_n) = (T_{n-1}^T \, T_{n-1}) + v_n v_n^T \, .$$

(5.29)

Although sufficiently simple to be feasible for
an air-air missile, this approach to range estimation
also failed for the same reasons:

     (a) Ill-conditioned matrix for some
           geometries,

     (b) High noise-sensitivity for short
           averaging times,

     (c) Large errors in range-rate estimates
           for longer averaging times due to
           the invalid assumption that $a_{T_r} = 0$.

When failure-mode (a) did not occur, and $a_{T_r} = 0$ was
valid, the algorithm yields estimate errors of the order
of 1%.

No attempt at estimating a_{T_r}, target acceleration
parallel to the LOS, by linear methods was successful.
Any algorithm which neglected $a_{T_r} \neq 0$ when it was signifi-
cant operated unsuccessfully; either excessive noise sensi-
tivity became a problem, or the neglected acceleration
caused excessive errors in the estimation of Range-Rate, $\hat{r}$.

In summary, except for encounter geometries which
yield ill-conditioned matrices, the matrix-inverse algorithms
work well with long-filtering times which eliminate noise
effects if the assumption that $a_{T_r} = 0$ is valid. If that

69

assumption is invalid, the matrix-inverse schemes fail
due to the bias in range-rate estimate caused by target
acceleration, or due to noise.

5.3 Observability

The failure of these various adaptive and matrix-
inverse parameter identification methods, whether continuous
or discrete, is fundamentally due to the existence of target
acceleration in the radial direction, parallel to the line of
flight. That acceleration component cannot be estimated
by linear techniques because it is "unobservable" in the
mathematical sense. This section relates the concept of
"observability" to this application and problem.

The state of a linear system with constant coefficents
in the dynamics and constant coefficients in the output
relation can be estimated from knowledge of the output pro-
vided the system is mathematically observable. For this
discussion, we view the quantities of range, range-rate,
etc., as states which are to be determined and consider the
signals of LOS-rate and missile acceleration as time-varying
parameters. In state-variable notation a plant may be
described as

Plant Dynamics: $\dot{x} = Ax + bu$

Output: $y = Hx + v$

$$(5.30)$$

where v is zero-mean Gaussian white noise, and x is an
N-component vector.

70

The observability of the system is specified by a
relationship between the A matrix, specifying the dynamics,
and the H matrix, relating the state to the output. If
the order of the system is N, then the matrix

$$O_N = [\ H^T \ \vdots \ A^T H^T \ \vdots \ (A^T)^2 H^T \ \vdots \ \dots \vdots (A^T)^{N-1} H^T \ ]$$

(5.31)

must have full rank for the system to be observable. Let
us now apply this to one of the possible formulations of
the problem. For the system definition, use the accelera-
tion-component equations from Section 2

accelerations

parallel to the $\quad \ddot{r} - r\dot{\sigma}^2 - a_{T_r} + a_{M_r} = 0$
LOS

(5.32)

Perpendicular to $\quad r\ddot{\sigma} + 2\dot{r}\dot{\sigma} - a_{T_\sigma} + a_{M_\sigma} = 0.$
the LOS

(5.33)

In order to cast this into the standard form of (5.30),
define state variables

$$
\begin{aligned}
x_1 &= \hat{r} \\
x_2 &= \hat{\dot{r}} \\
x_3 &= \hat{a}_{T_r} \\
x_4 &= \hat{a}_{T_\sigma}
\end{aligned}
\left.\begin{aligned}\ \\ \ \\ \ \\ \ \end{aligned}\right\}
$$

(5.34)

i.e. the variables x are the estimates of the unknown parameters. The last two lines of (5.34) express the fact that the two components of target acceleration must be estimated and are assumed to be unknown constants.

The state variable expression of the relationships among the several variables may be found from (5.32) and (5.34) as

$$
\begin{pmatrix} \dot{x}_1 \\ \dot{x}_2 \\ \dot{x}_3 \\ \dot{x}_4 \end{pmatrix} = \begin{pmatrix} 0 & 1 & 0 & 0 \\ \dot{\sigma}^2 & 0 & 1 & 0 \\ 0 & 0 & 0 & 0 \\ 0 & 0 & 0 & 0 \end{pmatrix} \begin{pmatrix} x_1 \\ x_2 \\ x_3 \\ x_4 \end{pmatrix} + \begin{pmatrix} 0 \\ -a_{m_r} \\ 0 \\ 0 \end{pmatrix} \quad .
$$

$$(5.35)$$

The first row of (5.35) expresses the differential equation relating range and range-rate estimates. The second row consists of (5.34) while the third and fourth rows express the assumption that the target's unknown accelerations a_{T_r} and a_{T_σ} are constant. From (5.35), the matrix A is

$$
A_n = \begin{pmatrix} 0 & 1 & 0 & 0 \\ \dot{\sigma}^2 & 0 & 1 & 0 \\ 0 & 0 & 0 & 0 \\ 0 & 0 & 0 & 0 \end{pmatrix}
$$

$$(5.36)$$

and N=4.

Equation (5.33) yields the output relationship

$$(\ -\ddot{\sigma} \quad -2\dot{\sigma} \quad 0 \quad 1 \ ) \begin{pmatrix} x_1 \\ x_2 \\ x_3 \\ x_4 \end{pmatrix} = \hat{a}_{M_\sigma} \ ; $$

(5.37)

comparison of the estimate, $\hat{a}_{M_\sigma}$, with the measured

acceleration a_{M_σ} yields an error whose minimization will

presumably yield optimal estimates of the range, x_1, and

range-rate, x_2. From (5.37),

$$H = (\ -\ddot{\sigma} \quad -2\dot{\sigma} \quad 0 \quad 1 \ ).$$

(5.38)

Combining (5.36) with (5.38) in the format of (5.35)

yields the observability matrix

$$O_4 = \begin{pmatrix} -\ddot{\sigma} & -2\dot{\sigma}^3 & -\dot{\sigma}^2 & -2\dot{\sigma}^5 \\ 2\dot{\sigma} & -\ddot{\sigma} & -2\dot{\sigma}^3 & -\dot{\sigma}^2\dddot{} \\ 0 & -2\dot{\sigma} & -\ddot{\sigma} & -2\dot{\sigma}^3 \\ 1 & 0 & 0 & 0 \end{pmatrix}.$$

(5.39)

The fourth column of (5.39) is exactly equal to $\dot{\sigma}^2$

times the second column, and the rank is less than the

order. This system is unobservable; experiment confirmed

this result.

73

Bell Aerospace Company

In realistic combat trajectories it is generally erroneous to assume that a_{T_r}, target acceleration in the range-direction, is zero. If, however, that assumption is valid for some situation, then we can simplify (5.35) by omitting the third row and column and similarly simplify H, so that if $a_{T_r} \equiv 0$, a priori, then

$$A_{31} = \begin{pmatrix} 0 & 1 & 0 \\ \dot{\sigma}^2 & 0 & 0 \\ 0 & 0 & 0 \end{pmatrix} \quad , \quad H_{31} = (-\ddot{\sigma} \quad -2\dot{\sigma} \quad 1)$$

and

$$O_{31} = \begin{pmatrix} -\ddot{\sigma} & -2\dot{\sigma}^3 & -\ddot{\sigma}\,\dot{\sigma}^2 \\ -2\dot{\sigma} & -\ddot{\sigma} & -2\dot{\sigma}^3 \\ 1 & 0 & 0 \end{pmatrix}.$$

$$(5.40)$$

In this case rank equals order and the system is observable if $\ddot{\sigma} \neq 0$ and $\dot{\sigma} \neq 0$. This result was experimentally confirmed.

Returning to (5.35), assume that the target acceleration perpendicular to the LOS, a_{T_σ}, is identically zero, i.e., $x_4 = \hat{a}_{T_\sigma} \equiv 0$, a priori, but the other component, $x_3 = \hat{a}_{T_r}$, is a non-zero constant. Then, making the appropriate changes in A and H, we have

$$\dot{A}_{32} = \begin{pmatrix} 0 & 1 & 0 \\ \dot{\sigma}^2 & 0 & 1 \\ 0 & 0 & 0 \end{pmatrix} \quad , \quad H_{32} = (-\ddot{\sigma} \quad -2\dot{\sigma} \quad 0)$$

and

$$
O_{32} = \begin{pmatrix}
-\ddot{\sigma} & -2\dot{\sigma}^3 & -\dot{\sigma}^2\ddot{\sigma} \\
-2\dot{\sigma} & -\ddot{\sigma} & -2\dot{\sigma}^3 \\
0 & -2\dot{\sigma} & 0
\end{pmatrix} .
$$

(5.41)

In this case the third column equals $\dot{\sigma}^2$ times the first; therefore the system is unobservable.

The result may now be stated: If the target has significant acceleration parallel to the line of sight, $(a_{T_r} \neq 0)$, it is not possible to estimate range and range-rate; the system is unobservable. If the target acceleration a_{T_r} is known to be zero, a priori; then the system is observable, and it may be reduced to a problem in the three states, $x_1 = \hat{r}$, $x_2 = \hat{\dot{r}}$ and $x_4 = \hat{a}_{T_\sigma}$. In this case, Equation (5.32) can be exactly instrumented. If $x_4 = \hat{a}_{T_\sigma} = $ constant is a reasonable assumption, it is possible to reduce the problem from three states to two by differentiating the output expression (5.37) and eliminating $x_4 = \hat{a}_{T_\sigma}$, as in (5.16).

It is, however, an important restriction that the theorems on observability do not apply perfectly to systems whose coefficients are time-varying. In our case the system dynamics are constant, while the observation matrix is not. Intuitively, it seemed possible that if

the coefficients of the output equation vary sufficiently in the observation interval, then a result might be obtained which is of value. Many variations of the above development, using different models of the system dynamics and output equations were therefore examined to pursue this question. The results were disappointing whenever $a_{T_r} \neq 0$, or $\dot{\sigma}$ was small. The system is unobservable, despite the uncertainty of the theory on this question, whenever $a_{T_r} \neq 0$.

Bell Aerospace Company

5.4 Other Linear Systems

It is advantageous to unify the results of the above discussions on kinematic linear parameter identification systems in order to form a basis for considering other possible linear systems. We therefore re-present the problem from a geometrical viewpoint and then consider possible extensions beyond the scope of this contract.

Consider the equation of acceleration components perpendicular to the LOS, from the kinematics,

$$r\ddot{\sigma} + 2\dot{r}\dot{\sigma} - a_{T_\sigma} + a_{m_\sigma} = 0.$$

$$(5.41)$$

Assume that the range acceleration, $\ddot{r}$, is zero, and may therefore be neglected. Assume further that a_{T_σ} is quasi-constant, i.e., cannot change significantly in less than 1/2 second. Then differentiation of (5.41) with a high pass filter such as $\dfrac{T_1}{T_1 s+1}$, where T_1 is of the order of 1/2 second or less, reduces (5.41) to

$$r v_1 + \dot{r} v_2 + v_o = 0 \qquad\qquad (5.42)$$

where $v_1 = \left(\dfrac{T_1 s}{T_1 s+1}\right)\ddot{\sigma}$; $v_2 = \left(\dfrac{2T_1 s\dot{\sigma}}{T_1 s+1} + \dfrac{T_1 \ddot{\sigma}}{(T_1 s+1)^2}\right)$, $v_o = \left(\dfrac{T_1 s}{T_1 s+1}\right) a_{m_\sigma}$.

If in (5.42) we replace r and $\dot{r}$ by the estimates $\hat{r}$ and $\hat{\dot{r}}$, (5.42) may be expressed as $\hat{r} v_1 + \hat{\dot{r}} v_2 + v_o = e_\sigma$; then the solution for $\hat{r}$ and $\hat{\dot{r}}$ lies on a locus such that $e_\sigma = 0$. In this

$$(5.43)$$

case (5.43) forms a straight line, as shown in the sketch below for some particular instant.

Fig. 5.1
Geometrical View of Equation Error.

The entire problem of estimation is based on the necessity of finding another line in the $(\hat{r}, \dot{\hat{r}})$ space:

(a) The multiple-error [4,6] adaptive process, by using a variety of values of T_i generates a number of other lines which are, more or less, linearly independent. This approach may be categorized as achieving distribution in the T_i-lag space at one instant of true time.

(b) The various single-error adaptive nets and the Kalman net take advantage of the fact that, at some other instant than that shown in Fig. 5.1, the line of zero error in the $(\hat{r}, \dot{\hat{r}})$ space is

78

differently oriented, if $\dot{\sigma} \neq 0$, and is therefore
linearly independent. These approaches thus
use the idea of distribution in true time, t,
rather than in the T_1 space.

(c) The matrix inverse schemes gather all lines
over the computing interval, thus achieving
distribution in time, and then find the solution.

A physically different approach to finding a second
linearly independent line in the $(\hat{r}, \dot{r})$ space is obviously
preferable if possible. Stadimetric ranging provides such
an approach. Seekers which enable measurement of some
function of the target size, or area, such as mosaic IR,
TV, area, or correlation, have this capability. In a
single plane we have the geometrical relationship

$$r\theta = D$$

(5.44)

where r Range

θ Angle Subtended by Target, assumed a small angle

D Target Size

as shown in the sketch below.

Assume that D is constant; this assumption is fair if D is the diameter of the least circle which contains the target as viewed from the seeker in both the maneuver and cross maneuver planes. From (5.44), by differentiating,

$$r\dot{\theta} + \dot{r}\,\theta = 0$$

and

$$\hat{r}\dot{\theta} + \dot{\hat{r}}\theta = e_7.$$

$$(5.45)$$

The choices of $\hat{r}$ and $\dot{\hat{r}}$ for which $e_7 = 0$ lie on a straight line which passes through the origin of the $(\hat{r}, \dot{\hat{r}})$ space at every instant. Combining this with the kinematic ranging sketch, Fig. 5.1, yields the sketch below.

Fig. 5.2
Combining Kinematic and Stadimetric Ranging.

If we solve (5.44) and (5.45 simultaneously, we get one equation for $\hat{r}$ and one for $\hat{\dot{r}}$. These are independent and their joint solution may therefore be determined. It is usually better to solve the two equations in a decoupled format as the solution can always be accomplished more rapidly, more simply and more accurately. A Least Magnitude algorithm may be used. They are analytically valid in such cases and are attractive for they estimate a moving parameter with smaller lag than quadratic algorithms, and thereby decrease the effect of target accelerations.

However, this argument rests on the rather uncertain base of the assumptions. One assumption is that the target cross-track acceleration (a_{T_σ}) is quasi-constant, i.e., changes negligibly within two time-constants of the high-pass filter $\dfrac{T_1 s}{T_1 s+1}$, in (5.42). The other assumption is that $\ddot{r} \approx 0$, or at least the unknown portion (a_{T_r}) thereof. In fact, in any maneuver of the target, a_{T_σ} and a_{T_r} change continuously and can change rapidly. This scheme is therefore less powerful than appears at first.

However, stadimetric data can be valuable in reducing the difficulty of range estimation. Equation (5.41) states one relationship between three of the unknowns in the kinematic ranging problem. Stadimetric data provides another relationship, so that the effective total number of unknowns may be reduced by one. The possibility therefore exists that linear estimation of range and range rate could be accomplished with acceptably small error, due to the unobservability of a_{T_r}, by combining kinematic and stadimetric methods.

It should be observed that stadimetric ranging has an advantage over kinematic ranging. In stadimetry, the sub-tended angle θ is positive-definite, and its rate $\dot{\theta}$ is zero if and only if $\dot{r} = 0$; this almost never occurs. On the other hand, in kinematic ranging, the objective of a proportional navigation homing system is to keep $\dot{\sigma} \approx 0$ at all times; consequently an ill-conditioned covariance matrix must result at least occasionally.

This observation leads to describing the possible weakness in the idea of combining kinematic and stadimetric ranging principles. In both schemes, express $\hat{\dot{r}}$ as a function of $\hat{r}$, and assume $\ddot{r} \approx 0$. Then, using (5.42) and (5.45)

$$\text{Kinematic:} \qquad \hat{\dot{r}} = \frac{v_0}{v_2} - \frac{v_1}{v_2} \, \hat{r}$$

$$(5.46)$$

$$\text{Stadimetric:} \qquad \hat{\dot{r}} = -\left(\dot{\theta}/\theta\right) \hat{r},$$

$$(5.47)$$

under the simplifying assumption that $a_{T_\sigma} = 0$.

As previously observed for the stadimetric method, in (5.47) θ is always positive, and $\dot{\theta}$ is almost always positive. Neglecting the rare and anomalous case of $\dot{\theta} \leq 0$, implying increasing range, $\dot{\theta}/\theta$ is positive and the solution for $\hat{\dot{r}}$ as a function of $\hat{r}$ passes through the origin with a time-varying negative slope which is a quotient of non-zero finite quantities. In the kinematic approach (5.46), the

coefficient of $\hat{r}$ will normally have a negative value but is a quotient in which the numerator and denominator rapidly approach small values and ultimately zero, in favorable geometries, and start and remain at small values in unfavorable geometries. The slope of (5.46) and the joint solution of (5.46) and (5.47), therefore are increasingly sensitive to instrument and computation noise as the maneuver becomes small. In geometric terms, the two lines in the $(\hat{r}, \dot{\hat{r}})$ space of Figure 5.2 become parallel as the maneuver becomes small.

In consequence, it is evident that the stadimetric/linear-kinematic method outlined above could be improved by use of the nonlinear kinematic method described in Section 4.

6. TECHNOLOGY ASSESSMENT

It appears that linear methods of kinematic ranging can work effectively only for favorable combat geometries and if the sensor noise levels are quite low. This implies high accuracy sensors, and frequent ineffectivity.

The nonlinear filter described in Section 4 estimates the target velocity-vector components and therefore can be used to deduce the target velocity and aspect angle. The filter also estimates the target's acceleration components, the turn-rate, and its derivative. It therefore estimates the entire specification of the target dynamics, and can be used to estimate the target future trajectory, and time to go. This may be useful not only to the air-air missile terminal-control guidance problem but also to a variety of terminal fire control systems in aircraft or helicopters instead of missiles. This nonlinear filter can also be used to eliminate impossible target accelerations from data provided by other tracking systems such as radar or laser rangers.

Many of the newer seekers of TV or IR types provide some indication of the target size or shape. Target size data can be used as a partial basis for a ranging system, as outlined in Section 5. In addition, information on the target shape or its aspect-angle can be used to provide clues enabling nonlinear filtering. For example, if the target is viewed from a head-on or tail-chase aspect it is clearly

difficult for the target to accelerate parallel to the Line of Sight; it can accelerate across the line of sight with relative ease.

Linear stadimetric ranging cannot by itself estimate range and range-rate, but only their ratio. However, combing linear stadimetry and kinematic schemes has the effect of reducing the number of unknown variables to be determined simultaneously. The parameter identification problem may in fact be reduced to a problem in 2-space, without using the poor assumptions that $\ddot{r}$, a_{T_r}, and a_{T_σ} are quasi-constant.

In this situation, two or (preferably) more independent measurement instants enable an unique solution. The problem of updating the hyperplane of Figs. 5.1 or 5.2 to another instant is then reduced. It is not eliminated, therefore the solution is not rigorously observable; however, the combination may be useful.

In a review of the present technology and an estimate of the trends and potentials, the interaction of cost with systems technology is perhaps most important in the air-air missile problem. These points stand out:

a) Seekers of all kinds are very expensive; a small radar seeker is very costly in weight, space and dollars. A TV seeker may be less expensive in each sense, but is not cheap. The various sophisticated IR seekers are cheaper but are still quite costly compared to the simplest IR seekers.

(b) Sensors such as rate gyros are an order of magnitude less costly than simple seekers.

c) The introduction of medium or large scale
    integrated digital and analog chips has at
    once improved the reliability of the computa-
    tion process and reduced the cost by
    orders of magnitude.

Taken together, these elements suggest that cost/effectivity
considerations lead to improving missile system performance
by combining a wide range of the inexpensive sensors with a
relatively sophisticated computation capability. This may
enable use of a relatively unsophisticated seeker of rela-
tively low cost.

The nonlinear range/range rate estimator shown in
Fig. 4.1 requires a considerable computation capability, and
requires input signals from a pair of accelerometers. It
also requires the missile airspeed components which may be
obtained from relatively inexpensive sensors or may be
estimated from accelerometer and rate-gyro data. But the
least sophisticated seeker is sufficient. Our approach was
to maximize the information which could be extracted from
an inexpensive seeker by combining several inexpensive sen-
sors with a relatively sophisticated yet inexpensive
computer which will soon be available.

Bell Aerospace Company

7. REFERENCES

1. Eyckhoff, P., "Aspects of Process Parameter Estimation," IEEE Transactions on Automatic Control, October, 1963.

2. Narendra, T. S., and L. E. McBride,"Multi-Parameter Self-Optimizing System Using Correlation Techniques," IEEE Transactions on Automatic Control, January, 1962.

3. Young, P. C., "The Use of Linear Regression and Related Procedures for the Identification of Dynamic Processes," IEEE Proceedings of the Seventh Symposium on Adaptive Processes, UCLA, December, 1968.

4. Lion, P. M., "Rapid Identification of Linear and Nonlinear Systems," AIAA Journal, Vol. 5, No. 10, October, 1967.

5. Bell Aerospace Company Report 9500-920183, "Adaptive Modeling and Control," F. D. Powell, June, 1970, Final Report on Office of Naval Research Contract Nonr-4864(00), NR049-207.

6. NASA Report 68-11-7, "Use of Integral Transforms in Parameter Estimation." H. C. Lessing and D. F. Crane, 1968.

7. Morrison, N., "Introduction to Sequential Smoothing and Prediction," McGraw-Hill Book Company, New York 1969.

8. Kalman, R. E., "A New Approach to Linear Filtering and Prediction Problems," Transactions of the A.S.M.E., Journal of Basic Engineering, Vol. 82, PP 35-45, March, 1960.

APPENDICES

APPENDIX A

The Nonlinear Estimator; Derivation and Instrumentation

It is possible, due to the particular form of the equations and constraints of the Mathematical Model of the system, to develop a nonlinear range and range-rate identifier. This type of identifier is discussed in this section.

A.1 Analysis

The key elements of the Mathematical Model are quoted from Section 3:

Velocity component equations parallel to the Line-of-Sight:

$$\dot{r} - V_T \cos(\gamma_T - \sigma) + V_M \cos(\gamma_M - \sigma) = 0,$$

or $\quad \dot{r} - V_{T_r} + V_{M_r} = 0.$

(A.1)

Velocity component equations perpendicular to the LOS

$$r\dot{\sigma} - V_T \sin(\gamma_T - \sigma) + V_M \sin(\gamma_M - \sigma) = 0,$$

or $\quad r\dot{\sigma} - V_{T_\sigma} + V_{M_\sigma} = 0.$

(A.2)

We also demonstrated that the acceleration component equations parallel and perpendicular to the LOS are, respectively:

$$\ddot{r} - r\dot{\sigma}^2 - a_{T_r} + a_{M_r} = 0$$

$$(A.3)$$

and

$$r\ddot{\sigma} + 2\dot{r}\dot{\sigma} - a_{T_\sigma} + a_{M_\sigma} = 0.$$

$$(A.4)$$

The target and missile velocity and acceleration components parallel and perpendicular to the LOS are:

Velocities:

Parallel: $V_{T_r} = V_T \cos \xi_T$

$$V_{M_r} = V_M \cos \xi_M$$

Perpendicular: $V_{T_\sigma} = V_T \sin \xi_T$

$$V_{M_\sigma} = V_M \sin \xi_M.$$

$$(A.5)$$

Accelerations:

Parallel: $a_{T_r} = \dot{V}_T \cos \xi_T - V_T \dot{\gamma}_T \sin \xi_T$

$$a_{M_r} = \dot{V}_M \cos \xi_M - V_M \dot{\gamma}_M \sin \xi_T$$

Perpendicular: $a_{T_\sigma} = \dot{V}_T \sin \xi_T + V_T \dot{\gamma}_T \cos \xi_T$ $\qquad (A.6)$

$$a_{M_\sigma} = \dot{V}_T \sin \xi_T + V_M \dot{\gamma}_M \cos \xi_T$$

where

Bell Aerospace Company

Angles: $\xi_T = \gamma_T - \sigma$

$\xi_M = \gamma_M - \sigma$.

(A.7)

The principle of this approach is simply to solve A.3 for $\ddot{r}$ as

$$\ddot{r} = r\dot{\sigma}^2 + a_{M_r} - a_{T_r}.$$

(A.8)

Integration of $\ddot{r}$ will yield $\dot{r}$ and r if the terms on the right of (A.8) are available.

The term $r\dot{\sigma}^2$ can be computed easily while a_{M_r}, the missile acceleration parallel to the LOS, can be measured directly. The problem therefore is now to estimate a_{T_r} in some way. It is assumed that initial values of $\hat{r}$ and $\hat{\dot{r}}$ are provided.

It was shown that the target acceleration in the range direction, a_{T_r}, can be determined from available data. The procedure is first to calculate V_T, the target airspeed, by use of (A.1) and (A.2) as

$$(\dot{r} + V_M \cos \xi_M)^2 + (r\dot{\sigma} + V_M \sin \xi_M)^2 =$$

$$V_T^2 \cos^2 \xi_T + V_T^2 \sin^2 \xi_T = V_{T_r}^2 + V_{T_\sigma}^2 = V_T^2.$$

(A.9)

It was stated in Section (4.1) that this expression may be differentiated to yield $V_{T_r} a_{T_r} + V_{T_\sigma} a_{T_\sigma} = V_T \dot{V}_T$; This is demonstrated below. Therefore, let us differentiate (A.9) with respect to time, yielding

$$2\{(\dot{r}+V_M \cos \xi_M)[\ddot{r}+(\dot{V}_M \cos \xi_M - V_M \dot{\gamma}_M \sin \xi_M)+V_M \dot{\sigma} \sin \xi_M]$$

$$+ (r\dot{\sigma}+V_M \sin \xi_M)[r\ddot{\sigma}+\dot{r}\dot{\sigma} +(\dot{V}_M \sin \xi_M+V_M \dot{\gamma}_M \cos \xi_M) -$$

$$V_M \dot{\sigma} \cos \xi_M]\} = 2 V_T \dot{V}_T.$$

90

Substitute from (A.5) the simplifying notation for the acceleration components of the missile, a_{M_r} and a_{M_σ}, parallel and perpendicular to the LOS, respectively; these accelerations are gathered in parenthesis within the same brackets in the expression above [( )].

This yields

$$(\dot{r} + V_M \cos \xi_M)(\ddot{r} + a_{M_r} + V_M \dot{\sigma} \sin \xi_M)$$
$$+ (r\dot{\sigma} + V_M \sin \xi_M)(r\ddot{\sigma} + \dot{r}\dot{\sigma} + a_{M_\sigma} - V_M \dot{\sigma} \cos \xi_M) =$$
$$V_T \dot{V}_T. \qquad (A.10)$$

Now solve (A.2) for $V_M \sin \xi_M$, multiply by $\dot{\sigma}$ and replace the term $(V_M \dot{\sigma} \sin \xi_M)$ on the first line of (A.10) by the term thus formed. Similarly, solve (A.1) for $V_M \cos \xi_M$, multiply by $\dot{\sigma}$ and eliminate the term $(V_M \dot{\sigma} \cos \xi_M)$ from the second line of (A.10). These substitutions yield

$$(\dot{r} + V_M \cos \xi_M)(\ddot{r} - r\dot{\sigma}^2 + a_{M_r} + \dot{\sigma}V_T \sin \xi_T) +$$
$$(r\dot{\sigma} + V_M \sin \xi_M)(r\ddot{\sigma} + 2\dot{r}\dot{\sigma} + a_{M_\sigma} - \dot{\sigma}V_T \cos \xi_T) =$$
$$V_T \dot{V}_T.$$

Keeping the right side of this expression, gather the coefficients of V_T on the left; this reduces to

$$(\dot{r} + V_M \cos \xi_M)(\ddot{r} - r\dot{\sigma}^2 + a_{M_r}) + (r\dot{\sigma} + V_M \sin \xi_M)$$
$$(r\ddot{\sigma} + 2\dot{r}\dot{\sigma} + a_{M_\sigma}) + \dot{\sigma} \{(\dot{r} + V_M \cos \xi_M)(V_T \sin \xi_T) -$$
$$-(r\dot{\sigma} + V_M \sin \xi_M)(V_T \cos \xi_T)\} = V_T \dot{V}_T. \qquad (A.11)$$

The term in curly braces { } in (A.11) is identically zero. This follows from (A.1), $\dot{r} + V_M \cos \xi_M = V_T \cos \xi_T$, while from (A.2), $r\dot{\sigma} + V_M \sin \xi_M = V_T \sin \xi_T$, so that the brace has the value $\{V_T \cos \xi_T (V_T \sin \xi_T) - V_T \sin \xi_T (V_T \cos \xi_T)\} = 0$.

As a consequence, (A.11) takes the simpler form

$$(\dot{r} + V_M \cos \xi_M)(\ddot{r} - r\dot{\sigma}^2 + a_{M_r}) + (r\dot{\sigma} + V_M \sin \xi_M)$$
$$(r\ddot{\sigma} + 2\dot{r}\dot{\sigma} + a_{M_r}) = V_T \dot{V}_T. \tag{A.12}$$

By use of (A.1) through (A.6), this may be expressed in the intuitively satisfying form $V_{T_r} a_{T_r} + V_{T_\sigma} a_{T_\sigma} = V_T \dot{V}_T$, (A.13) which is the form used in the discussion in Section 4, where we use the simplifying notation, from (A.5),

$$V_{T_r} = V_T \cos \xi_T$$

$$V_{T_\sigma} = V_T \sin \xi_T$$

to express the target velocity components parallel and perpendicular to the LOS.

The exact solution for a_{T_r} is thus

$$a_{T_r} = \frac{V_T \dot{V}_T - V_{T_\sigma} a_{T_\sigma}}{V_{T_r}} . \tag{A.14}$$

and

$$\ddot{r} = r\dot{\sigma}^2 - a_{M_r} + \frac{V_T \dot{V}_T - V_{T_\sigma} a_{T_\sigma}}{V_{T_r}} , \tag{A.15}$$

while

$$\frac{a_{T_\sigma}}{V_{T_r}} = \dot{\gamma}_T \quad \text{if } \dot{V}_T = 0.$$

Bell Aerospace Company

Usually $\dot{V}_T$ is small and can be neglected, and all other terms on the right of (A.15) can be estimated.

The mechanization of this algorithm is discussed in Section (A.2), following.

A.2 Mechanization of the Signals for the Ideal Algorithm

The range acceleration is given by (A.15); it may be integrated to yield $\dot{r}$ and r. The term $r\dot{\sigma}^2$ can then be formed, while the missile acceleration component, a_{M_r}, can be directly sensed.

The mechanization of (A.15) requires that missile airspeed V_M, the missile acceleration components a_{M_r} and a_{M_σ}, and the angle ξ_M be available as signals or be estimated. It will now be shown that this can be accomplished.

(a) Acceleration Components

The accelerometer components, a_{M_r}, and a_{M_σ}, are a special case; two easy solutions are available:

(1) Mount the accelerometers on the seeker; then one yields a_{M_r} and the other yields a_{M_σ} directly.

(2) Mount the accelerometers on the missile body; then their signals are a_{M_x}, and a_{M_y}, fore - aft and cross-body, respectively; and resolution of the signals from the accelerometer through

Bell Aerospace Company

the "look-angle," λ, yields

$$\begin{pmatrix} a_{M_r} \\ a_{M_\sigma} \end{pmatrix} = \begin{pmatrix} \cos\lambda & -\sin\lambda \\ \sin\lambda & \cos\lambda \end{pmatrix} \begin{pmatrix} a_{M_x} \\ a_{M_y} \end{pmatrix}. \qquad (A.16)$$

As the "look-angle," λ, between the missile centerline and the LOS can easily be made physically available in a seeker gimbal, the resolution of the acceleration components is easily accomplished.

(b) <u>Velocity Estimation</u>

If the missile body pitch rate, q, or equivalent, is an available signal, and further, if the cross-body acceleration of the missile, a_{M_y}, is also available as a signal, it is relatively easy to estimate missile velocity, V_M.

The pertinent equations of motion of the missile are,

$$\dot{\alpha} = q - \frac{a_{M_y}}{V_M} \qquad (A.17)$$

$$a_{M_y} = H\alpha + G\delta$$

where α angle of attack

    a_{M_y} cross-body acceleration

    δ control displacement

    q body pitch rate

    V_M airspeed

N, G cross-body accelerations per
radian, due to angle of attack
and control displacements,
respectively

Assuming quasi-constant conditions, the transfer
function defining acceleration is

$$a_{M_y} = \frac{N\,\alpha + G\,\delta}{s + N/V_M} \ . \tag{A.18}$$

The acceleration due to control displacement may
usually be neglected so that

$$a_{M_y} \simeq \frac{N\,\alpha}{s + N/V_M} = V_M \left(\frac{N/V_M}{s + N/V_M} \right)\, \alpha$$

$$= V_M \ \frac{\alpha}{Ts + 1} \tag{A.19}$$

where $T = V_M/N$. Then V_M may be estimated by the algorithms

$$\hat{\dot{V}}_M = k\, a_{M_y}\ (a_{M_y} - \hat{V}_M\, q) \tag{A.20}$$

or

$$\hat{\dot{V}}_M = k\ (\, |a_{M_y}| - \hat{V}_M\, |q| \,) \tag{A.21}$$

where $k > 0$ has the appropriate value.

Somewhat superior algorithms which will lag less
are achieved by biasing the algorithm given by the missile
longitudinal acceleration component a_{M_z}.

Algorithm (A.21) is obviously simple to instrument, requiring only one multiplication.

(c) Estimation of the Angle ξ_M

The angle ξ_M is defined as $\xi_M = \gamma_M - \sigma$.
But as $\gamma_M = \theta_M - \alpha$, where θ_M is the centerline attitude, then $\xi_M = \theta_M - \alpha - \sigma$, and as the angle from missile centerline to the seeker LOS is

$$\lambda = \sigma - \theta_M$$

we have $\xi_M = -\lambda - \alpha$ (A.22)

where α is the angle of attack between the missile centerline and the velocity vector. But this can easily be estimated as

$$\hat{\alpha} \simeq \frac{q}{Ts+1}$$ (A.23)

where T was defined above.

The missile velocity components V_{M_r} and V_{M_σ} can then be computed as $V_{M_r} = V_M \cos \xi_M$ and $V_{M_\sigma} = V_M \sin \xi_M$.

Bell Aerospace Company

APPENDIX B

Error Analysis Coefficients

The numerical data presented in this appendix represent
the time varying coefficients of the error equation. As dis-
cussed in Chapter 4, the error equation is of the form

$$\ddot{x} + a_1 \dot{x} + a_2 x = \sum_{i=1}^{7} b_i N_i,$$

and the data here represent the coefficients a_i and b_i tabulated
for every 0.25 seconds. There are six tables, representing a
selection of six choices of initial geometry configuration. They
are ordered, and correspond respectively to Figures 4.3 through
4.8 inclusive; however, each graph is labelled to show the initial
geometry. These data permit more general stochastic analyses of
the effects on the estimates due to errors in the   eral signals
which are used in the algorithm. The coefficients a_1 and a_2 are:

$$a_1 = 2\dot{\sigma} \tan \xi_T - \dot{\gamma}_T \tan \xi_T, \quad \text{and}$$

$$a_2 = -\dot{\sigma}^2 + \dot{\gamma}_T \dot{\sigma} + \ddot{\sigma} \tan \xi_T.$$

The coefficients b_i and error sources N_i are:

$b_1 = -1$ N_1 a_{M_r}, accel‖LOS error

$b_2 = \sec \xi_T$ N_2 $\dot{V}_T$, target airspeed change

$b_3 = -\dot{\gamma}_T \sec \xi_T \sin (\gamma_M - \gamma_T)$ N_3 $\hat{V}_M$, missile airspeed error

$$b_4 = -r\dot{\gamma}_T - 2\dot{r}\tan \xi_T + 2r\dot{\sigma} \qquad N_4 \quad \dot{\sigma}, \text{ LOS rate error}$$

$$b_5 = -V_M\dot{\gamma}_T \sec \xi_T \cos(\gamma_M - \gamma_T) \qquad N_5 \quad \hat{\xi}_M, \text{ error of estimating } \hat{\alpha}$$

$$b_6 = -r\tan \xi_T \qquad N_6 \quad \ddot{\sigma} \text{ LOS acceleration error}$$

$$b_7 = -\tan \xi_T \qquad N_7 \quad a_{M_\sigma}, \text{ accel. } \perp \text{ LOS, error}$$

All angles are in radian measure unless specifically stated otherwise.

The data of this appendix are presented in a conventional "exponential format" for digital output data. Thus the tabulated item 0.422E 01 is interpreted as $(0.422)10^{+1} = 4.22$, while $-0.244E-01$ is interpreted as $(-0.244)10^{-1} = -0.0244$.

TABLE B-1

Error Equation Coefficients a_i and b_i as functions of the time for the trajectory of Fig. 4.3 with initial conditions $\psi=90°$, $\phi=0$, $x_\circ=10,000$, $\dot{y}_\circ=1,000$.

TIME	A1	A2	P1	P2	B3	B4	B5	B6	B7
0.0	0.424E 01	0.451E 00	-0.100E 01	0.100E 02	-0.143E 01	0.445E 05	0.454E 00	-0.100E 00	-0.965E 01
0.250E 00	0.232E 01	-0.330E 00	-0.100E 01	0.572E 01	-0.104E 01	0.261E 05	0.275E 00	-0.535E 05	-0.463E 01
0.500E 00	0.160E 00	-0.265E 00	-0.100E 01	0.407E 01	-0.714E 00	0.134E 05	0.442E 00	-0.358E 05	-0.355E 01
0.750E 00	0.104E 01	-0.183E 00	-0.100E 01	0.322E 01	-0.531E 00	0.140E 05	0.536E 00	-0.263E 05	-0.306E 01
0.100E 01	0.764E 00	-0.130E 00	-0.100E 01	0.270E 01	-0.412E 00	0.112E 04	0.551E 00	-0.205E 05	-0.251E 01
0.125E 01	0.552E 00	-0.130E 00	-0.100E 01	0.234E 01	-0.326E 00	0.914E 04	0.565E 00	-0.166E 05	-0.213E 01
0.150E 01	0.406E 00	-0.455E-01	-0.100E 01	0.211E 01	-0.265E 00	0.765E 01	0.553E 00	-0.136E 05	-0.186E 01
0.175E 01	0.365E 00	-0.452E-01	-0.100E 01	0.193E 01	-0.223E 00	0.651E 04	0.583E 00	-0.115E 05	-0.165E 01
0.200E 01	0.304E 00	-0.501E-01	-0.100E 01	0.178E 01	-0.189E 00	0.563E 04	0.567E 00	-0.972E 04	-0.146E 01
0.225E 01	0.255E 01	-0.356E-01	-0.100E 01	0.167E 01	-0.162E 00	0.493E 04	0.553E 00	-0.331E 04	-0.134E 01
0.250E 01	0.213E 01	-0.251E-01	-0.100E 01	0.157E 01	-0.140E 00	0.430E 04	0.477E 00	-0.714E 04	-0.121E 01
0.275E 01	0.169E 01	-0.172E-01	-0.100E 01	0.149E 01	-0.123E 00	0.389E 04	0.522E 00	-0.415E 04	-0.111E 01
0.300E 01	0.166E 01	-0.110E-01	-0.100E 01	0.143E 01	-0.108E 00	0.350E 04	0.507E 00	-0.530E 04	-0.102E 01
0.325E 01	0.147E 01	-0.654E-02	-0.100E 01	0.137E 01	-0.955E-01	0.316E 04	0.444E 00	-0.457E 04	-0.943E 00
0.350E 01	0.131E 01	-0.333E-02	-0.100E 01	0.132E 01	-0.863E-01	0.286E 04	0.441E 00	-0.392E 04	-0.857E 00
0.375E 01	0.119E 01	-0.104E-02	-0.100E 01	0.127E 01	-0.776E-01	0.260E 04	0.445E 00	-0.333E 04	-0.767E 00
0.400E 01	0.107E 01	0.577E-03	-0.100E 01	0.123E 01	-0.699E-01	0.235E 04	0.454E 00	-0.289E 04	-0.722E 00
0.425E 01	0.965E 01	0.166E-02	-0.100E 01	0.117E 01	-0.630E-01	0.215E 04	0.442E 00	-0.241E 04	-0.641E 00
0.450E 01	0.874E 01	0.241E-02	-0.100E 01	0.117E 01	-0.567E-01	0.194E 04	0.441E 00	-0.202E 04	-0.641E 00
0.475E 01	0.790E 01	0.292E-02	-0.100E 01	0.114E 01	-0.510E-01	0.175E 04	0.438E 00	-0.147E 04	-0.556E 00
0.500E 01	0.711E 01	0.326E-02	-0.100E 01	0.112E 01	-0.458E-01	0.159E 04	0.425E 00	-0.137E 04	-0.492E 00
0.525E 01	0.637E 01	0.354E-02	-0.100E 01	0.110E 01	-0.409E-01	0.141E 04	0.420E 00	-0.116E 04	-0.445E 00
0.550E 01	0.568E 01	0.373E-02	-0.100E 01	0.108E 01	-0.363E-01	0.125E 04	0.414E 00	-0.862E 03	-0.400E 00
0.575E 01	0.499E 01	0.391E-02	-0.100E 01	0.106E 01	-0.319E-01	0.109E 04	0.409E 00	-0.655E 03	-0.354E 00
0.600E 01	0.434E 01	0.403E-02	-0.100E 01	0.105E 01	-0.274E-01	0.939E 03	0.405E 00	-0.485E 03	-0.305E 00
0.625E 01	0.370E 01	0.415E-02	-0.100E 01	0.103E 01	-0.238E-01	0.793E 03	0.402E 00	-0.340E 03	-0.265E 00
0.650E 01	0.308E 01	0.426E-02	-0.100E 01	0.102E 01	-0.200E-01	0.651E 03	0.399E 00	-0.220E 03	-0.223E 00
0.675E 01	0.246E 01	0.439E-02	-0.100E 01	0.102E 01	-0.163E-01	0.511E 03	0.396E 00	-0.127E 03	-0.180E 00
0.700E 01	0.185E 01	0.435E-02	-0.100E 01	0.101E 01	-0.127E-01	0.373E 03	0.394E 00	-0.573E 02	-0.133E 00
0.725E 01	0.244E 01	0.190E-01	-0.100E 01	0.100E 01	-0.939E-02	0.244E 03	0.392E 00	-0.117E 02	-0.916E-01

T	A1	A2	B1	B2	B3	B4	B5	B6	B7
0.0	0.249E 01	0.501E 00	-0.100E 01	0.100E 02	0.0	0.430E 05	0.0	-0.100E 00	-0.555E 01
0.025	0.177E 01	-0.367E 00	-0.100E 01	0.771E 01	0.0	0.329E 05	0.0	-0.729E 00	-0.744E 01
0.050	0.124E 01	-0.343E 00	-0.100E 01	0.633E 01	0.0	0.269E 05	0.0	-0.570E 00	-0.636E 01
0.075	0.244E 01	-0.404E 00	-0.100E 01	0.557E 01	0.0	0.228E 05	0.0	-0.448E 00	-0.545E 01
0.100	0.653E 00	-0.308E 00	-0.100E 01	0.505E 01	0.0	0.199E 05	0.0	-0.369E 00	-0.455E 01
0.125	0.404E 00	-0.238E 00	-0.100E 01	0.470E 01	0.0	0.178E 05	0.0	-0.349E 00	-0.459E 01
0.150	0.355E 00	-0.185E 00	-0.100E 01	0.446E 01	0.0	0.163E 05	0.0	-0.311E 00	-0.435E 01
0.175	0.260E 00	-0.144E 00	-0.100E 01	0.430E 01	0.0	0.152E 05	0.0	-0.280E 00	-0.414E 01
0.200	0.186E 00	-0.112E 00	-0.100E 01	0.418E 01	0.0	0.144E 05	0.0	-0.254E 00	-0.446E 01
0.225	0.136E 00	-0.870E-01	-0.100E 01	0.409E 01	0.0	0.138E 05	0.0	-0.231E 00	-0.367E 01
0.250	0.956E-01	-0.686E-01	-0.100E 01	0.404E 01	0.0	0.134E 05	0.0	-0.211E 00	-0.341E 01
0.275	0.659E-01	-0.561E-01	-0.100E 01	0.397E 01	0.0	0.131E 05	0.0	-0.153E 00	-0.367E 01
0.300	0.435E-01	-0.365E-01	-0.100E 01	0.397E 01	0.0	0.129E 05	0.0	-0.175E 00	-0.344E 01
0.325	0.276E-01	-0.263E-01	-0.100E 01	0.395E 01	0.0	0.128E 05	0.0	-0.158E 00	-0.332E 01
0.350	0.164E-01	-0.160E-01	-0.100E 01	0.394E 01	0.0	0.127E 05	0.0	-0.142E 00	-0.381E 01
0.375	0.891E-02	-0.116E-01	-0.100E 01	0.394E 01	0.0	0.127E 05	0.0	-0.126E 00	-0.381E 01
0.400	0.417E-02	-0.695E-02	-0.100E 01	0.393E 01	0.0	0.126E 05	0.0	-0.110E 00	-0.360E 01
0.425	0.133E-02	-0.374E-02	-0.100E 01	0.393E 01	0.0	0.126E 05	0.0	-0.943E-01	-0.360E 01
0.450	-0.375E-03	-0.176E-02	-0.100E 01	0.393E 01	0.0	0.126E 05	0.0	-0.785E-01	-0.380E 01
0.475	-0.155E-02	-0.113E-02	-0.100E 01	0.393E 01	0.0	0.126E 05	0.0	-0.626E-01	-0.360E 01
0.500	-0.336E-02	-0.172E-02	-0.100E 01	0.394E 01	0.0	0.126E 05	0.0	-0.470E-01	-0.381E 01
0.525	-0.730E-02	-0.454E-01	-0.100E 01	0.394E 01	0.0	0.126E 05	0.0	-0.312E-01	-0.381E 01
0.550	-0.202E-01	-0.408E-01	-0.100E 01	0.394E 01	0.0	0.126E 05	0.0	-0.154E-01	-0.381E 01

TABLE B-2

Error Equation Coefficients a_i and b_i as functions of the time for the trajectory of Fig. 4.4 with initial conditions $\psi=90°$, $\varphi = 0°$, $x_T = 10,000$, $y_T = 1,000$.

$$b_1 = -1$$

$$b_2 = \sec \xi_T$$

$$b_3 = -\dot{Y}_T \sec \xi_T \sin (\gamma_M - \gamma_T)$$

$$b_4 = -r\dot{Y}_T - 2\dot{r} \tan \xi_T + 2r\dot{\sigma}$$

$$b_5 = -V_M \dot{Y}_T \sec \xi_T \cos (\gamma_M - \gamma_T)$$

$$b_6 = -r \tan \xi_T$$

$$b_7 = -\tan \xi_T$$

$$a_1 = 2\dot{\sigma} \tan \xi_T - \dot{Y}_T \tan \xi_T$$

$$a_2 = -\dot{\sigma}^2 + \dot{Y}_T \dot{\sigma} + \ddot{\sigma} \tan \xi_T$$

N_1 a_M, accel ⊥LOS error

N_2 $\dot{V}_T$, target airspeed change

N_3 $\hat{V}_M$, missile airspeed error

N_4 $\dot{\sigma}$, LOS rate error

N_5 ξ_M, error of estimating σ

N_6 $\ddot{\sigma}$ LOS acceleration error

N_7 a_{γ_σ}, accel. ⊥LOS error

100

TIME	A1	A2	B1	B2	B3	B4	B5	B6	B7
0.0	0.579E 00	0.541E 00	-0.100E 01	0.100E 02	0.193E 01	0.412E 05	-0.454E 00	-0.100E 06	-0.999E 01
0.250E 00	0.571E 00	-0.549E 00	-0.100E 01	0.118E 02	0.216E 01	0.490E 05	-0.147E 02	-0.112E 06	-0.118E 02
0.500E 00	0.351E 00	-0.850E 00	-0.100E 01	0.151E 02	0.274E 01	0.626E 05	-0.581E 02	-0.136E 06	-0.150E 02
0.750E 00	-0.192E 00	-0.150E 01	-0.100E 01	0.224E 02	0.403E 01	0.932E 05	-0.145E 04	-0.192E 04	-0.224E 02
0.100E 01	-0.230E 01	-0.335E 01	-0.100E 01	0.539E 02	0.958E 01	0.224E 06	-0.473E 04	-0.430E 06	-0.539E 02
0.125E 01	0.620E 01	0.464E 01	-0.100E 01	-0.875E 02	-0.154E 02	-0.364E 06	0.898E 06	0.653E 06	0.875E 02
0.150E 01	0.214E 01	0.100E 01	-0.100E 01	-0.224E 02	-0.392E 01	-0.933E 05	0.248E 05	0.155E 06	0.223E 02
0.175E 01	0.144E 01	0.471E 00	-0.100E 01	-0.124E 02	-0.216E 01	-0.520E 05	0.140E 04	0.793E 05	0.123E 02
0.200E 01	0.111E 01	0.271E 00	-0.100E 01	-0.841E 01	-0.147E 01	-0.356E 05	0.933E 03	0.453E 05	0.835E 01
0.225E 01	0.921E 00	0.173E 00	-0.100E 01	-0.629E 01	-0.111E 01	-0.270E 05	0.659E 03	0.334E 05	0.621E 01
0.250E 01	0.787E 00	0.117E 00	-0.100E 01	-0.499E 01	-0.883E 00	-0.216E 05	0.474E 03	0.237E 05	0.486E 01
0.275E 01	0.687E 00	0.832E-01	-0.100E 01	-0.411E 01	-0.734E 00	-0.180E 05	0.339E 03	0.172E 05	0.355E 01
0.300E 01	0.608E 00	0.613E-01	-0.100E 01	-0.349E 01	-0.628E 00	-0.154E 05	0.234E 03	0.126E 05	0.335E 01
0.325E 01	0.544E 00	0.465E-01	-0.100E 01	-0.303E 01	-0.548E 00	-0.135E 05	0.149E 03	0.918E 04	0.286E 01
0.350E 01	0.492E 00	0.364E-01	-0.100E 01	-0.267E 01	-0.486E 00	-0.119E 05	0.779E 02	0.655E 04	0.248E 01
0.375E 01	0.447E 00	0.294E-01	-0.100E 01	-0.239E 01	-0.436E 00	-0.106E 05	0.170E 02	0.448E 04	0.217E 01
0.400E 01	0.409E 00	0.252E-01	-0.100E 01	-0.216E 01	-0.394E 00	-0.953E 04	-0.362E 04	0.281E 04	0.192E 01
0.425E 01	0.378E 01	0.271E-01	-0.100E 01	-0.198E 01	-0.359E 00	-0.858E 04	-0.834E 04	0.147E 04	0.170E 01
0.450E 01	0.367E 01	0.185E 00	-0.100E 01	-0.182E 01	-0.327E 00	-0.773E 04	-0.126E 04	0.361E 03	0.152E 01

$$a_1 = 2\dot{\sigma}\tan\xi_T - \dot{\gamma}_T\tan\xi_T$$

$$a_2 = -\dot{\sigma}^2 + \dot{\gamma}_T\dot{\sigma} + \ddot{\sigma}\tan\xi_T$$

TABLE B-3

Error Equation Coefficients a_i and b_i as functions of the time for the trajectory of Fig. 4.5 with initial conditions $\psi=90°$, $\phi=80°$, $x_T = 10,000$, $y_T = 1,000$.

$$b_1 = -1$$

$$b_2 = \sec\xi_T$$

$$b_3 = -\dot{\gamma}_T\sec\xi_T\sin(\gamma_M-\gamma_T)$$

$$b_4 = -r\dot{\gamma}_T - 2\dot{r}\tan\xi_T + 2r\dot{\sigma}$$

$$b_5 = -V_M\dot{\gamma}_T\sec\xi_T\cos(\gamma_M-\gamma_T)$$

$$b_6 = -r\tan\xi_T$$

$$b_7 = -\tan\xi_T$$

N_1 a_{M_r}, accel $\parallel$ LOS error

N_2 $\dot{V}_T$, target airspeed change

N_3 $\hat{V}_M$, missile airspeed error

N_4 $\dot{\sigma}$, LOS rate error

N_5 $\hat{\xi}_M$, error of estimating $\hat{\xi}$

N_6 $\ddot{\sigma}$ LOS acceleration error

N_7 a_{M_σ}, accel. $\perp$ LOS, error

101

TIME	A1	A2	B1	B2	B3	B4	B5	B6	B7
0.0	0.160E 00	0.152E-03	-0.100E 01	0.100E 01	0.0	-0.133E 04	-0.393E 04	0.100E 04	0.100E 00
0.250E 00	0.964E-02	0.242E-02	-0.100E 01	0.100E 01	0.632E-02	-0.163E 04	-0.392E 04	0.541E 03	0.574E-01
0.500E 00	0.254E-02	0.306E-02	-0.100E 01	0.100E 01	0.113E-01	-0.147E 04	-0.391E 04	0.147E 03	0.155E-01
0.750E 00	-0.375E-02	0.353E-02	-0.100E 01	0.100E 01	0.159E-01	-0.130E 04	-0.390E 04	-0.235E 03	-0.260E-01
0.100E 01	-0.945E-02	0.476E-02	-0.100E 01	0.100E 01	0.203E-01	-0.115E 04	-0.390E 03	-0.600E 03	-0.673E-01
0.125E 01	-0.157E-01	0.406E-02	-0.100E 01	0.101E 01	0.245E-01	-0.999E 03	-0.390E 03	-0.937E 03	-0.100E 00
0.150E 01	-0.216E-01	0.424E-02	-0.100E 01	0.101E 01	0.366E-01	-0.850E 03	-0.391E 03	-0.125E 04	-0.150E 00
0.175E 01	-0.274E-01	0.431E-02	-0.100E 01	0.102E 01	0.265E-01	-0.702E 03	-0.392E 03	-0.155E 04	-0.192E 00
0.200E 01	-0.333E-01	0.433E-02	-0.100E 01	0.103E 01	0.345E-01	-0.554E 03	-0.394E 03	-0.192E 04	-0.234E 00
0.225E 01	-0.394E-01	0.430E-02	-0.100E 01	0.104E 01	0.405E-01	-0.403E 03	-0.397E 03	-0.207E 04	-0.275E 00
0.250E 01	-0.456E-01	0.424E-02	-0.100E 01	0.105E 01	0.450E-01	-0.250E 03	-0.400E 03	-0.231E 04	-0.322E 00
0.275E 01	-0.519E-01	0.415E-02	-0.100E 01	0.107E 01	0.494E-01	-0.936E 02	-0.405E 03	-0.252E 04	-0.367E 00
0.300E 01	-0.565E-01	0.403E-02	-0.100E 01	0.109E 01	0.539E-01	0.682E 02	-0.407E 03	-0.272E 04	-0.414E 00
0.325E 01	-0.655E-01	0.384E-02	-0.100E 01	0.110E 01	0.517E-01	0.236E 03	-0.412E 03	-0.290E 04	-0.462E 00
0.350E 01	-0.725E-01	0.373E-02	-0.100E 01	0.112E 01	0.635E-01	0.411E 03	-0.419E 03	-0.305E 04	-0.512E 00
0.375E 01	-0.805E-01	0.355E-02	-0.100E 01	0.115E 01	0.692E-01	0.595E 03	-0.424E 03	-0.316E 04	-0.565E 00
0.400E 01	-0.895E-01	0.334E-02	-0.100E 01	0.118E 01	0.750E-01	0.788E 03	-0.431E 03	-0.331E 04	-0.620E 00
0.425E 01	-0.973E-01	0.310E-02	-0.100E 01	0.124E 01	0.813E-01	0.993E 03	-0.439E 03	-0.341E 04	-0.673E 00
0.450E 01	-0.107E 00	0.264E-02	-0.100E 01	0.124E 01	0.915E-01	0.121E 04	-0.448E 03	-0.344E 04	-0.731E 00
0.475E 01	-0.117E 00	0.254E-02	-0.100E 01	0.128E 01	0.954E-01	0.145E 04	-0.458E 03	-0.353E 04	-0.204E 00
0.500E 01	-0.127E 00	0.219E-02	-0.100E 01	0.133E 01	0.104E 00	0.170E 04	-0.470E 03	-0.355E 04	-0.874E 00
0.525E 01	-0.136E 00	0.160E-02	-0.100E 01	0.138E 01	0.113E 00	0.197E 04	-0.482E 03	-0.354E 04	-0.945E 00
0.550E 01	-0.152E 00	0.134E-02	-0.100E 01	0.144E 01	0.123E 00	0.227E 04	-0.496E 03	-0.350E 04	-0.103E 01
0.575E 01	-0.167E 00	0.820E-03	-0.100E 01	0.150E 01	0.134E 00	0.260E 04	-0.512E 03	-0.342E 04	-0.112E 01
0.600E 01	-0.183E 00	0.203E-03	-0.100E 01	0.158E 01	0.147E 00	0.296E 04	-0.530E 03	-0.331E 04	-0.122E 01
0.625E 01	-0.201E 00	-0.546E-03	-0.100E 01	0.166E 01	0.161E 00	0.336E 04	-0.573E 03	-0.314E 04	-0.133E 01
0.650E 01	-0.221E 00	-0.137E-02	-0.100E 01	0.176E 01	0.178E 00	0.382E 04	-0.600E 03	-0.292E 04	-0.145E 01
0.675E 01	-0.245E 00	-0.245E-02	-0.100E 01	0.188E 01	0.197E 00	0.434E 04	-0.630E 03	-0.263E 04	-0.155E 01
0.700E 01	-0.273E 00	-0.355E-02	-0.100E 01	0.201E 01	0.220E 00	0.494E 04	-0.666E 03	-0.226E 04	-0.175E 01
0.725E 01	-0.305E 00	-0.572E-02	-0.100E 01	0.218E 01	0.247E 00	0.564E 04	-0.666E 03	-0.176E 04	-0.163E 01
0.750E 01	-0.346E 00	-0.973E-02	-0.100E 01	0.237E 01	0.280E 00	0.647E 04	-0.709E 03	-0.117E 04	-0.215E 01
0.775E 01	-0.366E 00	-0.407E-01	-0.100E 01	0.262E 01	0.320E 00	0.748E 04	-0.760E 03	-0.361E 03	-0.242E 01

TABLE B-4

Error Equation Coefficients a_i and b_i as functions of the time for the trajectory of Fig. 4.6 with initial conditions $\psi=0°$, $\phi = 80°$, $x_T = 16,000$; $y_T = 1,000$.

102

TIME	A1	A2	B1	B2	B3	B4	B5	B6	B7
0.0	0.120E-01	0.652E-02	-0.100E 01	-0.101E 01	-0.424E-04	-0.184E 04	-0.393E 03	0.101E 04	0.100E 00
0.250E 00	0.816E-02	0.742E-02	-0.100E 01	-0.100E 01	-0.336E-02	-0.161E 04	-0.392E 03	0.572E 03	0.617E-01
0.500E 00	0.317E-02	0.402E-02	-0.100E 01	-0.100E 01	-0.628E-02	-0.140E 04	-0.391E 03	0.180E 03	0.213E-01
0.740E 00	-0.353E-02	0.657E-03	-0.100E 01	-0.100E 01	0.111E-01	-0.114E 04	-0.391E 03	-0.164E 03	-0.213E-01
0.100E 01	-0.120E 01	-0.193E-02	-0.100E 01	-0.100E 01	0.179E-01	-0.841E 03	-0.390E 03	-0.455E 03	-0.659E-01
0.125E 01	-0.221E-01	-0.444E-02	-0.100E 01	-0.101E 01	0.265E-01	-0.496E 03	-0.390E 03	-0.650E 03	-0.113E 00
0.150E 01	-0.340E-01	-0.660E-02	-0.100E 01	-0.101E 01	0.368E-01	-0.110E 03	-0.388E 03	-0.865E 03	-0.162E 00
0.175E 01	-0.475E-01	-0.632E-02	-0.100E 01	-0.102E 01	0.489E-01	0.316E 03	-0.386E 03	-0.974E 03	-0.213E 00
0.200E 01	-0.626E-01	-0.551E-02	-0.100E 01	-0.104E 01	0.625E-01	0.778E 03	-0.382E 03	-0.101E 04	-0.268E 00
0.225E 01	-0.790E-01	-0.558E-02	-0.100E 01	-0.105E 01	0.776E-01	0.127E 04	-0.376E 03	-0.979E 03	-0.325E 00
0.250E 01	-0.964E-01	-0.543E-02	-0.100E 01	-0.107E 01	0.939E-01	0.180E 04	-0.368E 03	-0.865E 03	-0.395E 00
0.275E 01	-0.114E 00	-0.723E-02	-0.100E 01	-0.110E 01	0.111E 00	0.234E 04	-0.357E 03	-0.666E 03	-0.449E 00
0.300E 01	-0.131E 01	-0.127E-02	-0.100E 01	-0.113E 01	0.129E 00	0.290E 04	-0.342E 03	-0.377E 03	-0.517E 00

TABLE B-5

Error Equation Coefficients a_i and b_i as functions of the time for the trajectory of Fig. 4.7 with initial conditions $\psi = 180°$, $\phi = 80°$, $x_T = 10,000$, $y_T = 1,000$.

$$a_1 = 2\dot{\sigma} \tan \xi_T - \dot{Y}_T \tan \xi_T$$

$$a_2 = -\dot{\sigma}^2 + \dot{Y}_T \dot{\sigma} + \ddot{\sigma} \tan \xi_T$$

$b_1 = -1$ N_1 a_{M_r}, accel # LOS error

$b_2 = \sec \xi_T$ N_2 $\dot{V}_T$, target airspeed change

$b_3 = -\dot{Y}_T \sec \xi_T \sin (Y_M - Y_T)$ N_3 $\hat{V}_M$, missile airspeed error

$b_4 = -r\dot{Y}_T - 2\dot{r} \tan \xi_T + 2r\dot{\sigma}$ N_4 $\dot{\sigma}$, LOS rate error

$b_5 = -V_M \dot{Y}_T \sec \xi_T \cos (Y_M - Y_T)$ N_5 $\hat{\xi}_M$, error of estimating

$b_6 = -r \tan \xi_T$ N_6 $\ddot{\sigma}$ LOS acceleration error

$b_7 = -\tan \xi_T$ N_7 a_{N_σ}, accel. $\perp$ LOS, error

103

TIME	a1	a2	b1	b2	b3	b4	b5	a6	a7
0.0	-0.793E-C3	-0.622E-C4	-0.1C0E 01	-0.100E 01	0.0	-0.999E 00	0.0	0.101E 04	0.502E-01
0.250E 00	-0.807E-03	0.160E-03	-0.1C0E 01	-0.100E 01	0.0	-0.307E 02	0.0	0.100E 04	0.522E-01
0.500E 00	-0.785E-03	0.154E-C3	-0.1C0E 01	-0.100E 01	0.0	-0.720E 02	0.0	0.969E 03	0.541E-01
0.750E 00	-0.759E-C3	0.148E-C3	-0.1C0E 01	-0.100E 01	0.0	-0.111E 03	0.0	0.987E 03	0.559E-01
0.100E 01	-0.730E-03	0.143E-03	-0.100E 01	-0.100E 01	0.0	-0.147E 03	0.0	0.971E 03	0.575E-01
0.125E 01	-0.697E-03	0.138E-03	-0.100E 01	-0.100E 01	0.0	-0.181E 03	0.0	0.951E 03	0.590E-01
0.150E 01	-0.661E-03	0.133E-C3	-0.100E 01	-0.100E 01	0.0	-0.213E 03	0.0	0.726E 03	0.605E-01
0.175E 01	-0.623E-C3	0.129E-C3	-0.100E 01	-0.100E 01	0.0	-0.242E 03	0.0	0.499E 03	0.618E-01
0.200E 01	-0.584E-03	0.124E-03	-0.100E 01	-0.100E 01	0.0	-0.269E 03	0.0	0.666E 03	0.630E-01
0.225E 01	-0.542E-03	0.119E-C3	-0.100E 01	-0.100E 01	0.0	-0.293E 03	0.0	0.611E 03	0.641E-01
0.250E 01	-0.500E-C3	0.115E-03	-0.100E 01	-0.100E 01	0.0	-0.316E 03	0.0	0.793E 03	0.651E-01
0.275E 01	-0.457E-03	0.110E-C3	-0.100E 01	-0.100E 01	0.0	-0.336E 03	0.0	0.752E 03	0.660E-01
0.300E 01	-0.414E-03	0.106E-C3	-0.100E 01	-0.100E 01	0.0	-0.354E 03	0.0	0.709E 03	0.665E-01
0.325E 01	-0.371E-03	0.101E-C3	-0.100E 01	-0.100E 01	0.0	-0.371E 03	0.0	0.663E 03	0.574E-01
0.350E 01	-0.328E-C3	0.967E-04	-0.100E 01	-0.100E 01	0.0	-0.385E 03	0.0	0.616E 03	0.682E-01
0.375E 01	-0.286E-C3	0.920E-04	-0.100E 01	-0.100E 01	0.0	-0.398E 03	0.0	0.557E 03	0.688E-01
0.400E 01	-0.244E-C3	0.872E-04	-0.100E 01	-0.100E 01	0.0	-0.409E 03	0.0	0.517E 03	0.653E-01
0.425E 01	-0.205E-03	0.821E-04	-0.100E 01	-0.100E 01	0.0	-0.418E 03	0.0	0.465E 03	0.697E-01
0.450E 01	-0.167E-03	0.765E-04	-0.100E 01	-0.100E 01	0.0	-0.426E 03	0.0	0.412E 03	0.700E-01
0.475E 01	-0.131E-03	0.712E-04	-0.100E 01	-0.100E 01	0.0	-0.432E 03	0.0	0.359E 03	0.703E-01
0.500E 01	-0.970E-04	0.651E-04	-0.100E 01	-0.100E 01	0.0	-0.437E 03	0.0	0.304E 03	0.705E-01
0.525E 01	-0.602E-04	0.586E-C4	-0.100E 01	-0.100E 01	0.0	-0.440E 03	0.0	0.250E 03	0.706E-01
0.550E 01	-0.343E-C4	0.512E-04	-0.100E 01	-0.100E 01	0.0	-0.443E 03	0.0	0.194E 03	0.707E-01
0.575E 01	-0.136E-04	0.441E-04	-0.100E 01	-0.100E 01	0.0	-0.444E 03	0.0	0.139E 03	0.708E-01
0.600E 01	0.107E-04	0.477E-04	-0.100E 01	-0.100E 01	0.0	-0.445E 03	0.0	0.334E 02	0.708E-01
0.625E 01	0.734E-04	0.362E-03	-0.1C0E 01	-0.100E 01	0.0	-0.445E 03	0.0	0.275E 02	0.708E-01

TABLE B-6

Error Equation Coefficients a_i and b_i as functions of the time for the trajectory of Fig. 4.8 with initial conditions $\psi=180°$, $\phi = 0°$, $x_T = 20,000$, $y_t = 1,000$.

DOCUMENT CONTROL DATA - R & D

(Security classification of title, body of abstract and indexing annotation must be entered when the overall report is classified)

1. ORIGINATING ACTIVITY *(Corporate author)*	2a. REPORT SECURITY CLASSIFICATION
Bell Aerospace Company P.O. Box 1 Buffalo, New York 14240	Unclassified 2b. GROUP

3. REPORT TITLE

Kinematic Ranging in an Air-Air Missile

4. DESCRIPTIVE NOTES *(Type of report and inclusive dates)*

Final Report; March, 1971 to October, 1972

5. AUTHOR(S) *(First name, middle initial, last name)*

Ronald J. LaSpisa and Frederic D. Powell

6. REPORT DATE	7a. TOTAL NO. OF PAGES	7b. NO. OF REFS
October 1972	104	6

| 8a. CONTRACT OR GRANT NO
Contract N00019-71-C-0259
b. PROJECT NO
WF 20-344
c.
d. | 9a. ORIGINATOR'S REPORT NUMBER(S)
Bell Aero. Report #9500-920294

9b. OTHER REPORT NO(S); *(Any other numbers that may be assigned this report)*
- |

10. DISTRIBUTION STATEMENT

Statement No. 2: This document is subject to special export controls and each transmittal to foreign governments or foreign nationals may be made only with prior approval of NAVAIR (Air-C02).

| 11. SUPPLEMENTARY NOTES
- | 12. SPONSORING MILITARY ACTIVITY
Naval Air Systems Command
Code Air-53322C
Washington, D.C. 20360 |

13. ABSTRACT

Methods are explored for estimating Range and Range-Rate from the geometry and kinematics of the air-air homing-missile combat situation rather than from direct measurements. The methods reported herein use the various signals available from the missile autopilot, plus the inertial rotation-rate of the Line of Sight provided by the seeker.

It is shown that acceleration of the target in the radial direction, parallel to the Line of Sight, precludes successful estimation by the classical techniques such as adaptive parameter identification, Kalman filter estimation, or the various minimum-variance estimation methods. A nonlinear estimator is described which estimates the target acceleration and velocity components and can yield accurate range and range-rate estimates if correctly initialized at launch. This estimator is able to take advantage of the many inequalities which constrain the maneuvering of an air-air target. Errors and performance of this estimator are demonstrated by computer simulations.

14 KEY WORDS	LINK A		LINK B		LINK C	
	ROLE	WT	ROLE	WT	ROLE	WT
Air-Air Missiles						
Kinematics						
Ranging						
Parameter Identification						
Nonlinear Filtering						

DISTRIBUTION

Commander, Naval Air Systems Command
Washington, D.C. 20360
Attention: Code AIR-5332-2C
                    (3)

Commander, Naval Air Systems Command
Washington, D.C. 20360
Attention: Code AIR-604
                    (2)

Commander, Navail Air Systems Command
Washington, D.C. 20360
Attention: Ccde AIR-604 (DDC)
                    (12)

Commander, Naval Air Systems Command
Washington, D.C. 20360
Attention: Code AIR-5332-2B
                    (1)

Commander, Naval Ordnance Systems Command
Washington, D.C. 20360
Attention: Code ORD-034
                    (1)

Commander, Naval Weapons Center
China Lake, California 93557
Attention: Code 4041
                    (1)

Commander, Naval Ordnance Systems Command
Washington, D.C. 20360
Attention: Code ORD-9132
                    (1)

Commander, Naval Weapons Center
China Lake, California 93557
Attention: Code 5571
                    (1)

Commander, Naval Ordnance Systems Command
Washington, D.C. 20360
Attention: Code ORD-62211
                    (1)

Commander, Naval Weapons Center
China Lake, California 93557
Attention: Code 3051
                    (1)

Office of Naval Research
Department of the Navy
Washington, D. C. 20360
Attention: Code 461
                    (1)

Commander, Naval Weapons Center
China Lake, California 93558
Attention: Code 3023
                    (1)

Office of Naval Research
Department of the Navy
Washington, D. C. 20360
Attention: Code 430:C
                    (1)

Office of Naval Research
Department of the Navy
Washington, D.C. 20360
Attention: Code 432
                    (1)

U.S. Army Missile Command
Redstone Arsenal, Alabama 35809
Attn: AMSMI-RE, Bldg. 5400
        Mr. Maurice F. Belrose
                    (1)

U.S. Army Missile Command
Redstone Arsenal, Alabama 35809
Attention: AMSMI-R, Bldg. 4509
                Mr. James J. Fagan
                    (1)

U.S. Army Missile Command
Redstone Arsenal, Alabama 35809
Attn: AMCPM-MDEI
        Capt. William Stender
                    (1)

U.S. Army Missile Command
Redstone Arsenal, Alabama 35809
Attn: AMCPM-MDER, Mr. Wallace E. Wood
                    (1)

Wright Patterson Air Force Base　　Wright Patterson Air Force Base
Ohio　45433　　　　　　　　　　Ohio　45433
Attn: ASD/ENVWA, Mr. H. L. Williams　Attn: AFFDL/FGL, Mr. A. F. Barfield
　　　　　　　　(1)　　　　　　　　　　　　　　　　　　(3)

Wright Patterson Air Force Base　　Wright Patterson Air Force Base
Ohio　45433　　　　　　　　　　Ohio　45433
Attn:　SSL, Librarian　　　　　Attn:　AFAL/CD, Mr. J. V. Burke
　　　　　　(1)　　　　　　　　　　　　　　　　　(1)

Air Force Armament Development & Test Center
Eglin AFB, Florida　32542
Attn: DLWS,　George Blackshaw
　　　　　　　　　　(1)

H. E. Brown　　　　　　　　　　Capt. G. L. Chatwood
Armament Development & Test Center　Armament Development & Test Center
Attn:　DLQM　　　　　　　　　　Attn:　DLJM
Eglin AFB, Florida　32542　　　Eglin AFB, Florida　32524
　　　　　　　　(1)　　　　　　　　　　　　　　　(1)

Major Alan Gale　　　　　　　　Dr. W. W. Metz
Armament Development & Test Center　Armament Development & Test Center
Attn:　DLWS　　　　　　　　　　Attn:　DLQ
Eglin AFB, Florida　32542　　　Eglin AFB, Florida　32542
　　　　　　　　(1)　　　　　　　　　　　　　　(1)

Bell Aerospace Company　　　　　Bell Aerospace Company
P.O. Box One　　　　　　　　　P.O. Box One
Buffalo, New York　14240　　　Buffalo, New York　14240
Attn:　Dr. J. Goerner　　　　　Attn:　Dr. P. LaSpisa
　　　　　　(1)　　　　　　　　　　　　　　(1)

Bell Aerospace Company　　　　　Bell Aerospace Company
P.O. Box One　　　　　　　　　P.O. Box One
Buffalo, New York　14240　　　Buffalo, New York　14240
Attn: F. Powell　　　　　　　　Attn:　Library
　　　　　(2)　　　　　　　　　　　　　　(1)

Bell Aerospace Company
P.O. Box One
Buffalo, New York　14240
Attn:　Tech. Com. Dept.
　　　　　　(2)